2014-05-03

Observations and Modeling of Microbial Water Quality at Recreational Beaches

Zhixuan Feng
University of Miami, zfeng@rsmas.miami.edu

UNIVERSITY OF MIAMI

OBSERVATIONS AND MODELING OF MICROBIAL WATER QUALITY AT RECREATIONAL BEACHES

By

Zhixuan Feng

A DISSERTATION

Submitted to the Faculty
of the University of Miami
in partial fulfillment of the requirements for
the degree of Doctor of Philosophy

Coral Gables, Florida

May 2014

UNIVERSITY OF MIAMI

A dissertation submitted in partial fulfillment of
the requirements for the degree of
Doctor of Philosophy

OBSERVATIONS AND MODELING OF MICROBIAL WATER QUALITY AT RECREATIONAL BEACHES

Zhixuan Feng

Approved:

_____ Adrianus Reniers, Ph.D. Professor of Applied Marine Physics	_____ John D. Wang, Ph.D. Professor of Applied Marine Physics
_____ Brian K. Haus, Ph.D. Professor of Applied Marine Physics	_____ Lora E. Fleming, M.D. Ph.D. Professor of Epidemiology University of Exeter Medical School
_____ Helena M. Solo-Gabriele, Ph.D. Professor of Civil, Architectural and Environmental Engineering	_____ M. Brian Blake, Ph.D. Dean of the Graduate School

FENG, ZHIXUAN (Ph.D., Applied Marine Physics)

Observations and Modeling of Microbial Water Quality at Recreational Beaches (May 2014)

Abstract of a dissertation at the University of Miami.

Dissertation supervised by Professors Ad Reniers and Brian Haus
No. of pages in text. (146)

To comply with federal law Beach Environmental Assessment and Coastal Health Act (BEACH Act), and the U.S. Environmental Protection Agency guidelines, beach monitoring programs have been adopted and implemented to protect beachgoers from health risks caused by harmful microorganisms. Present monitoring programs around the United States heavily rely on sparse water sampling (usually daily to weekly) with time-consuming microbial laboratory analysis, thereby potentially causing unnecessary beach closures or human health risks for beaches that remain open. The objective of this dissertation is to use both field observations and numerical models to investigate the linkages between microbiological, hydrological, and morphological processes at nonpoint source beaches. The scales cover intra-day to inter-annual variations, and from a single case study beach to hundreds of beaches in the State of Florida. This objective is accomplished through three studies.

In the first study, a coupled microbe-hydrodynamic-morphological model is developed. The unique feature of this model is its capability of simulating the release of microbes attached to beach sands as a result of combined wave and tidal forcing. The microbe transport-decay equation, coupled to the nearshore process model XBeach, includes source functions that account for microbial release from mobilized sand, groundwater flow, entrainment through pore water diffusion, rainfall-runoff loading, and

a fate function that accounts for solar inactivation effects. The model has skills in simulating observed temporal patterns of enterococci levels at a municipal beach in Miami, FL through an intensive 10-day field experiment, including the reproduction of diel cycles due to solar inactivation and patterns associated with semidiurnal tides. The spatial patterns are shown as rapid decreases of enterococci levels from the shoreline to offshore.

The second study develops a new numerical mass balance model for enterococci levels on nonpoint source beaches. This is a model similar to more general horizontal grid numerical models, but simplified as it is limited to calculation of transient cross-shore microbial distributions for a beach with fairly alongshore uniform source and environmental conditions. The inputs to the model are readily-available environmental factors (i.e., wind, tide, wave, solar radiation, and precipitation), which are used in the mass balance considerations of source loading, transport, and biological decay. The significant advantage of this model is its easy implementation and a detailed description of the cross-shore distribution of enterococci which should be useful for beach management purposes. The performance of the balance model is evaluated by comparing predicted exceedances of a beach advisory threshold value to field data, and to a traditional regression equation model. Both the balance model and regression equation predicted approximately 70% the advisories correctly at the knee depth and > 90% at the waist depth. The balance model has the advantage over the regression equation in its ability to simulate spatiotemporal variations of microbial levels and is recommended for making more informed beach management decisions.

In the third study, decade-long weekly monitored indictor bacteria levels (enterococci and fecal coliform) at 262 Florida recreational beaches, provided by the Florida Healthy Beaches Program, are analyzed to examine spatiotemporal patterns of microbial levels and microbial responses to hydrological and hydrometeorologic fluctuations (i.e., wave height, water temperature, solar radiation, and precipitation). Results showed that low-wave-energy beaches exceed the EPA thresholds significantly more than high-wave-energy ones ($p < 0.01$), and Gulf of Mexico beaches also exceed the thresholds significantly more than Atlantic ones ($p < 0.01$). Percent exceedances negatively correlate with both long-term mean wave height and beach slope, suggesting that beach wave energy level is an important factor in determining water quality. In general, the higher wave energy, the better beach water quality is. In addition, we found that seasonal bacterial variations in Atlantic and Gulf of Mexico beaches are generally out of phase. There are opposite correlations in seasonal mean log-transformed bacterial levels and environmental variables (i.e., wave height, water temperature, solar radiation, and precipitation) between Atlantic versus Gulf of Mexico beaches. Microbial variations on each of Florida coasts are likely controlled by different mechanisms, which would require different beach management strategies to minimize microbial water quality exceedances.

In summary, this dissertation explores innovative modeling techniques and highlights physical and biological interactions in controlling nearshore microbial water quality. The new model tools and knowledge can be applied in beach management practice, water quality assessment, and decision support across the United States.

ACKNOWLEDGEMENTS

I would like to express my sincere gratitude to my co-advisers, Drs. Ad Reniers and Brian Haus, for their continuous support, guidance, and wisdom throughout my study and research. I am truly grateful to my dissertation committee members, Drs. Helena Solo-Gabriele, John Wang, and Lora Fleming, who helped me tremendously and offered me their insightful and invaluable advices.

I cannot achieve this dissertation without considerable support from the Oceans and Human Health Center (OHH) at the University of Miami. Numerous people participated and contributed to the 10-day field experiment in June 2010, including Sharon Smith, Josefina Olascoaga, Peter Minnett, James Klaus, Lisa Plano, Chris Sinigalliano, Maribeth Gidley, Mathew Phillips, Amir Abdelzaher, Alan Piggot, Julie Hollenbeck, Laura Fiorentino, Samir Elmir, Amber Enns, Laura Vogel, Yifan Zhang, and many others. I thank my colleagues and friends, Patrick Rynne, Bjorn Lund, Henry Potter, Jingshuang Xue and others, for being around me in the past few years.

This dissertation work is funded by the National Science Foundation (NSF) and National Institute of Environmental Health Sciences (NIEHS) OHH Program (NIEHS # P50 ES12736 and NSF #OCE0432368/0911373/1127813). I acknowledge Deltares for sharing XBeach model source codes, Robert McCall and Arnold van Rooijen for their technical assistance. David Polk of Florida Department of Health provided historical water quality monitoring data.

Most of all, thanks to my family and friends, especially my parents and girlfriend Yujie, for their love, support, and encouragement. Lastly, thank you, the entire RSMAS and University of Miami family! You made my past five years enjoyable and memorable.

TABLE OF CONTENTS

Page

LIST OF FIGURES

LIST OF TABLES

Chapter 1 INTRODUCTION

1.1 Background

1.1.1 Prior Research in Microbial Pollution

In recent years, inter-relationships between oceans and human health have been increasingly recognized as both regional and worldwide issues, one of which is microbial water contamination by pathogenic and/or non-pathogenic bacteria, viruses, parasites, protozoa, and other microorganisms (Fleming et al., 2006; Stewart et al., 2011). Globally, it has been estimated that a total of 120 million cases of gastrointestinal diseases and 50 million cases of respiratory diseases occur every year in relation to bathing/swimming in impaired marine waters (Shuval, 2003). To protect human health in recreational waters, the United States Environmental Protection Agency (EPA) recommends the use of fecal indicator bacteria (FIB) (i.e., enterococci for both seawater and freshwater; *Escherichia coli* for freshwater only) as standards to determine whether or not health advisories should be issued (US EPA, 1986). In 2000, the Beaches Environmental Assessment and Coastal Health (BEACH) Act that amended the Clean Water Act was signed into a federal law. The BEACH Act required states and tribes to adopt new or revised recreational water quality criteria and to develop and implement beach monitoring and assessment programs. In 2012, new recreational water quality criteria have been released to provide more accurate estimates of health risk and tools for assessing and managing recreational waters and for developing alternative site-specific criteria (US EPA, 2012).

Since the early 2000s, researchers at the Oceans and Human Health Center (OHH) at the University of Miami, funded jointly by the National Science Foundation (NSF) and National Institute of Environmental Health Sciences (NIEHS), have conducted

a series of interdisciplinary research projects on water quality and associated human health impact assessment of subtropical marine beaches. These studies have focused at Hobie Beach (Miami, FL) study site since it is characterized by frequent exceedances of EPA criteria and beach closures. An early pilot study on epidemiology found no significant correlations between multiple traditional indicator microbes and human health effects (Fleming et al., 2004; Shibata et al., 2004). Later studies focused on estimations of amounts of enterococci and *Staphylococcus aureus* shed by bathers (Elmir et al., 2007) and further distinguished bacterial contributions from two distinct age groups: adults and toddlers (Elmir et al., 2009; Plano et al., 2011). Another study quantified the average enterococci loads from dog, bird, and shrimp feces, and showed that dog feces contribute a substantially greater amount of enterococci (at least two orders of magnitude higher) than the other two possible sources (Wright et al., 2009). In addition, an innovative surveillance camera system was developed to enumerate instantaneous, short-term, and long-term average visitations of humans and animals and to further estimate total amounts of enterococci contributed by bathers, birds, and dogs, respectively (Wang et al., 2010). Abdelzaher et al. (2010) evaluated the inter-relationships between multiple FIB, environmental conditions and a number of potential pathogens in both water and sand samples. The detections of pathogenic *Vibrio vulnificus*, *Cryptosporidium spp.*, and *Giardia spp.* coincided with the elevated and excessive FIB levels (Abdelzaher et al., 2010).

In regard to identifying and tracking sources of microorganisms, early and recent studies all suggested that intertidal sediments can be significant indigenous sources of both indicator microorganisms and pathogens (Shibata et al., 2004; Wright et al., 2011;

Shah et al., 2011). Samples taken from storm runoff through the beach surface were observed with high enterococci concentrations of order of 10^4 CFU/100 mL or higher, which may explain the elevated bacterial indictors and detections of disease-causing *Cryptosporidium spp.*, *Giardia spp.*, and enterovirus after major rainfall events (Wright et al., 2011; Abdelzaher et al., 2011). Biofilms on the sand surface may provide a suitable habitat for FIB and pathogens and it was found that enterococci levels peak at intermediate levels of extracellular polymeric substance, a major component of biofilms (Piggot et al., 2012). A sand core experiment showed that only an average of 10% of total enterococci within the sand was released through shallow groundwater flows induced by hydraulic head gradients (Philips et al., 2011b). Beach renovation activities in 2010, including importation of new and clean sand, stormwater infrastructure upgrade, and parking improvement, significantly reduced enterococci and biofilm levels in the sand and also enterococci exceedances of the water (Hernandez et al., 2014).

Beach Exposure Assessment and Characterization Health Epidemiology Study (BEACHES) demonstrated that bathers have significantly higher health risk of gastrointestinal, respiratory, and dermatologic diseases than non-bathers (Fleisher et al., 2010; Sinigalliano et al., 2010). The BEACHES study also involved evaluations and comparisons of conventional (i.e., enterococci) and alternative (i.e., Bacteroidales) indicator organisms using both culture-based and rapid molecular methods (Sinigalliano et al., 2010; Shibata et al., 2010). Subsequent analyses only showed a statistically significant positive dose-response relationship between skin illness and enterococci level and antecedent rainfall, and an inverse relationship between acute febrile respiratory illness and water temperature, but no other statistically significant associations between

self-reported symptoms and any of the indicator organisms (Fleisher et al., 2010; Sinigalliano et al., 2010). In addition, the BEACHES study also found that measurements by quantitative polymerase chain reaction (qPCR) may not be comparable to either membrane filtration or chromogenic substrate for marine waters (Shibata et al., 2010; Sinigalliano et al., 2010).

Modeling can provide better understanding of water quality patterns observed from epidemiologic and environmental studies. A hydrodynamic model with water quality capacity that incorporates three nonpoint sources (i.e., bather shedding, dog feces, and beach sands) indicated that dog fecal events may be partially responsible for the observed high enterococci levels near the shoreline (Zhu et al., 2011). Simulated flow fields were further utilized to extract Lagrangian Coherent Structures (LCS) and LCS results demonstrated that local water circulation at the study site may favor the retention of pollutants originated from the shoreline (Fiorentino et al., 2012). In addition, a Delft3D circulation and water quality model was developed for this site, and the simulations revealed different patterns of enterococci distribution impacted by four different types of nonpoint sources of enterococci (Feng et al., 2012).

Many studies have demonstrated that indicator and/or pathogenic microorganisms may enter coastal waters through a variety of pathways, such as sewage outfalls and spills (Nevers and Whitman, 2005), rivers and creeks (Kim et al., 2004), urban and agricultural runoff (Sanders et al., 2005), contaminated soils and sands (Solo-Gabriele et al., 2000; Shah et al., 2011), submerged aquatic vegetation (Badgley et al., 2011), groundwater discharge (Boehm et al., 2004a), animals (Wright et al., 2009), and bathers (Elmir et al., 2007; Elmir et al., 2009; Plano et al., 2011). Moreover, the spatial and

temporal variations of microbes in the beach environments are heavily impacted by nearshore circulation and mixing which are typically driven by tides, waves, density gradients and/or winds with additional topographic and bathymetric influences (Grant and Sanders, 2010). Bacteria can persist within the sand for a long time and even replicate under favorable conditions (Desmarais et al., 2002; Yamahara et al., 2009); however, assessments of microbial water quality in tropical and subtropical environments typically do not monitor beach sediments under present EPA guidelines. In addition, although previous environmental studies did indicate that tidal washing of intertidal sand may be responsible for the observed high microbial levels during high tide (Shibata et al., 2004; Wright et al., 2011; Abdelzaher et al., 2011), the mechanisms of bacterial release from the sand grains to the water column is unclear and few studies have paid attention to the wave influence and related sediment resuspension and transport.

1.1.2 Models in Beach Water Quality Research

Well-developed models can be powerful, effective, and efficient beach management tools to supplement existing beach monitoring programs and epidemiologic studies. Models may benefit management from at least two points: (1) models are efficient tools to evaluate the impacts of various pollutant sources and controlling mechanisms on water quality scenarios; (2) models can predict microbe levels in the near future in order to forecast potential beach advisories and closures (Palmer et al., 2008). The methodologies that various models rely on can be fundamentally different: from statistical regression models (e.g., Nevers and Whitman, 2005; Frick et al., 2008); to conceptual models that solve the microbial mass balance equation under simplified transport and decay processes (e.g., Grant et al., 2005; Boehm et al., 2005; Grant and

Sanders, 2010); to two- (i.e., depth-averaged or depth-integrated) or three-dimensional hydrodynamic models with microbial source input, transport, and fate capacities (e.g., Sanders et al., 2005; Liu et al., 2006; Hipsey et al., 2008; Zhu et al., 2011; Ge et al., 2012a; Thupaki et al., 2013).

The most explored and widely used statistical models are multivariable linear regression models. They are intended to identify linear or quasi-linear relationships between levels of indicator bacteria (e.g., *E. coli* and enterococci) and various ambient environmental conditions. Within the context of these regression models, the environmental conditions are usually quantified by specific hydrometeorologic and hydrologic parameters (e.g., wave height, turbidity, solar radiation, rainfall, tide, river discharge, and wind) to determine relative contributions of explanatory variables and corresponding regression coefficients. For examples of such models, refer to Olyphant (2005), Nevers and Whitman (2005), Frick et al. (2008) and Ge et al. (2010). Based on such methodologies, the EPA has developed "Virtual Beach" software, a user-friendly prediction tool freely available to scientific communities and beach managers (Frick et al., 2008; Cyterski et al., 2012).

Conceptual/analytical models only retain important physical and biological processes associated with microbial dynamics while neglecting and/or simplifying unimportant ones, making the complex microbial mass balance equation easy to solve and analyze. Those models may not be capable of adequately predicting real-time bacterial levels at the beach; however, they can reveal the characteristics and relative importance of contamination sources and related physical and biological processes. For example, Grant et al. (2005) developed a conceptual surf zone model considering point

source bacterial loads from two tidal inlets, under processes of advection and turbulent mixing in the alongshore, advective loss in the cross-shore, and sunlight inactivation. Another surf zone model has solved a known point source, governed by the physical processes of dilution by rip currents and alongshore littoral drift and by the biological processes of solar inactivation and grazing mortality (Boehm et al., 2005). A beach boundary layer was constructed and applied to embayed beaches with minimal wave action (Grant and Sanders, 2010). Both analytical and numerical solutions were achieved under the assumption of steady-state balance between cross-shore turbulent diffusion and longshore advection, and were further used to predict bacterial concentrations and environmental impacts of a variety of beach-side pollutant loads (Grant and Sanders, 2010).

Deterministic modeling usually requires comprehensive understanding of the complex physical, chemical, and biological processes and mechanisms and also abundant datasets from field observations or laboratory experiments for model calibration, parameterization, validation, and hindcast. The two- or three-dimensional hydrodynamic and water quality models numerically solve continuity, momentum, and microbe transport-fate equations to yield spatial and temporal distributions of microbial concentrations. One of the difficulties lies in proper quantification and formulation of pollutant source fluxes and uncertainties associated with bacterial loading terms, especially those of nonpoint sources (Sanders et al., 2005). In addition, although some of previous modeling efforts admitted the importance of sediment as a bacterial reservoir and source loading (e.g., Sanders et al., 2005; Zhu et al., 2011), few have resolved

separately for wave propagation, sediment transport, morphological variation, and concomitant bacterial release.

1.2 Dissertation Overview

The primary goal of the dissertation is to assess microbial water quality at recreational beaches, particularly nonpoint source beaches, through a combination of field observations, data analyses, and numerical models. Specifically, this dissertation explores innovative modeling techniques and highlights physical and biological interactions in controlling nearshore beach water quality. Ultimately, the new model tools and knowledge can be applied in beach management practice, water quality evaluation, and decision support to achieve better human health protection at recreational beaches across the United States.

In Chapter 2, a coupled microbe-hydrodynamic-morphological model is developed to simulate the release of sediment-bound enterococci as a result of wave and tidal forcing. This model couples an existing nearshore process model (XBeach) with microbe transport-decay equation, which includes source functions that account for microbial release from mobilized sand, groundwater flow, entrainment through pore water diffusion, rainfall-runoff loading, and a fate function that accounts for solar inactivation effects. The model shows skills in simulating observed spatiotemporal patterns of enterococci levels at a case study beach (in Miami, FL) through an intensive 10-day field experiment. Chapter 2 was published in 2013 and is reprinted with permission from the journal, *Water Resources Research*.

In Chapter 3, a new numerical mass balance model for transient distributions of enterococci in beach water is developed for nonpoint source beaches where sand and

runoff are primary sources. The main difference between the balance model of this chapter and the coupled process model of the previous chapter is that the balance model takes an empirical approach to directly parameterize bacterial loading with wave and tidal conditions, which saves considerable time and computational resources. The performance of the balance model is further evaluated by comparing predicted exceedances of a beach advisory threshold to field data, and to a traditional multivariable linear regression model.

Chapter 4 expands the scope of this dissertation from one case study beach to 262 recreational beaches throughout the State of Florida. Historical water quality records of weekly monitored enterococci and fecal coliform from 2000 to 2009 are analyzed along with relevant environmental factors including beach slope, wave, sea surface temperature, solar radiation, and precipitation. Interesting water quality patterns emerge in seasonal FIB variations and in comparisons of high- versus low-wave-energy beaches and Atlantic versus Gulf of Mexico beaches. This study not only provides a big picture evaluation of microbial water quality in Florida, but also reveals the dominant hydrologic, hydrometeorologic, and geomorphic factors that affect spatiotemporal patterns of FIB.

Chapter 5 summarizes this dissertation and draws overall conclusions of important findings from previous three chapters. Recommendations on future microbial water quality modeling research will also be presented.

Chapter 2 MODELING SEDIMENT-RELATED ENTEROCOCCI LOADING, TRANSPORT, AND INACTIVATION AT AN EMBAYED NONPOINT SOURCE BEACH

2.1 Introductory Remarks

The utilization of coastal waters and shorelines at beach sites as recreation and tourism resources requires regular monitoring of water quality to protect human health. When levels of fecal indicator bacteria (FIB) exceed regulatory thresholds, set at 104 Colony Forming Units (CFU) per 100 mL for enterococci in a single water sample, beach advisories or even closures may be issued by local beach managers (US EPA, 1986). Traditional culture-based methods need at least 18 to 24 hours for laboratory analysis so that exceedance of FIB cannot be identified until the second day, resulting in delays in issuing beach advisories. Model approaches, on the other hand, can be timely, effective, and powerful tools in beach management to supplement existing beach monitoring programs.

Traditionally, regression models have been used to predict FIB levels based on local hydrodynamic and hydrometeorological conditions (e.g., Olyphant, 2005; Nevers and Whitman, 2005; Frick et al., 2008). Another type of model is the conceptual /analytical model, which largely simplifies physical and biological processes in order to achieve analytical solutions for particular beach systems. Two good examples are conceptual surf zone model (Boehm et al., 2005; Grant et al., 2005) and enclosed beach boundary layer model (Grant and Sanders, 2010). More recently, process-based models have been applied to hindcast microbial concentrations in aquatic environments, in order to evaluate influences of various pollutant sources and environmental conditions on beach water quality and to determine the subsequent transport and fate of bacteria of

interest (e.g., Sanders et al., 2005; Hipsey et al., 2008; Zhu et al., 2011; Ge et al., 2012a). Those models resolve detailed hydrodynamics, coupled with a microbial balance and appropriate biotic and non-biotic processes representing source loading, transport and fate and can include sediment resuspension effects (Sanders et al., 2005; Hipsey et al., 2008; Ge et al., 2012a).

Beach sediment has been recognized as an important non-point microbial source (e.g., Whitman and Nevers, 2003; Shibata et al., 2004; Yamahara et al., 2007; Halliday and Gast, 2011; Shah et al., 2011). Bacteria can live and persist within the sand and even replicate under favorable conditions (Yamahara et al., 2009). Previous environmental studies suggested that tidal washing of intertidal sand may be responsible for the observed high microbial levels after high tide (Shibata et al., 2004; Wright et al., 2011; Abdelzaher et al., 2011). However, the mechanisms responsible for the bacterial release from bed sediment to the water column are unclear, impeding quantification of the bacterial fluxes across the sediment-water interface.

Past process-model studies accounted heuristically for the release of microorganisms during sediment resuspension through a critical bed shear stress (Sanders et al., 2005; Ge et al., 2012) or an organism concentration balance in the sediment (Hipsey et al., 2008), but all ignored the sediment transport processes. At beach sites, ignoring wave-related bacterial source contributions from the mobilized sediment may lead to model underestimation of microbial levels. This study aims to develop a uniquely coupled microbe-hydrodynamic-morphological model with source and fate functions capable of simulating the transport of microbes from coastal beach sands. The source functions include the transfer of microbes: attached to mobilized sand grains, between the

water column and sand pore water (i.e. entrainment), from groundwater exchange, and from rainfall runoff overland flow. The fate term accounted for the die-off of microbes due to solar radiation. Model performance was evaluated using temporally intense measurements of enterococci levels at a recreational beach. The significance of various transport, forcing, and source/fate functions was evaluated through scenarios that individually removed processes from the model. Model outputs were further examined through local sensitivity analysis by individually varying key parameters by ±50% of optimized or literature values.

2.2 Materials and Methods

2.2.1 Site Description

The study site, Hobie Beach, is a subtropical marine beach on Virginia Key to the southeast of the city of Miami, Florida, United States of America (Figure 2.1). The beach is about 1,600 m long, straight and oriented in a northwest-southeast direction. It is located within a coastal embayment, Biscayne Bay, and sheltered from waves from the Atlantic Ocean due to the layout of two barrier islands, Virginia Key and Key Biscayne. Locally-generated wind waves within the bay may have impacts on the beach, but are moderate to small because of the limited fetch and shallow water depth (most areas are less than 4.0 m). In addition, nearby waters are heavily used for recreational boating, especially during weekends and holidays, and thus the beach may also be influenced by boat-generated waves. The tide is dominated by the principal lunar semidiurnal (M2) constituent with an approximate tidal range of 0.6 m. Although tidal currents in the adjacent Bear Cut inlet channel are fairly strong (up to 1.0 m/s) (Fiechter, et al., 2006), their magnitudes decrease significantly near the beach (Zhu et al., 2011). No known point

source is found to have a direct impact on the beach (Shibata et al., 2004). Local water circulation, demonstrated by Lagrangian coherent structures, may favor the retention of pollutants originating from the shoreline (Fiorentino et al., 2012). The beach sediments are mainly composed of medium sand with an average medium grain diameter of 0.39 ± 0.05 mm (Phillips et al., 2011b).

2.2.2 Field Measurements

2.2.2.1 Topographic Survey

The beach topography (Figure 2.1) was obtained from a walking survey in June 2010, using a GPS backpack unit (Trimble TSC1, Sunnyvale, CA, USA).

2.2.2.2 Water and Sediment Sampling and Analysis

From 1 to 11 June 2010, water and sediment samples were collected hourly at knee-depth (~0.3 m deep) locations. Every six hours, the seawater was also sampled at waist-depth (~1.0 m deep) locations and subtidal, intertidal, and supratidal sand samples were also collected at that time. Concentrations of culturable enterococci in the water and sediment were measured by a membrane filtration method, expressed for water as CFU/100 mL and for sand as CFU/g of the dry sand. Turbidity of water samples was also measured in the laboratory using a nephelometer (TD-40, Turner Designs, Sunnyvale, CA, USA) with units expressed as nephelometric turbidity units (NTU). For details of field sampling and laboratory analysis refer to Enns et al. (2012).

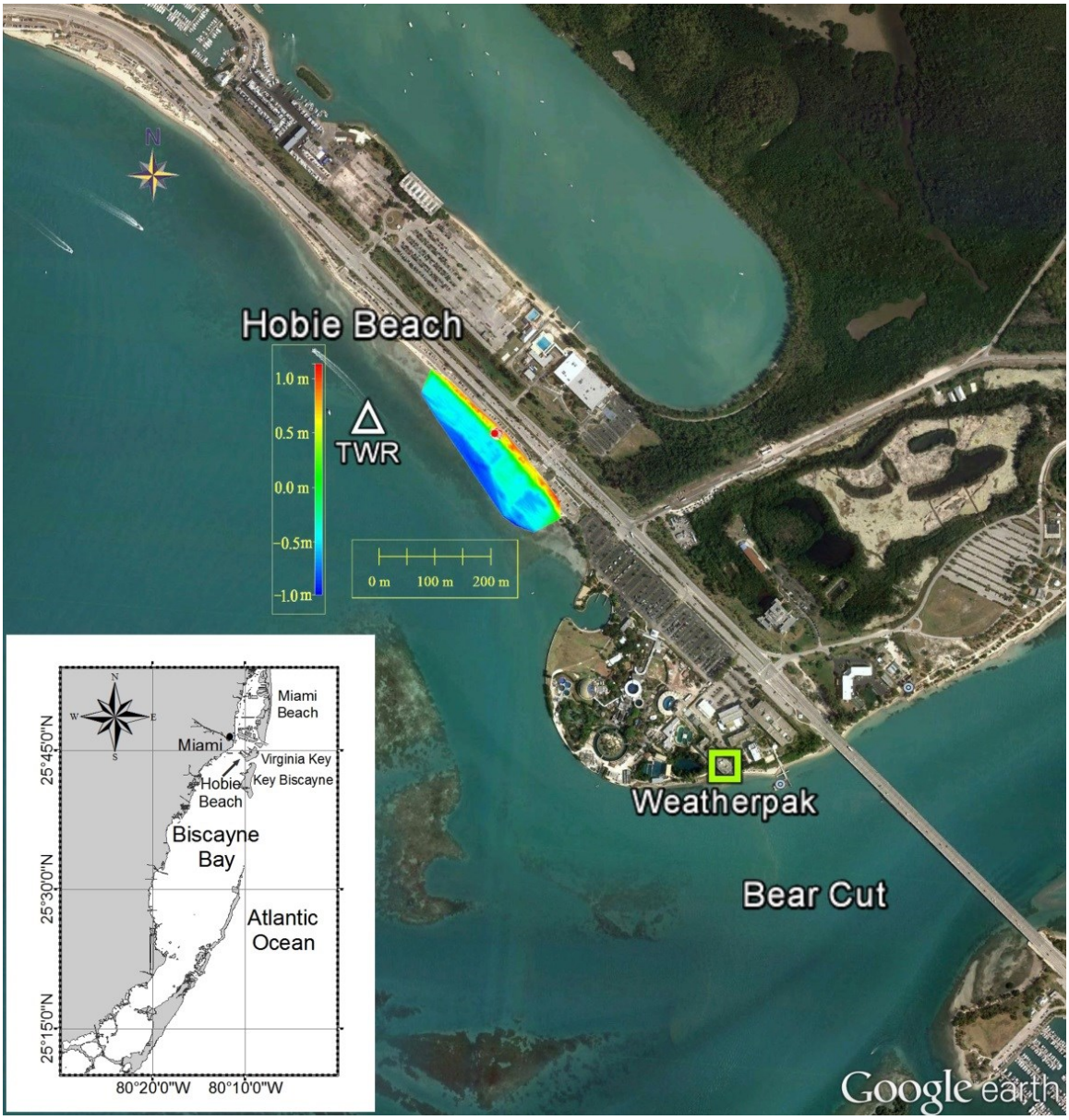

Figure 2.1 Geographical location and Google Earth aerial photo of Hobie Beach. Surveyed topography is illustrated by a color contour and color bar shows depth from -1.0 to 1.0 m with respect to mean sea level (MSL). The position of tide and wave recorder (TWR) is indicated by the white triangle. Water and sand were sampled along a transect oriented normally to the beach offshore of the pole location (red dot). The hydrometeorological measurements are obtained from the Weatherpak station (green square).

2.2.3 Environmental Conditions

A tide and wave recorder (RBR TWR-2050, Ottawa, ON, Canada) was bottom-mounted to measure waves and tides at a mean depth of 2.35 m, approximately 190 m offshore of the sampling site (Figure 2.1). Water elevations were sampled every 32 s to obtain the tidal conditions. Wave conditions were also measured every 20 min with a burst mode that recorded 4 Hz surface elevations for a total of 512 samples. The elevations were processed with the WAFO (Wave Analysis for Fatigue and Oceanography) Matlab toolbox (Brodtkorb et al., 2000) to obtain significant wave heights and peak wave periods from the variance density spectra. Hydrometeorological parameters, such as wind speed and direction, solar insolation and rainfall rate, were measured every 2 min at a research weather station (Weatherpak, Seattle, WA, USA) on the roof of a building at the University of Miami Rosenstiel School campus (Figure 2.1), which is about 1 km southeast of the beach site (http://yyy.rsmas.miami.edu/etc/download-weatherpak.cgi). Note that solar insolation was measured using an Eppley Precision Spectral Pyranometer (PSP) that directly senses whole sunlight spectrum.

2.2.4 Coupled Microbe-Hydrodynamic-Morphological Model

2.2.4.1 Model Concept

In simulating nearshore beach water quality, the variations of microbial levels are controlled by the processes that relate to loading, transport, and fate of microbes (Figure 2.2). Note that in terms of a certain beach, not all loads and processes are important; in other words, controlling mechanisms are site-specific. As for Hobie Beach, beach sand in the intertidal zone is known to be a major reservoir of bacteria (Wright et al., 2011; Shah

et al., 2011); thus the priority of the model is to include bacterial loading from the sand, which further requires resolving current and wave dynamics and related sediment transport. Additional processes considered include groundwater flow since a portion of microbes is found to reside in the pore water (Phillips et al., 2011b), rainfall runoff since very high levels of microbes have been observed in the runoff (Wright et al., 2011), and solar radiation as local observations have shown a strong influence on FIB levels (Abdelzaher et al., 2010; Enns et al., 2012).

Processes and sources not considered include: (1) exchange of microbes across the air-sea interface, although airborne transport may be occasionally influential (e.g., in the case of airborne transport of harmful algal toxins (Pierce et al., 2003)), (2) animal fecal events although studies have shown that dog fecal events, may intermittently affect water quality (Wright et al., 2009; Zhu et al., 2011), and (3) human shedding (Elmir et al., 2007; Enns et al., 2012), which has been demonstrated to impact the bacterial quality of water especially for bacteria of skin origin (Plano et al., 2011).

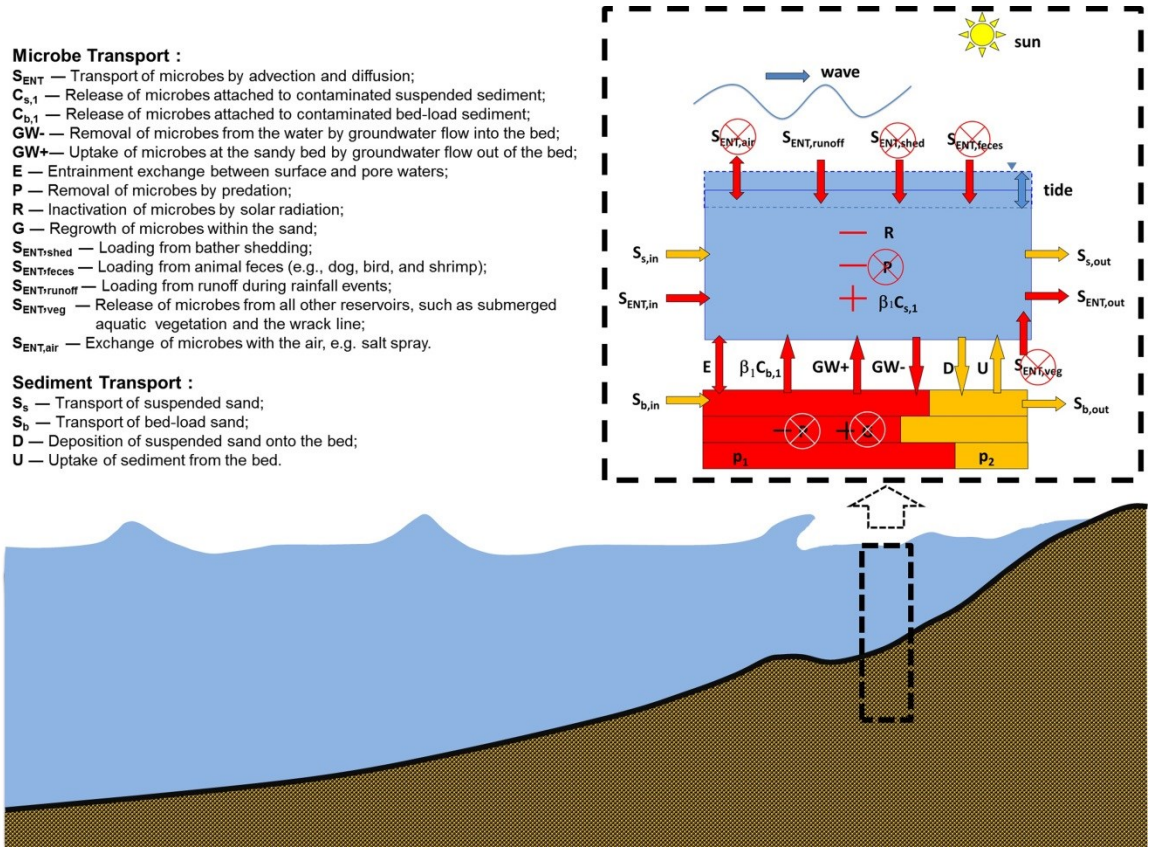

Figure 2.2 Cross-shore section of a beach and a control volume corresponding to one model cell (box of dark dashed line), which is exaggerated to illustrate detailed model components. Within the box, surface water column is shown with light blue, affected by both waves and tides. Contaminated and clean sands are shown with red and yellow colors, the factions (*p1* and *p2*) of which can vary with depth. Yellow arrows indicate processes related to the sediment transport, while red arrows indicate processes related to microbe transport. The microbial processes and loads not taken into account in the model are crossed out.

2.2.4.2 Coupling Microbe Module into XBeach

XBeach is an open source modeling tool in the nearshore community, which has been widely used to simulate a variety of small-scale hydrodynamic and morphological phenomenon, such as barrier island and dune erosion due to tropical storms (Roelvink et al., 2009; McCall et al., 2010), megacusp formation in a rip-channeled beach (Orzech et al., 2011), wave-driven circulations on coral reefs (Symonds et al., 2011), evolution of a gravel beach profile (Williams et al., 2012), and sediment transport in the swash zone (van Rooijen, 2011; Reniers et al., 2012). XBeach solves coupled two-dimensional depth-averaged equations for wave propagation (i.e., wave action balance equation for evolution and roller energy balance equation for breaking), water circulation (i.e., shallow water equations), groundwater, sediment transport, and bottom changes on the time scale of wave groups (Roelvink et al., 2009).

In this study, we coupled a microbe transport-decay equation with XBeach to link microbial water quality with hydrodynamic and sediment transport processes. The interrelationships between primary model components are shown in Figure 2.3. The microbe module solves the depth-averaged microbial balance within the water column, which accounts for non-point source loads, i.e., sediment attached, pore water trapped, and rainwater-runoff microbe loading. The pore water component includes inputs through groundwater advection and diffusion-like entrainment. Solar inactivation was the only fate term incorporated into the model.

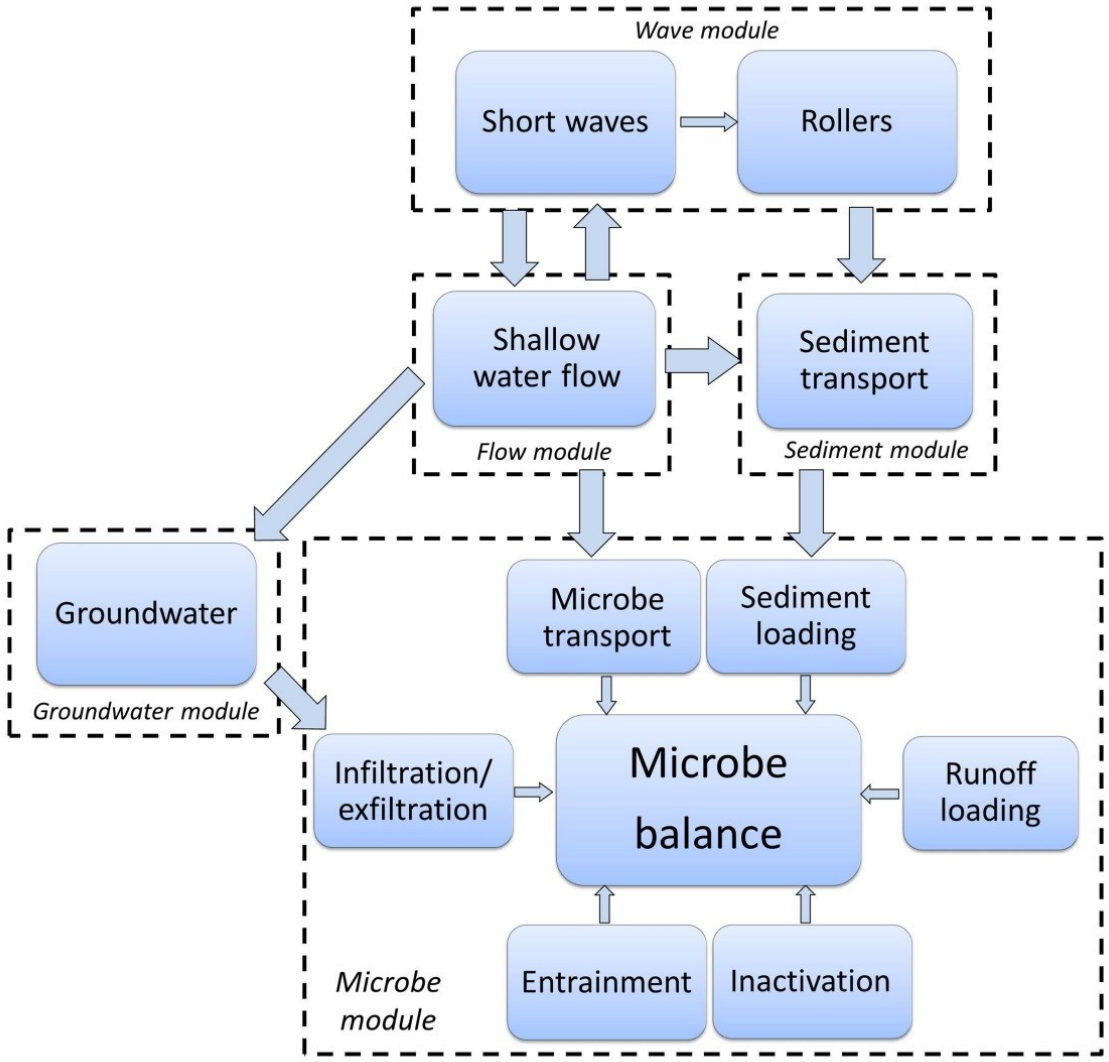

Figure 2.3 A flow diagram for wave, flow, sediment, groundwater and microbe computations and linkages between primary model components.

2.2.4.3 Microbe Transport-Decay Equation

The transport, source loading, and die-off of microbes (i.e., enterococci in this paper) in Figure 2.2 can be expressed by a depth-averaged microbe transport-decay equation:

$$\frac{\partial \mathrm{hENT}}{\partial \mathrm{t}} + \frac{\partial \mathrm{hENTu^L}}{\partial \mathrm{x}} + \frac{\partial \mathrm{hENTv^L}}{\partial \mathrm{y}} - \frac{\partial}{\partial \mathrm{x}}\left[\mathrm{D_m h}\frac{\partial \mathrm{ENT}}{\partial \mathrm{x}}\right] - \frac{\partial}{\partial \mathrm{y}}\left[\mathrm{D_m h}\frac{\partial \mathrm{ENT}}{\partial \mathrm{y}}\right] =$$

$$\beta_1 \mathrm{h}\left[\mathrm{C_{s,1}} + \mathrm{C_{b,1}}\right] - \beta_2 \mathrm{p_1 w_{bed}}\delta\left(\frac{\mathrm{w_{bed}}}{|\mathrm{w_{bed}}|} + 1\right) - \mathrm{ENT\ w_{bed}}\,\delta\left(\frac{\mathrm{w_{bed}}}{|\mathrm{w_{bed}}|} - 1\right) + \beta_3(\beta_2 \mathrm{p_1} -$$

$$\mathrm{ENT}) + \beta_4 \mathrm{I_r} - \beta_5 \mathrm{h I_s ENT} \qquad (1)$$

where h is water depth (in m), ENT is a depth-averaged concentration of culturable enterococci (in CFU/m^3), u^L and v^L are Lagrangian velocities (in m/s; see Roelvink et al., 2009 for details), and D_m is the microbe diffusion coefficient (in m^2/s). In XBeach, the low-frequency and mean flows (i.e. u^L and v^L) are directly solved from shallow water equation using a depth-averaged Generalized Lagrangian Mean (GLM) formulation (Roelvink et al., 2009). Assuming isotropic and homogeneous diffusion, the diffusion coefficient is set a constant 0.03 m^2/s. The waist-depth samples are used to find the physically appropriate value of D_m showing that by including diffusive transport the predictions are of the same order as the observations. The lumped coefficient D_m represents the combined effects of turbulent diffusion and tidal dispersion. The terms on the right hand side (RHS) of equation (1) represent source loading or die-off rates, which are explained one by one in the following subsections. Note that all β coefficients are fixed and therefore are independent of space and time.

2.2.4.3.1 Model Treatment of Sand Contaminated with Microbes

We utilize the multiple sediment class formulation in XBeach to assign contamination and distribution of microbes in the sand by artificially dividing sediment into two classes, which allows for the tracking of each sediment class during computations. Two distinct classes are assigned, contaminated sand (class-1) and clean sand (class-2) and their corresponding fractions were denoted by p_1 and p_2 (= 1 - p_1) (Figure 2.2). Two classes are then calculated separately with sediment transport formulations (see Appendix-A for details). If there is no contaminated sand, p_1 equals zero and consequently there are no microbes within the sand. In effect, the distribution of p_1 describes the availability of microbes in the sand ready for mobilization by the bed shear stress, groundwater flow, and entrainment. The model input values of p_1 are fitted to field data, which are described in subsection 2.2.4.4.1.

2.2.4.3.2 Enterococci Released from Mobilized Sand

The model assumes that once the sand is mobilized, a portion of enterococci attached to the grains is directly desorbed and enters the water column. The mobilized suspended and bed-load sediment are in a dynamic equilibrium, i.e. there is continuous exchange of sediment between the bed and the fluid layer while maintaining the sediment concentration, bringing up new sediment with enterococci from the bed reservoir, thus acting as a conveyer belt for the enterococci uptake. Through a dimensional calibration factor β_1 (in CFU/m^3/s), the release flux of enterococci from sand is linked to the total instantaneous concentration of mobilized contaminated sand, a combination of suspended load ($C_{s,1}$ is suspended volumetric concentration of contaminated suspended sediment in L/L) and bed load ($C_{b,1}$ is volumetric concentration of contaminated bed-load sediment).

However, there is no existing research/literature that provides guidance in choosing the value of β_1 to date. Thus, the model calculations used a calibrated β_1 value of 8.0×10^7 CFU/m^3/s, obtained by fitting and optimizing simulated and observed enterococci levels. Developing robust β_1 values in the laboratory based on controlled wave conditions and microbial sources in the sand is a subject of future research.

2.2.4.3.3 Groundwater Transport

Groundwater exfiltration (from the ground into the open water column) or infiltration (from the open water column into the ground) is the bidirectional advective exchange of materials across sediment-water interface, similar to the hyporheic exchange between stream and streambed (Grant et al., 2011). β_2 is a dimensional calibration coefficient (in CFU/m^3) representing a maximum enterococci concentration of bed pore water for the transport across the bottom boundary. The vertical groundwater flow rate, w_{bed}, is defined positive downward and negative upward (see Appendix-B). The Kronecker delta function is used to determine the direction of w_{bed}. If w_{bed} <0 (i.e., exfiltration), an enterococci flux associated with pore water joins surface water; otherwise, if w_{bed} >0 (i.e., infiltration), an enterococci flux of surface water goes into the bed.

To relate the standard unit, CFU/g of the dry sand, to CFU/m^3 of the bulk sediment volume (including sand grains and pore spaces), we used the following relation (Grant et al., 2011):

$$\mathrm{ENT}_{\mathrm{CFU/m^3}} = \left(1000\rho_s \mathrm{ENT}_{\mathrm{CFU/g}}\right)\left(1 - n_p\right) \quad (2)$$

where the sand grain density ρ_s is set to a standard value of 2.65×10^3 kg/m^3 (Soulsby, 1997) and porosity n_p (= 0.4) is locally measured (Phillips et al., 2011b). This yields a

level of ENT_{max} = 1.6×10^{8} CFU/m^3 at the shoreline. Previous sand core experiments using local sand determined an average of 10% of total enterococci reside in the pore water, from which we may estimate β_2 of 1.6×10^{7} CFU/m^3, ($\beta_2 = 0.1 \times 1.6 \times 10^8 \mathrm{CFU/m^3} = 1.6 \times 10^7 \mathrm{CFU/m^3}$) (Phillips et al., 2011b). Notice that $\beta_2 p_1$ represents spatial dependent enterococci concentration in the pore water. If p_1 equals 1 then the water that flushes from the bed into the surface water has a maximum concentration of β_2. This also implies that the release rate of enterococci does not increase with increasing groundwater flow velocity, consistent with the microbe release from the laboratory experiments (Phillips et al., 2011b).

The groundwater flow velocity is calculated according to Darcy's law (see Appendix-B) and this module has been tested by another study (Williams et al., 2012). Measured hydraulic conductivity may vary by two orders of magnitude, from 4.0×10^{-5} to 4.0×10^{-3} m/s (Phillips et al., 2011b). For model calculations, we applied a value of 2.9×10^{-4} m/s, least-square fitted from 16 sets of measured head difference and volumetric rate relationships in Phillips et al. (2011b).

2.2.4.3.4 Entrainment Exchange Across Sediment-Water Interface

The entrainment exchange is diffusional transfer between water column and underlying pore water across the bottom boundary layer, most likely due to coherent turbulence in this case (Grant and Marusic, 2011). Molecular microbial diffusion is unimportant based on the small diffusion coefficient for fecal bacteria, in the order of 10^{-13} m^2/s (van der Mei et al., 1994). The flux of entrainment exchange is assumed proportional to the difference in concentrations across the interface according to Grant and Marusic (2011). The entrainment coefficient ($\beta_3 = 1.0 \times 10^{-5}\mathrm{m/s}$) was given

according to the mass transfer coefficient for the sand bed from experiments and also derived from a diffusive sub-layer model (Reidenbach et al., 2010).

2.2.4.3.5 Rainfall-Runoff Loading

To quantify the rainfall runoff loading rate, the measured rainfall intensity I_r (in m/s) was utilized and filtered with an hourly moving average window. β_4 is a lumped coefficient (in CFU/m^3) for the enterococci flux associated with rainfall runoff and determined from the rational formula, which relates the runoff flux to rainfall rate and land usage, population density and degree of imperviousness (Lindeburg, 1986). Therefore, total enterococci flux (Q_r) flushed into the beach water via overland flow is:

$$Q_r = \sum_i \left(D_i A_{d,i}\right) ENT_r I_r == \sum_i \left(D_i W_{d,i} L_{d,i}\right) ENT_r I_r \quad (3)$$

where D_i, $A_{d,i}$, $W_{d,i,}$ and $L_{d,i}$ are the drainage coefficients, areas, widths and lengths of various ground types i = 1, 2, …). At Hobie Beach, there are two distinct drainage types: paved asphalt road and sandy beach (see Figure 2.1), the drainage coefficients of which are 0.9 and 0.6, respectively (Elmir, 2006). The width of paved road is 6 m while beach width depends on tidal elevations with an average of 20 m. ENT_r is the enterococci concentration in the runoff that varies by two to three orders of magnitude based on prior field experiments and we gave an average of 1.5×10^8 CFU/m^3 in this study (Wright et al., 2011).

In reality, runoff drains through spaced runnels on the beach, which eventually results in non-uniform runoff influx alongshore the beach. Therefore, instead of assigning an unrealistic point source to the 1D model, we created a line source for runoff loading by assuming that when runoff water joins beach water, associated microbes immediately

distribute along an X_r (= 10 m, width of intertidal zone) wide wedge of water extended from shoreline. Hence,

$$\beta_4 I_r = \frac{\sum_i (D_i W_{d,i} L_r) ENT_r}{A_r} I_r = \frac{\sum_i (D_i W_{d,i}) ENT_r}{X_r} I_r \quad (4)$$

where A_r, X_r, and L_r are the surface area, cross-shore and alongshore lengths of the receiving water body ($A_r = X_r \times L_r$) assuming two land types have the same alongshore length as receiving water body. Finally, the lumped coefficient is:

$$\beta_4 = 2.6 \times 10^8 CFU/m^3 \quad (5)$$

2.2.4.3.6 Solar Inactivation

The solar inactivation follows the widely used first-order exponential decay (e.g., Sinton et al., 2002; Sanders et al., 2005; Zhu et al., 2011). The sunlight inactivation coefficient ($\beta_5 = 3.68 \times 10^{-7}$ m^2/J) was determined from an in situ experiment at this beach and was used in a previous study (Zhu et al., 2011). Recorded solar radiation intensity I_s (in W/m^2) was filtered with a one-hour moving average window before input to the model.

2.2.4.4 Model Implementation

In this study, calculations were performed in a mode that neglected bathymetric evolution based on the fact that profile change is very little for this low-energy beach in a relatively short 10-day period. We also assumed steady state concentrations of microbes within the bed. This implies that any microbe lost from the sand and interstitial water is (continuously) compensated by concomitant regrowth in the bed. It is a reasonable approximation if the released amount of microbes is relatively small, with respect to the whole bed reservoir. The other reason for this assumption is that regrowth, competition, and predation of microbes in the sand are very complex microbiological processes,

dependent on a number of environmental conditions (e.g., moisture content, salinity, temperature, and nutrients) and sand characteristics (e.g., minerals, grain size, and biofilms) as well as microbial communities (Yamahara et al., 2007; Yamahara et al., 2009; Piggot et al., 2012). Therefore, the formulations of those processes need further study and are not investigated in this paper. We will only briefly discuss the steady state bed reservoir assumption in subsection 4.2.

2.2.4.4.1 Cross-shore Distribution of Sand Enterococci Source

The enterococci levels within the sand during the experiment exhibited significant spatial and temporal variability. At the upper beach face (permanently dry), the observed levels of enterococci in the sand vary between 0.4 and 718 CFU/g with an observed mean of approximately 100 CFU/g. This also holds for the sand sampled at knee-depth locations, varying by three orders of magnitude, (Figure 2.4-A). This variation can arise from the fact that the microbes attached to the sand are patchy and spatially and temporally inhomogeneous. As a consequence, the (initial) fractional distribution of contaminated sand that corresponds to enterococci levels within the sand, a prerequisite for model initialization, was unknown.

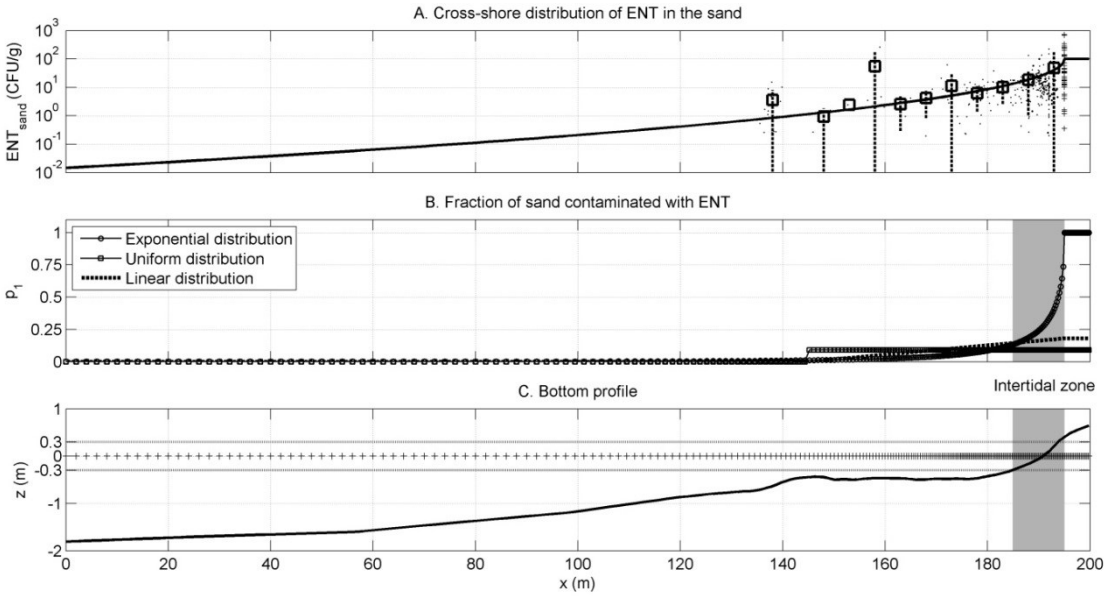

Figure 2.4 Model setup. (A) Observed cross-shore distributions of enterococci concentrations 8within the sand (dots), spatially-averaged (at 5 m intervals) arithmetic mean values (squares) and corresponding standard deviations (dashed vertical lines). Observed dry beach samples are marked by crosses. Exponential fit curve as initial cross-shore distribution of enterococci is shown by the solid line. (B) Fractional distribution of sand contaminated with enterococci for three cases: exponential (corresponding to above exponential fit), uniform and linear (used later in the scenario tests of Section 3.3.7). The shadows indicate intertidal zone in the model domain between 185 m and 195 m. (C) Bottom profile (solid line) and a tidal elevation envelope of ±0.3 m (light dotted lines) around mean sea level (cross markers shown at grid points).

Using the arithmetic mean enterococci concentrations (i.e. averaged over time and space), a simple exponential fit was used to describe the initial cross-shore distribution, referred to as an exponential distribution (Figure 2.4-A):

$$\mathrm{ENT_{sand}(x)} = \begin{cases} \mathrm{CFU_{max}} \exp\left[-\left(\frac{195-\mathrm{x}}{2.5}\right)^{0.5}\right], & \mathrm{x} < 195\mathrm{m} \\ \mathrm{CFU_{max}}, & \mathrm{x} \geq 195\mathrm{m} \end{cases} \quad (6)$$

And corresponding distribution of fraction of contaminated sand is (Figure 2.4-B):

$$\mathrm{p_1(x)} = \begin{cases} \exp\left[-\left(\frac{195-\mathrm{x}}{2.5}\right)^{0.5}\right], & \mathrm{x} < 195\mathrm{m} \\ 1, & \mathrm{x} \geq 195\mathrm{m} \end{cases} \quad (7)$$

where x = 195 m corresponds to the higher high tide line where dry beach sand was sampled and CFU_{max} = 100 CFU/g is the maximum enterococci level of the sand prescribed in the model. The resultant fraction of contaminated sand decreases rapidly offshore (Figure 2.4-B), which also agrees with a prior field experiment (Wright et al., 2011). It reduces to below 15% beyond the low tide line and becomes almost negligible in the areas between 0 and 140 m. This also implies there are no distant sand enterococci sources for the purposes of this model.

2.2.4.4.2 Model Setup

Model simulations were performed for a single cross-shore transect (i.e., one-dimensional computations); in other words, we neglected all alongshore variations in the y-direction. The bottom profile was alongshore averaged using the surveyed bathymetric data at the microbe sampling site (Figure 2.1). This shows the presence of a small sand bar, around x = 145 m (Figure 2.4-C). Offshore of the sand bar, the subtidal terrace illustrates a mild slope of 1:120, while a flat terrace of about 40 m width is located onshore of the bar. The upper beach face is much steeper (a slope of 1:20), leading up to

a dry berm of approximately 0.8 m above Mean Sea Level (MSL). The model grid spacing is variable with a 2 m coarser resolution offshore ($x < 90$ m), gradually decreasing to 0.25 m near the low tide line and a 0.25 m resolution in the intertidal and supratidal areas ($x > 175$ m) (Figure 2.4-C). The time step for the model calculation is determined by the Courant stability criterion and is calculated automatically based on a Courant number of 0.9. In this study, the model applies the same time step for all modules that involve updating in time. The model uses a cold start as initial conditions of water depth, current velocity, and enterococci level of the water. Given the fact that the model domain is small (i.e. 200 m) and response time scales are short, the spin-up time is only minutes for hydrodynamics and in the order of one hour for enterococci levels.

The offshore boundary was located along a shore-parallel line at a distance where the tide and wave recorder was deployed. At this boundary, an absorbing-generating or weakly-reflective boundary condition was used to prevent re-reflection of long waves generated in the surf and swash zones, in combination with prescribed tidal elevations recorded by the sensor (Figure 2.5-A). Normally incident waves were specified with a parametric JONSWAP (Joint North Sea Wave Project) spectra entering into the computational domain, defined by the measured significant wave heights (H_{m0}) and peak frequencies (T_p) (Figure 2.5-B and -C). The wave propagation and breaking were then calculated based on wave and roller energy balance equations (see Roelvink et al., 2009 for details on the model description).

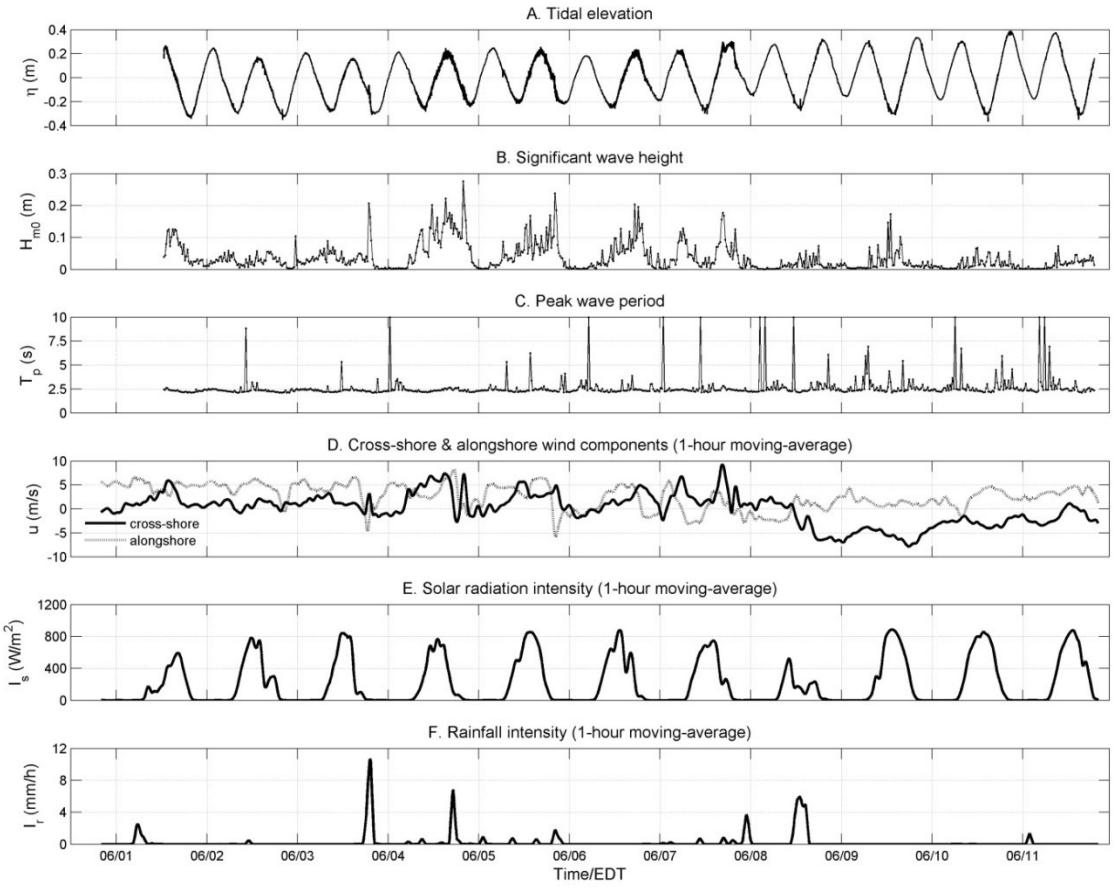

Figure 2.5 Time series measurements of environmental conditions during the 10-day intensive study at Hobie Beach. (A) Surface elevations measured by the tide and wave recorder (see Figure 1 for equipment location). (B) Corresponding significant wave heights measured by the recorder. (C) Peak wave periods. (D) Hourly moving-averaged cross-shore (dark line) and alongshore (light-colored line) wind speeds. (E) Hourly moving-averaged solar insolation. (F) Hourly moving-averaged rainfall intensities.

Table 2.1 List of model parameter settings

Module	*Parameter*	*Description*	*Value*
Flow	*nuh*	Background horizontal eddy viscosity	0.03 m^2s^{-1}
	C	Chezy bottom roughness coefficient	65.0 $m^{1/2}s^{-1}$
	CFL	Courant number	0.9
Wave	*gamma*	Breaker parameter in dissipation model	0.45
	alpha	Dissipation parameter	1.0
	beta	Slope of breaking wave front in roller model	0.1
	n	Power in breaking probability function	10
	gammajsp	Peak enhancement factor in JONSWAP spectrum	3.3
	s	Directional spreading coefficient in JONSWAP spectrum	1000
	fnyq	Highest frequency to create JONSWAP spectrum	1.0 Hz
	dfj	Step size frequency to create JONSWAP spectrum	0.01 Hz
Sediment	D_h	Sediment diffusion coefficient	0.03 m^2s^{-1}
	f_{mor}	Morphological speed-up factor	0
	α_b	Bed slope factor	0
	ngd	Number of sediment classes	2
	nd	Number of sediment layers	2
	dzg	Thickness of sediment layers	0.25 m
	D50	Uniform D50 sediment diameter	0.0004 m
	D90	Uniform D90 sediment diameter	0.0005 m
Ground-water	k_x,k_y	Horizontal hydraulic conductivity	2.9×10^{-4} $m\cdot s^{-1}$
	k_z	Vertical hydraulic conductivity	2.9×10^{-4} $m\cdot s^{-1}$
	n_p	Porosity	0.4
	$d_{wetlayer}$	Thickness of wet layer	0.1 m
	$Z_{b,aquifer}$	Bed level of the aquifer	-5.0 m
Microbe	β_1	Sediment-related enterococci release coefficient	8.0×10^{7} $CFU\cdot m^{-3}s^{-1}$
	β_2	Pore water enterococci concentration coefficient	1.6×10^{7} $CFU\cdot m^{-3}$
	β_3	Entrainment mass transfer coefficient	1.0×10^{-5} $m\cdot s^{-1}$
	β_4	Rainfall-runoff loading coefficient	2.6×10^{8} $CFU\cdot m^{-3}$
	β_5	Sunlight inactivation coefficient	3.68×10^{-7} m^2J^{-1}
	D_m	Microbe diffusion coefficient	0.03 m^2s^{-1}
	CFU_{max}	Maximum reference enterococci concentration in the sand	100 $CFU\cdot g^{-1}$

For the groundwater calculation, since a barrier island beach with tidal influence tends to have an elevated water table above MSL, the initial groundwater head 0.1 m was given according to the water table overheight approximation deduced from the Boussinesq equation (Nielsen, 1990; Nielsen, 1999). All relevant model parameters and corresponding values were summarized in Table 2.1.

2.2.4.4.3 Model Skill

The skill of the model was evaluated by comparing $\log_{10}$-transformed model results with observations at both the knee-depth and waist-depth sampling locations in terms of the correlation coefficient and refined Willmort index of agreement.

Correlation coefficient:

$$r = \frac{COV(P, O)}{\sigma_P \sigma_O} \tag{8}$$

Refined Willmort index of agreement (Willmort, et al., 2011):

$$d_r = \begin{cases} 1 - \frac{\sum_{i=1}^{n} |P_i - O_i|}{2 \sum_{i=1}^{n} |O_i - \overline{O}|}, & \text{if } \sum_{i=1}^{n} |P_i - O_i| \leq 2 \sum_{i=1}^{n} |O_i - \overline{O}| \\ \frac{2 \sum_{i=1}^{n} |O_i - \overline{O}|}{\sum_{i=1}^{n} |P_i - O_i|} - 1, & \text{if } \sum_{i=1}^{n} |P_i - O_i| > 2 \sum_{i=1}^{n} |O_i - \overline{O}| \end{cases} \tag{9}$$

where COV and σ refer to covariance and standard deviation. P and O represent model-predicted and field-observed $\log_{10}$-transformed enterococci levels. Willmort index provides dimensionless measure of model-observation agreement, which is bounded between -1.0 (i.e., poor agreement) and 1.0 (i.e., perfect agreement).

2.3 Results

2.3.1 Environmental Observations

Tidal elevations were predominantly semidiurnal with a range of about 0.6 m (Figure 2.5-A). Significant wave heights were less than 0.3 m with a dominant peak period of around 2.5 s (Figure 2.5-B and -C). The onshore direction roughly aligned with the longest wind wave fetch and wave heights correlated well with onshore wind speeds (r = 0.71; Figure 2.5-D) This indicates that waves affecting Hobie Beach are locally wind-generated inside Biscayne Bay but wave height is limited by relatively short fetch and shallow depth of the bay environment (Young, 1997). Solar radiation intensity illustrated predominant diel cycles but could be occasionally suppressed in the daytime when the weather was overcast or rainy (Figure 2.5-E). During the 10-day period, rainfall events were short-lived and episodic, most of which were local convective thunderstorms (Figure 2.5-F).

2.3.2 Model Simulations

2.3.2.1 Hydrodynamic and Morphological Simulations

We modeled a period of 10-day, starting from 12:30 pm, 1 June, 2010 when the first wave measurement was recorded. The hydrodynamic model was driven by observed tides and waves at the offshore boundary. The root-mean-square (RMS) wave orbital velocities at the knee depth were quasilinear to wave heights, with magnitudes ranging from 0 to 0.25 m/s (Figure 2.6-A). Meanwhile, both the Lagrangian and Eulerian (cross-shore) velocities were one order of magnitude lower than wave orbital velocities, less than 0.05 m/s. The presence of waves increased Eulerian velocities, showing small peaks of return (offshore) flows. Such results agreed with other studies at this beach, suggesting

that cross-shore velocities in the nearshore shallow region were minimal (Zhu et al., 2011; Fiorentino et al., 2012). One important implication of the velocities was that wave orbital velocity dominated Eulerian velocity in terms of initiating incipient bed sediment motion and therefore sediment-bounded microbe release. This notion was also supported by modeled suspended sediment concentrations at the knee depth, which were correlated well RMS orbital velocities ($r = 0.87$).

Bed-load sediment concentrations followed the same trend as suspended load, but their magnitudes were always lower (Figure 2.6-B). Suspended and bed-load sediment concentrations at the waist depth also corresponded to incoming waves, but were at least one order of magnitude lower than those of the knee depth (Figure 2.6-D). This indicated that majority of sediment resuspension occurred in the nearshore shallow region. Correlations were found between simulated suspended sediment concentrations of both knee-depth ($r = 0.30$) and waist-depth ($r = 0.35$) water with respect to corresponding turbidity measurements (Figure 2.6-C to -E). Although turbidity, an indication of occurrence of sediment resuspension, corresponded to incident waves, we did not observe perfect correlations to suspended sediment concentrations, mainly because turbidity measurement is more sensitive to smaller particles (Hannouche et al., 2011). Suspended solids at the site were a combination of fine silt and medium sand, which confounded the correlation between turbidity and modeled sand sediment concentrations. Overall, the model was satisfactory in hindcasting hydrodynamics and sediment transport.

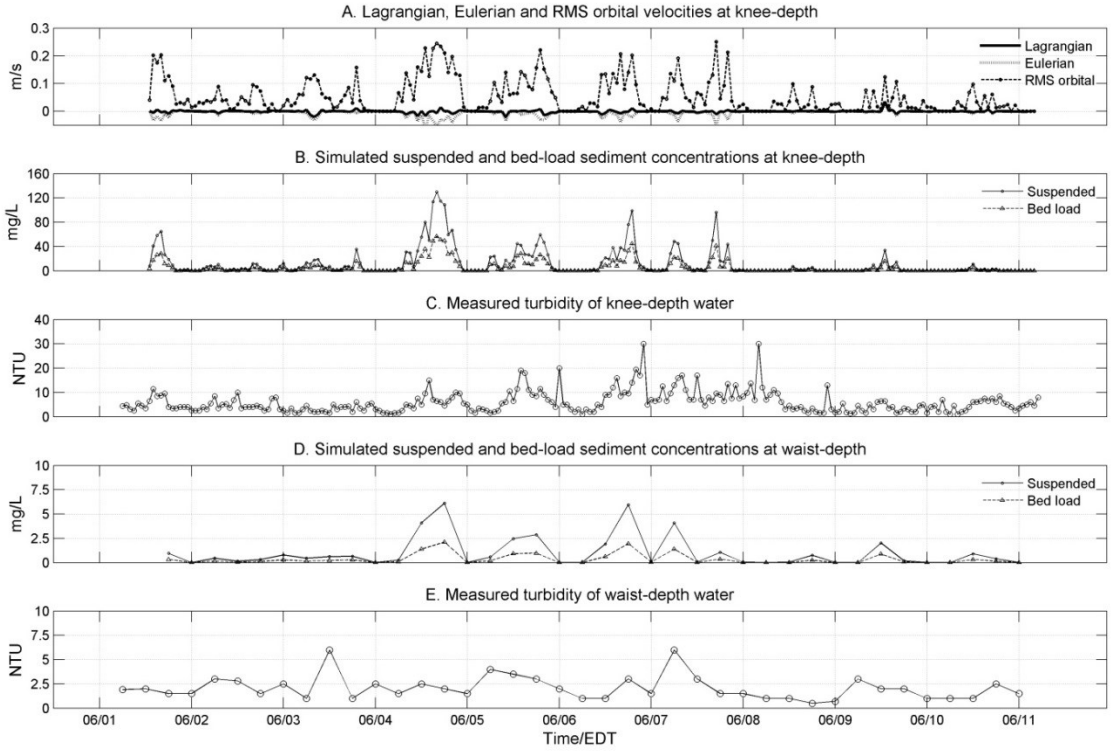

Figure 2.6 Model results of currents and sediment concentrations and turbidity measurements. (A) Modeled Lagrangian, Eulerian, and RMS wave orbital velocities (in m/s) at the knee depth. (B) Hourly moving-averaged suspended and bed-load sediment concentrations (in mg/L) at the knee depth. (C) Measured turbidity (in NTU) of hourly knee-depth water samples. (D) Hourly moving averaged suspended and bed-load sediment concentrations at the waist depth (only shown in the time spots corresponding to 6-hourly sampled waist-depth water). (E) Measured turbidity of 6-hourly waist-depth water samples.

2.3.2.2 Microbial Simulations

The model reproduced the spatial and temporal trends and patterns of enterococci variation in beach water for the 10-day period (Figure 2.7-A). Spatially, enterococci levels were always highest next to the waterline and then decreased rapidly in the offshore direction, by one to two orders of magnitude in a 100-m distance away from the shore. This pattern was coincident with two earlier field studies (Shibata et al., 2004; Wright et al., 2011). This could be explained by the facts that: (1) the most important microbe reservoir, beach sand, has a maximum microbial concentration above the shoreline in the dry sand, followed by gradually decreasing concentrations from the high to low tide line within the intertidal sand, while in the subtidal region, their concentrations become even lower to minimal; (2) two loading mechanisms, wave-induced resuspension and bottom boundary layer entrainment, occur predominantly in the narrow water wedge just below the high tide line, explained in more details in subsection 3.3; (3) during rainfall events, runoff that contains large amounts of microbes washed off from the upper beach face initially flows into the nearshore water through local ditches and afterward dilutes further offshore; (4) the cross-shore beach profile is gently sloping so that microbes are concentrated in the shallow shoreline region since the model is in 2-D depth-averaged mode.

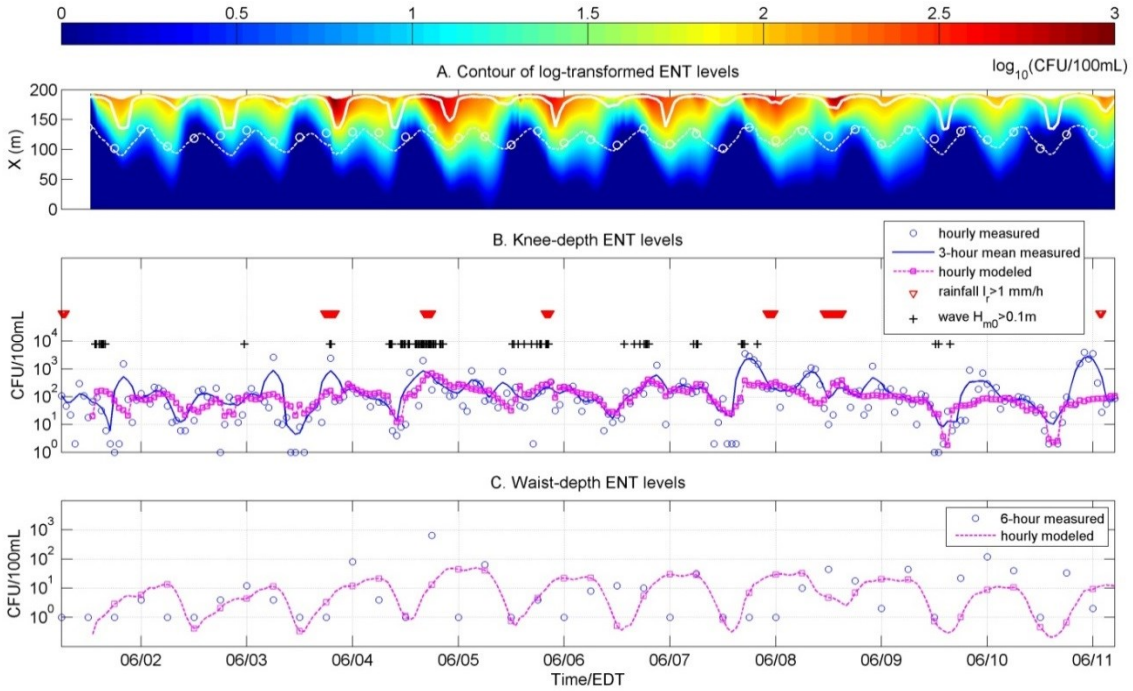

Figure 2.7 Model results of enterococci levels during the 10-day study. (A) Contour of $\log_{10}$-transformed enterococci levels (in CFU/100 mL), showing the cross-shore transect from beach shoreline to offshore boundary. Solid white line indicates corresponding knee-depth sampling locations in the model domain. Dashed white line indicates the 1-m isobath, approximating to the waist depth and white circles are exact waist-depth sampling locations in the model domain. (B) Comparisons of simulated and measured enterococci levels at knee-depth locations. The red triangles and black crosses illustrate rainfall events (rainfall rates larger than 1.0 mm/h) and wave events (offshore significant wave heights larger than 0.1 m), respectively. (C) Comparisons of simulated and measured enterococci levels at waist-depth locations. Note that magenta squares illustrate simulated enterococci levels at corresponding waist-depth water sampling times.

Temporally, $\log_{10}$-transformed enterococci levels demonstrated strong diel and tidal cycle signals (Figure 2.7-A). High levels predominantly occurred and persisted longer in the nighttime when solar radiation became minimal, allowing bacteria to remain viable and culturable. During the daytime, on the contrary, sunlight can effectively inactivate released enterococci. For the constant deactivation coefficient (β_5) given in Table 2.1, the time duration for a certain percent die-off is inversely proportional to the solar radiation intensity. It takes 2.2 hours to deactivate 90% of the total enterococci at noon time with a near maximum solar insolation of 800 W/m^2. Within one tidal cycle, the highest predicted enterococci concentration was typically found tens of minutes to several hours after high tide, which was consistent with the analysis using hourly measurements of enterococci levels at knee-depth locations (Enns et al., 2012). The highly elevated enterococci levels that occurred for five consecutive nights from 3 to 7 June also coincided with high tides, locally medium to high waves ($H_{m0} > 0.1$ m), and occasionally rainfall events ($I_r > 1$ mm/h). Those patterns apparently indicate that the concurrence of high tides particularly on the ebb phase, local wind waves, and/or rains at night can greatly elevate microbial levels, which may result in exceedances of indicator bacteria levels for several hours or even throughout the night.

Simulated enterococci levels were compared with field measurements at both knee- and waist-depth locations (Figure 2.7-B and -C). The arithmetic mean (and standard deviation) of $\log_{10}$-transformed hourly measurements at knee-depth, $\log_{10}$ (ENT_knee) = 1.87 (± 0.74), compared well with that of the model, 1.96 (± 0.41). The standard deviation calculated from the model results was lower than that from the measurements. As a result, model predictions were smoother and unable to capture most

transient spikes or extremely high levels (those of enterococci levels around or above 1,000 CFU/ 100 mL). To reduce the bias of those extreme values on statistical scores, we used the 3-hour moving averaged time series to calculate statistics for this case and later test cases (Table 2.2). The correlation (r = 0.612) and index of agreement (d_r = 0.595) at the knee-depth were fairly good, considering the fact that observations were so highly variable. The model also yielded the correct pattern that enterococci concentrations of the waist-depth samples were significantly lower than those of the knee-depth samples, since waist depths are farther away from the enterococci sources. At the waist depth, however, both correlation (r = 0.267) and index of agreement (d_r = 0.467) were not as good as those at the knee depth and no significant correlation was found ($p_{N=37}$ = 0.111).

Table 2.2 Summary of error statistics for each scenario test

Scenario	r		d_r	
	Knee	Waist	Knee	Waist
Baseline	0.612	0.267	0.595	0.467
No diffusion	0.584	0.288	0.472	0.432
No waves	0.524	0.297	0.445	0.485
No groundwater	0.610	0.270	0.578	0.468
No entrainment	0.494	0.209	0.456	0.404
No rainfall	0.610	0.254	0.571	0.466
No sunlight	0.397	0.122	0.520	0.230
Uniform distribution	0.507	0.266	0.539	0.438
Linear distribution	0.547	0.244	0.567	0.422

2.3.3 Scenario Tests

To assess the contributions of the various processes described in section 2.3 on the loading, transport, and fate of enterococci, we performed a series of calculations in which different processes were either turned off or modified. This was done to evaluate and compare the relative importance of each of the processes in affecting beach water quality from a mechanistic point of view. The result of Figure 2.7-A was used as the baseline scenario and differences were calculated by subtracting enterococci levels of scenario experiments from those of the baseline (Figure 2.8). The scenarios focused on evaluating the importance of cross-shore diffusion, waves, source functions (groundwater, entrainment, rainfall), and the solar radiation fate. Waves were considered to represent a surrogate to evaluate the influence of mobilized sediment (the first term on the RHS of equation 1). Moreover, the impact of different spatial distributions of enterococci within in the intertidal sand was also evaluated.

2.3.3.1 No Cross-shore Diffusion

To deactivate cross-shore diffusion, we set both sediment and microbe diffusivity to be zero. In this scenario, most enterococci are constrained to a narrow strip next to the waterline, which causes the persistence of high levels in the intertidal zone and overestimation at knee depth while underestimation at waist depth (Figure 2.8-A). This suggests that turbulent diffusion is a crucial process in far-field mixing. It should be noted that diffusion not only mixes free-living microbes that exist in the water, but also bacteria-contaminated sand in the form of suspended load and concomitant release.

2.3.3.2 No Waves

Without any wave forcing, the Eulerian current alone is too weak to suspend sediment. In this case, the release from the bed sediment is almost negligible, which causes a remarkable underestimation of microbe influxes and levels, especially in the middle part of the 10-day period (Figure 2.8-B). Model skill is clearly better when waves are present resulting in a smoother observed microbe response which is well matched by the model (Figure 2.7-B). By comparing model results between baseline and no-wave experiments, we could identify a threshold significant wave height of approximately 0.05-0.1 m before apparent wave-induced release of bacteria at this beach site occurs.

2.3.3.3 No Groundwater

The difference between the cases with and without groundwater is small and indiscernible most of the time (Figure 2.8-C), which suggests that the role of groundwater in microbial balance is insignificant. Slight differences occur around low tide when the highest groundwater head gradient is achieved, which generates the largest groundwater flow. This result is consistent with sand core experiments, which showed that pore water flow releases a relatively small amount of enterococci from the sands at this site (Phillips et al., 2011b).

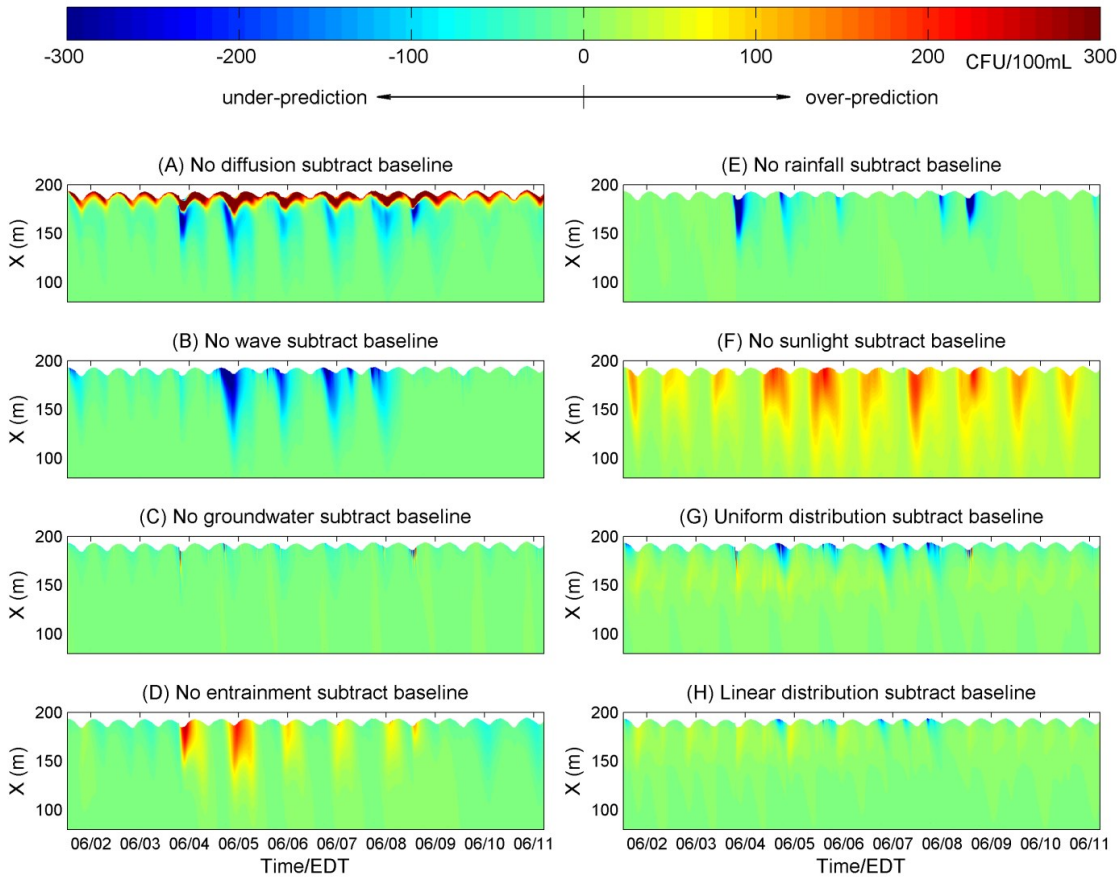

Figure 2.8 Model simulations for different scenario experiments compared with baseline, only showing the model domain from beach shoreline to about 120 m offshore. (A) Contour of differences in enterococci levels between no-diffusion and baseline. Note that color bar is in the conventional linear unit scale of CFU/100 mL. (B) Contour of differences in enterococci levels between no-wave and baseline. (C) Contour of differences in enterococci levels between no-groundwater and baseline. (D) Contour of differences in enterococci levels between no-entrainment and baseline. (E) Contour of differences in enterococci levels between no-rainfall and baseline. (F) Contour of differences in enterococci levels between no-sunlight and baseline. (G) Contour of differences in enterococci levels between uniform distribution and baseline. (H) Contour of differences in enterococci levels between linear distribution and baseline.

2.3.3.4 No Entrainment

The entrainment coefficient was set to zero so that diffusive exchange across the bottom boundary layer is prevented. The role of entrainment is to slowly redistribute the enterococci between the open water column and the pore water within the sediment bed, and the rate of the entrainment is dependent on the concentration difference between the two reservoirs. Within the intertidal zone, the open water column has generally lower concentrations except when other influxes dominate and subsequently increase enterococci levels in it (e.g., during thunderstorms with a large quantity of runoff influx or during wave events that release enterococci from the bed). Therefore, entrainment mostly acts as a one-way microbial influx process to the beach water within the intertidal zone, previously termed "tidal washing" (Abdelzaher et al., 2011; Wright et al., 2011; Enns et al., 2012). However, when enterococci levels are sometimes highly elevated, the direction of entrainment will reverse with enterococci transfer into the bed, which provides another potential mechanism to mitigate extremely high levels of bacteria in the water column in addition to sunlight deactivation, advection, and diffusion. Note that there is no empirical evidence showing microbial flux from surface water into the bed, which could be an area of future research both in the laboratory and field. Without entrainment, these high levels would last several hours longer (see red and yellow areas in Figure 2.8-D). While at other times when rain is absent and waves are minimal, neglecting entrainment would result in slight under-prediction of enterococci levels especially during the ebb tide (see blue areas in Figure 2.8-D).

2.3.3.5 No Rainfall

Runoff associated with rainfall is a direct but episodic microbial source to the beach water in the 10-day period. Without the rainfall runoff loading, several events of elevated enterococci concentrations were clearly missed with the most significant difference observed for the night of 4 June (Figure 2.8-E). Another potential effect of rainfall on beach water quality is to raise groundwater level and increase exfiltration rate but that process cannot be examined at present without further groundwater monitoring.

2.3.3.6 No Sunlight

By turning off sunlight deactivation, the over-predictions of enterococci levels spread across almost the entire 10-day period and expand from the waterline to nearly 100 m offshore, especially in the daytime (Figure 2.8-F). In this case, the model certainly overestimates both knee- and waist-depth enterococci levels. Again, solar inactivation is a key process to reduce enterococci levels during the day and responsible for both observed and modeled diurnal fluctuations of enterococci levels.

2.3.3.7 Uniform and Linear Distributions of Sand Enterococci Levels

To understand the model sensitivity to different distributions of the sand enterococci source, we tested two scenarios: (1) a constant level (9.0 CFU/g) within145 to 200 m and zero everywhere else, referred to as uniform distribution; (2) a linear increase from 0 CFU/g at 145 m to the maximum 18.0 CFU/g at 195 m, referred to as linear distribution (Figure 2.4-B). Those two distributions ensure the total enterococci reservoir of the area from the subtidal point (x = 145 m) to higher high water line (x = 195 m) equals that of the exponential distribution used before. It is not surprising that major differences are found in the intertidal zone where the latter two distributions

provide fewer amount of available enterococci, resulting in underestimations of enterococci levels in that area, especially when tide is ebbing (Figure 2.8-G and -H). Nevertheless, the general spatial and temporal patterns do not change much, compared to the baseline case. Overall, the linear distribution slightly better fits the baseline result than the uniform one because of its relatively higher concentrations of contaminated sand in the intertidal zone. In summary, sand enterococci source distribution influences the levels of enterococci observed in the water column and the best fit to the data occurs when the sediments higher upon the shore are characterized by higher enterococci levels.

2.3.4 Sensitivity Analysis

Sensitivity analysis was conducted as a further evaluation of model performance and to better understand its behavior in response to parameter changes. As illustrated in scenario tests, six parameters in equation (1) may have substantial influences on model output of enterococci level of beach water, by controlling physical transport (D_m), source loading (β_1, β_2, β_3, β_4), or biological decay (β_5). Due to the complexity and large sets of parameters in this model, we only applied simple local sensitivity analysis method by perturbing one factor at a time (i.e., OAT approach) to two proportions (50% and 150%) of corresponding calibrated or literature value, plus or minus 50% variations (Saltelli et al., 2000). Again, we used the result of Figure 2.7-A as the baseline or control and percentages of variation with respect to the control were calculated (Figure 2.9).

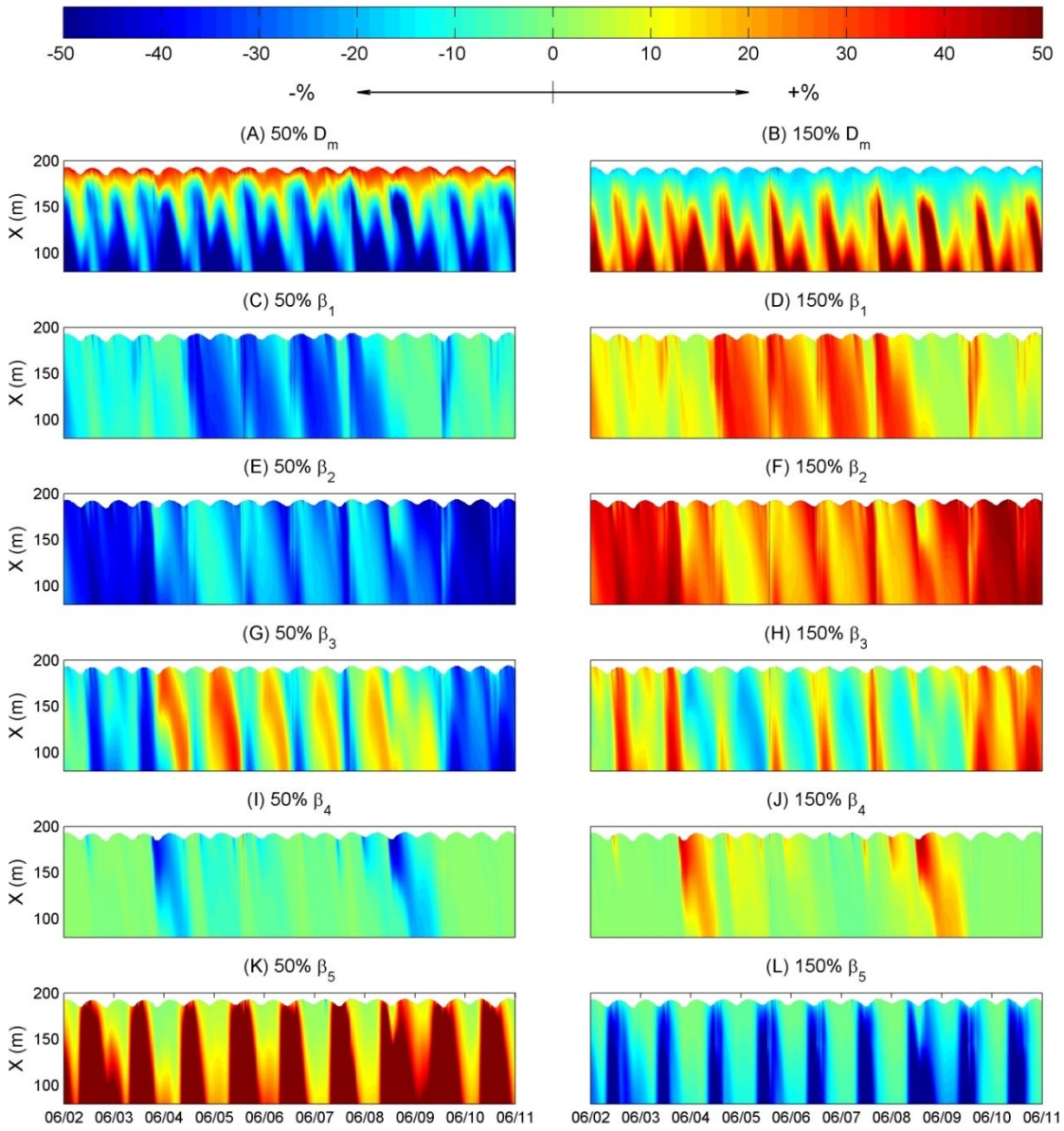

Figure 2.9 Sensitivity analyses on six key parameters. Percentage variations of enterococci levels when microbe diffusion coefficient D_m decreases by 50% (A) or increases by 50% (B). Percentage variations of enterococci levels when sediment-related enterococci release coefficient β_1 decreases by 50% (C) or increases by 50% (D). Percentage variations of enterococci levels when pore water enterococci concentration coefficient β_2 decreases by 50% (E) or increases by 50% (F). Percentage variations of enterococci levels when entrainment mass transfer concentration coefficient β_3 decreases by 50% (G) or increases by 50% (H). Percentage variations of enterococci levels when rainfall-runoff loading coefficient β_4 decreases by 50% (I) or increases by 50% (J). Percentage variations of enterococci levels when sunlight inactivation coefficient β_5 decreases by 50% (K) or increases by 50% (L).

2.3.4.1 Microbe Diffusion Coefficient D_m

The model responses to the changes of diffusion coefficient showed opposite variational patterns between nearshore and offshore regions. The decrease of D_m weakens diffusive transport of enterococci from high concentration intertidal zone to further offshore. Therefore, the smaller D_m is, the more enterococci stay near the waterline while the less are transported away. In general, 50% decrease of D_m causes enterococci levels to increase by less than 40% in the nearshore while to increase more than 50% in the offshore (Figure 2.9-A). Changing D_m to 1.5 times of calibrated value results in less than 20% decrease of enterococci levels in the nearshore and greatly above 50% increase in the offshore (Figure 2.9-B). Such results demonstrate the nonlinearity of diffusion process in the model, which can also be deduced from equation (1) that diffusion terms are second order derivatives.

2.3.4.2 Enterococci Sediment Release Coefficient β_1

Increasing (decreasing) β_1 means larger (smaller) enterococci loading rate from sediment when sediment suspension and transport occur, resulting in rise (fall) of enterococci levels throughout the spatial domain in the beach water when waves are present (Figure 2.9-C and -D). The simulated enterococci levels respond quasi-linearly to the variation of coefficient $\beta_1$when wave heights are noteworthy.

2.3.4.3 Pore Water Concentration Coefficient β_2

Since β_2 represents the abundance of enterococci in the pore water, it can indicate the proportions of enterococci living in the interstitial as oppose to attaching to the sand grain. This will affect both advective exchange by groundwater infiltration/exfiltration and diffusive exchange due to entrainment, with the latter being more important.

Reducing (enlarging) β_2 means lower (higher) enterococci concentrations in the pore water, which will decrease (increase) pore water enterococci loading flux. When sediment or runoff loading is insignificant in the beginning and ending of the 10-day period, lowering β_2 to half will cause around 40-50% decrease in enterococci levels; otherwise, the reductions of enterococci levels are generally less than 20% (Figure 2.9-E). Increasing β_2 leads to exactly opposite patterns (Figure 2.9-F).

2.3.4.4 Entrainment Coefficient β_3

The model responses to entrainment coefficient are fairly complicated. The increase (decrease) of β_3 will facilitate (suppress) the diffusive exchange across the bottom boundary. As previously discussed, pore water generally has higher enterococci levels than surface water, so the decrease of β_3 will reduce enterococci transfer rate from higher pore water to lower overlaying water column and therefore lower enterococci levels of surface water. However, when enterococci levels are highly elevated in the surface water, becoming higher than those in the pore water at nights in the middle nights of the 10-day period, enterococci levels contrarily increase by 10-40% in the case of reducing β_3 by 50% (Figure 2.9-G). We observed just opposite patterns with the case of 150% β_3 (Figure 2.9-H).

2.3.4.5 Rainfall-Runoff Loading Coefficient β_4

The changes of runoff loading coefficient have few impacts on enterococci levels except during rainfall periods, showing quasi-linear responses to coefficient change (Figure 2.9-I and -J). The magnitudes of enterococci level variations seem smaller than coefficient changes, and never exceed 40%.

2.3.4.6 Sunlight Inactivation Coefficient β_5

The influence of inactivation coefficient varies significantly with time and is highly nonlinear. The change of enterococci levels due to coefficient change is generally very small in the nighttime when sunlight is nonexistent. However in the daytime, modeled enterococci levels are quite sensitive to the changes of β_5. Reducing it to half leads to more than 100% to up to 10 times increase in enterococci levels, which are beyond the uniform color scale (±50%) used for all figure panels (Figure 2.9-K). If β_5 becomes 1.5 fold of literature value, the enterococci levels decrease by 10% to 80% of baseline values, with offshore areas having larger variations than the nearshore (Figure 2.9-L). This suggests that β_5 is an important coefficient to correctly predict enterococci levels in the daytime due to the exponential decay feature of the sunlight inactivation process.

2.4 Discussion

2.4.1 Model-Observation Comparisons

The comparisons between model results and field measurements raise the question why the diurnal maxima of enterococci concentrations were under-predicted by the model. This may be attributed to both inherent inhomogeneity of natural sediment and other potential microbial loads not represented in our model, such as dog feces, human activities, and seaweed debris. For example, one fecal event from a small dog may contribute 1.5×10^8 CFU enterococci (Wright et al., 2009). If we assume this microbial load is well mixed and distributed in the water volume with depths from 0 m (i.e., waterline) to 0.3 m (i.e., knee-depth), a mean slope 1/25 in the intertidal zone, and a 10 m long shoreline, it would yield a mean concentration of 1.3×10^3 CFU/100 mL, which is in

the same order as typically observed spikes. Previous model studies also suggested that dog fecal events may have transient impacts (hundreds of CFU/100 mL) in a limited area for several hours (Zhu et al., 2011). Other possibilities can be bathers, dogs and/or samplers walking in the water and stirring up bottom sediment and attached microbes and the signals may be captured by the water samples. Such artificial disturbances are more influential during high tide than low tide because of the geographical location and relative abundance of microbial sources. This partly explains the fact that extreme elevations are more frequently observed around high tides (Enns et al., 2012). In addition, an abnormally wide and thick wrack line was formed in this beach site during the last four days of the field experiments and covered the entire shoreline from the dry berm to nearly 10 m offshore. Seaweed is not only potential microbial sources themselves (Grant et al., 2001; Badgley et al., 2011), but may also provide favorable environments for bacteria survival and growth in the sand underneath (Shibata et al., 2004).

The model has a better skill in hindcasting enterococci levels in the water closer to the shore (knee depth) than farther offshore (waist depth). The lack of observations and the low levels of enterococci at offshore locations may contribute to the lower skill offshore. Moreover, in present model setup, the cross-shore exchange is primarily controlled by diffusion rather than advection. This is due to extremely weak cross-shore currents in the order of 10^{-2} m/s or lower for the whole period (Figure 2.6-A). Other processes not resolved due to the 1-D model setting, specifically alongshore advection, may be as important as cross-shore diffusion. Alongshore uniform assumption should be valid at the central portion of the beach. The bathymetry at the experiment site is mostly alongshore uniform (see Figure 2.1). The longshore current velocity at the site, observed

with GPS-equipped drifters, is also quite uniform with velocities in the order of 10^{-1} m/s (Fiorentino et al., 2012). Although there is significant spatial variability in the enterococci levels within the sand, these spatial scales are much smaller than the scales associated with the alongshore bathymetry, O (100 m), and hydrodynamics; therefore, that can be considered alongshore uniform after local averaging. We examine the relative importance of alongshore advection and cross-shore diffusion by estimating Reynolds number for two different zones: nearshore and offshore. Reynolds number is the ratio of two terms in left hand side of equation (1):

$$R_e = \frac{\left[\frac{\partial hENTv^L}{\partial y}\right]}{\left[\frac{\partial}{\partial x}\left(D_m h \frac{\partial ENT}{\partial x}\right)\right]} = \frac{VL_x^2}{D_m L_y} \tag{10}$$

where V is a mean alongshore velocity (in m/s), D_m is diffusion coefficient (in m^2/s), and L_x and L_y are characteristic cross-shore and alongshore length scales (in m).

If we consider a mean alongshore velocity of 0.1 m/s offshore the beach, a diffusivity of 0.03 m^2/s, and cross-shore and alongshore characteristic lengths of 10 m and 100 m respectively, a Reynolds number of 3.3 is obtained for the offshore region, which suggests alongshore advection and cross-shore diffusion are of the same order of magnitude in transporting microbes. However, since concentration gradient is so high in the narrow and shallow nearshore region, the cross-shore length scale (L_x = 1 m) there is much smaller. In addition, due to the increased friction in such shallow water, the mean longshore velocity is reduced to 0.05 m/s. Then, we obtain a Reynolds number of 0.016 for the nearshore region, which indicates that nearshore is dominated by cross-shore diffusion. The Reynolds number analysis also explains why model performance is not as

good in the offshore as in the nearshore because of the missing of longshore transport. To achieve better predictions in the offshore, a 2-D model configuration that can include longshore transport mechanism is required, which will be our following work.

2.4.2 Constant Bed Reservoir Assumption

There is another interesting question from this modeling effort: is the growth of enterococci in the sand able to replenish the loss of enterococci due to the release? To answer this question, we have to investigate what occurred in the bed reservoir during the 10-day period although the model assumes constant enterococci reservoir within the bed. Due to depletion and regrowth, the total amount of enterococci in the bed reservoir is time dependent in reality. The observations show that the enterococci levels in hourly sampled knee-depth sands are highly variable, spatially and temporally inhomogeneous (Figure 2.10-A). Sand closer to the high tide line (x = 195 m) generally have higher enterococci levels, while those in the subtidal zone have much lower levels. Such spatial distribution is one of the most important characteristics of this type of enterococci source, which we have extensively explained in subsection 2.2.4.4.1. To achieve a good estimation of the reservoir using this sparse data set, we calculate daily mean enterococci levels and compare them with model-based constant enterococci level of the sand (Figure 2.10-B). Note that the daily mean calculation excludes the samples taken beyond a subtidal line (x = 170 m), which is outside intertidal zone, the prevailing source region. The model-based constant enterococci level of the sand is spatially averaged between 195 m and 170 m using equation (6), corresponding to where most knee-depth sand samples locate. The daily mean enterococci levels of the reservoir are fairly stable in those 10 days, slightly oscillating around model-based constant level. This suggests that the

removal of enterococci by the tides and waves have little impact on the total availability of enterococci within the bed, which is consistent with the model assumption of steady state reservoir. The replenishing of removed enterococci is hypothesized to be due to regrowth within the sand, which should be fully explored in the future. In that way, instead of assuming a stable source, a time-varying source function, dependent on environmental parameters and constrains (e.g., temperature, nutrient, and salinity) and sand characteristics (e.g., grain size, mineral, and biofilm), can be applied to the model.

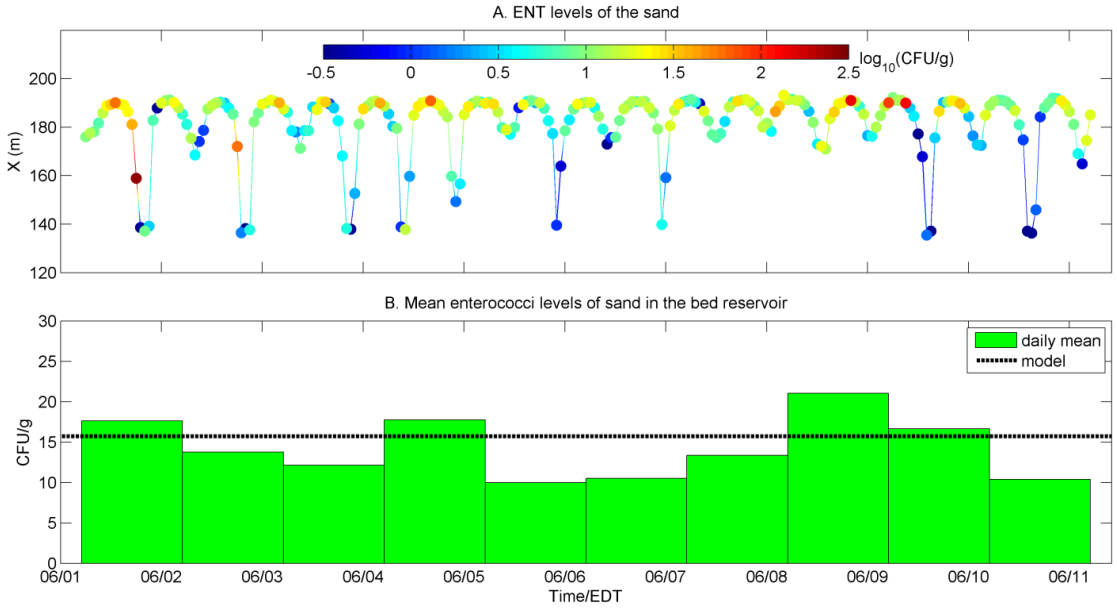

Figure 2.10 (A) Measured knee-depth enterococci levels of the sand (colors of dots demonstrate enterococci levels in log10-transformed CFU/g dry sand); (B) Mean enterococci levels in the bed reservoir (in CFU/g). The histograms show daily mean measured enterococci levels of the sand, an indicator of the mean enterococci levels in the bed reservoir, which average knee-depth samples between 170 m and 195 m within a full day. The dashed line is the model-based constant spatially-averaged enterococci levels of the sand in the area from 170 m to 195 m.

2.4.3 The Importance and Role of the Tide

One of the most unique features making marine beaches differ from freshwater and inland counterparts, like those around the Great Lakes, is tide. Tidal oscillations create a dynamic intertidal zone, superimposed with wave-induced motions. Tides may also elevate the water table above mean sea level and drive water table variations (Nielsen, 1990). The interactions of tides with other coastal processes are fairly complex. This effort elucidates the roles of the tide in beach microbial dynamics in the following aspects, from high to low importance. First of all, the tide periodically changes the location of waterline and surf zone, and therefore the abundance and availability of bacterial sources. In general, high tide initiates the elevation of microbial levels that is more evident in the ebb tidal phase. Second, high tide typically facilitates diffusive exchange from bed pore water to the open water column because of the high concentration differences between pore and surface water near the high tide line. Third, tides are also the major generating force of water table fluctuations and groundwater flows, and thereby bed interfacial advective exchange.

Note that there are also some other tide-related processes that may affect beach water quality but are not investigated in this paper. At first, the 1-D beach-scale model developed in present study is not capable of simulating currents associated with bay-scale circulation, generated by tidal waves propagation in the outer ocean and continental shelf and modulated by the bathymetry and geomorphology in the coastal zone. Circulation pattern and features (e.g., longshore currents, eddies, and coherent structures) are different among tidal phases, which affect transport and dilution of fecal bacteria in the water (Zhu et al., 2011; Fiorentino et al., 2012). Second, tidal stages will determine the

inundated duration of the wrack line and can control the additional contributions of bacteria from seaweed debris washed off to beach water (Shibata et al., 2004). Moreover, tides may also influence the activities of birds, dogs and bathers, all of which are potential fecal bacterial sources (Wright et al., 2009; Wang et al., 2010).

2.4.4 Beach Management Implications

From beach management perspective, our model results address the question concerning when an elevated level of enterococci would be expected during regular open beach hours. The model simulations suggest that locally energetic waves, generated by strong and persistent onshore or southwest winds, occurring at high tide (especially in the ebb phase), will very likely yield exceedances of enterococci levels at this beach. The other environmental factor that should be considered is rainfall, particularly heavy and/or long rains. The persistence of high fecal bacterial levels usually depends on the severity of the exceedance and the intensity of solar inactivation. It should also be noted that exceedances more often occurred in the nighttime are of less concern to human health, given the fact that Hobie Beach is routinely closed from sunset to sunrise by Miami-Dade County. However, if an extraordinary elevation is reached by a combination of several favorable conditions, like the one that occurred in the night of 4 June, the very high levels cannot be reduced fast enough so that the exceedance persists until the next morning, thereby triggering beach advisories and a potential of negative human health impact.

In addition, the model results suggest that the microbial quality of sand, in terms of the abundance of microbes within the sediment, is a fundamental factor in determining overall beach water quality. This is also confirmed by the surveys of multiple south

Florida beaches, which found that beaches with high levels of enterococci in the sand had more reported exceedances of EPA standards (Phillips et al., 2011a).

2.4.5 Applications and Limitations of the Model

Although we have showed a case study in an embayed subtropical beach with relatively low wave energy and small tidal range, the coupled microbe-hydrodynamic-morphological model can be adapted to model bacterial release at other beaches. The approach illustrated herein may be useful for beaches where the pervasive fecal bacteria source comes from the shoreline sand. It may also be useful in different environmental settings such as rip-channeled beaches, where XBeach can be used to reproduce the circulation cells on top of rip channels and shoals (Orzech et al., 2011). In that case, the pollutants originated from the beach may have long retention times in the surf zone (Reniers et al., 2009).

The limitations of the model are associated with the need: for additional parameter calibration and to carefully evaluate the model initial conditions and assumptions. The parameterization issues may be resolved in the future with more field studies and extensive model validations against new data sets, as well as well-designed laboratory experiments in wave flumes to determine appropriate sediment-related enterococci release coefficient β_1. Furthermore, one must pay attention to the initial conditions and basic assumptions made in this study when applying the model to other time periods or beach sites. For instance, Hobie Beach was completely renourished months after the 10-day study. In that case, the initial distribution of microbes in the sand used in this study does not represent the microbial beach environment after the nourishment, and consequently a modified initial condition based on new field

experiments must be established before model simulations. Also, the cross-shore distribution of microbes in the sand is assumed to be stable over the simulation time, which is unlikely to be the case during times of significant beach changes under the impact of storms (Gast et al., 2011).

2.5 Concluding Remarks

In this chapter, an innovative coupled microbe-hydrodynamic-morphological model has been developed. The unique feature of this model is its capability of simulating the release of microbes attached to coastal beach sands as a result of combined wave and tidal forcing. A nearshore process model (XBeach) was coupled with a microbe transport-decay equation. This equation included source functions that accounted for microbial release from mobilized sand, groundwater flow, entrainment through pore water diffusion, rainfall-runoff loading, and a fate function that accounted for solar inactivation effects. The model successfully simulated observed spatial and temporal patterns of enterococci in the beach water, including the reproduction of diel and tidal fluctuations and the rapid decrease of enterococci levels from the waterline to offshore. Primary processes for enterococci loading to the water column included wave-induced sediment resuspension and tidal washing for the entrainment of enterococci from the pore water in the intertidal zone. Diffusion was the major mechanism to transport enterococci from intertidal zone to offshore. Sunlight inactivation was a key process to reduce enterococci levels during the day and to produce the diurnal cycles. Rainfall runoff was found to be an intermittent source of enterococci to beach water whereas groundwater exchange was of secondary importance. Sensitivity analyses suggested that the processes and coefficients related to enterococci loading have quasilinear characteristics, while

model results of enterococci levels were sensitive to both diffusion and sunlight inactivation coefficients, showing high nonlinearity and spatial and temporal dependence.

Chapter 3 A SIMPLIFIED PREDICTIVE MODEL FOR MICROBIAL COUNTS ON BEACHES WHERE INTERTIDAL SAND IS THE PRIMARY SOURCE

3.1 Introductory Remarks

In response to the U.S. Environmental Protection Agency guidelines (US EPA, 1986) and other federal laws, such as Beaches Environmental Assessment and Coastal Health Act (BEACH Act) of 2000, beach monitoring programs have been adopted and implemented around the U.S. coasts as well as the Great Lakes to protect beachgoers from health risks caused by potentially harmful bacteria. Implementation traditionally includes sparse water sampling with time-consuming laboratory analysis required to measure microbial levels. For instance, under the Florida Healthy Beaches Program, all 34 coastal counties in the State of Florida collect beach water samples weekly, reporting beach advisories on the basis of enterococci and fecal coliform measurements 24-48 hours after sample collection. The water sample analysis is useful in terms of guiding beach warnings and advisories; however, due to the one-day laboratory time requirement by the culture method and high spatiotemporal variability associated with fecal indicator bacteria (FIB) in the nearshore water (Boehm, 2007; Ge et al., 2012a; Enns et al., 2012), this method may not be timely and sufficient for decision making, thereby potentially causing unnecessary beach closures and human health risks for beaches that remain open. Recently, many beach managers have begun to utilize predictive tools, of which the most widely applied are models developed through multivariable linear regression (e.g., Olyphant, 2005; Nevers and Whitman, 2005; Frick et al., 2008). In addition, process-based models, which couple hydrodynamic models with a microbe transport-fate model involving microbial loading, transport and fate processes (e.g., Sanders et al., 2005; Hipsey et al., 2008; Feng et al., 2013; Thupaki et al., 2013) can in principle be used to

make predictions. However, for local beach managers or public health agencies, process-based models are usually challenging to build and less accessible due to their intrinsic complexity and high computational demands.

In the past, pollutant transport models along with mass balance analysis have been applied to quantify bacterial source loading rates from well-defined point sources (e.g., rivers and tidal inlets), and to predict FIB levels in the surf zone of marine beaches (Kim et al., 2004; Grant et al., 2005), as well as in the freshwater beaches of the Great Lakes (Thupaki et al., 2010). However, these models are not directly applicable to many beaches without known point sources.

In the U.S., about half of the beach closing/advisory days (12,596 and 11,588 days in 2010 and 2011, respectively) were attributed to unknown sources of pollution (National Resources Defense Council, 2011 & 2012). Stormwater runoff with high bacterial levels has been identified as one type of nonpoint source of pollutants to beach water (e.g., Reeves et al., 2004; Ahn et al., 2005; Parker et al., 2010). More significantly, beach sediments have been found to be ubiquitous nonpoint sources of FIB (e.g., Whitman and Nevers, 2003; Shibata et al., 2004; Yamahara et al., 2007; Halliday and Gast, 2011; Byappanahalli et al., 2012) and also harbor potentially pathogenic microbes (Goodwin et al., 2009; Shah et al., 2011; Yamahara et al., 2012). A multi-beach survey suggested that beaches with relatively higher abundance of enterococci in the sand would also have higher exceedance rates (Phillips et al., 2011a).

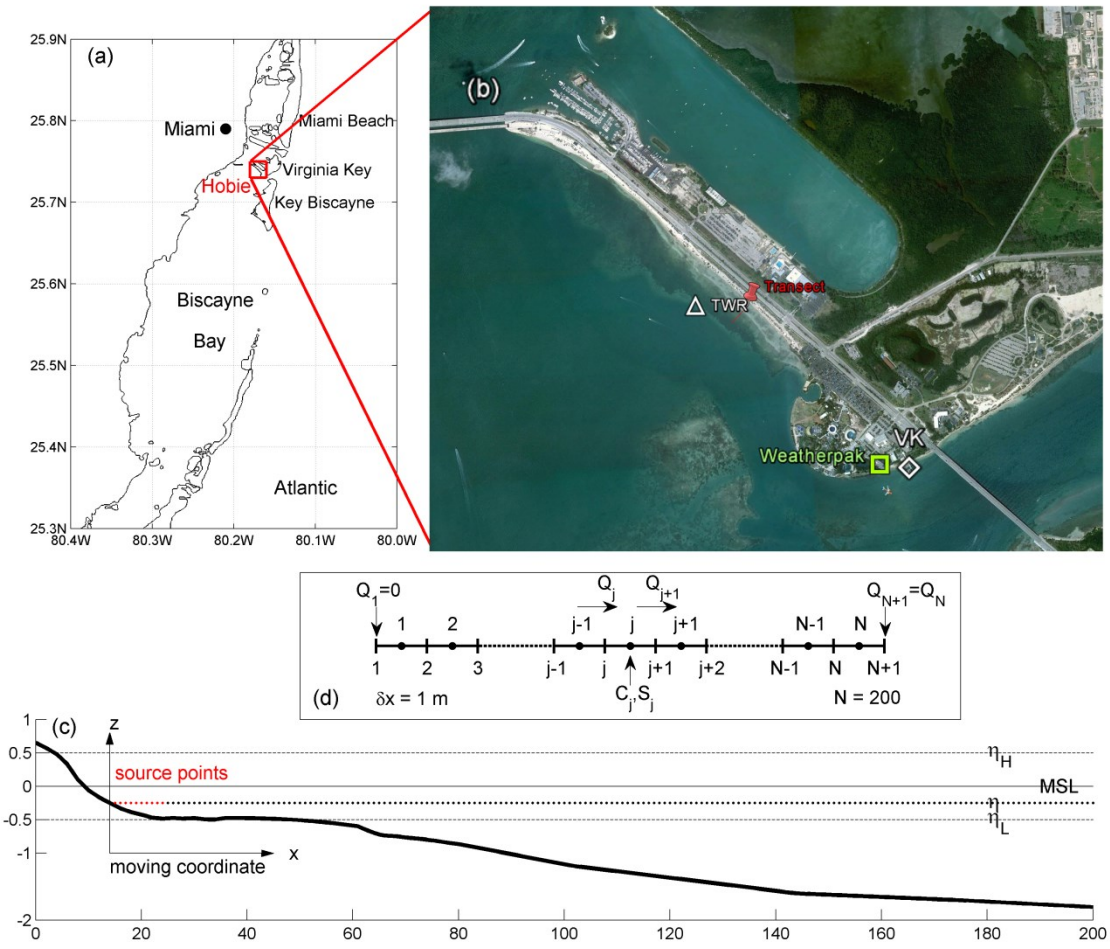

Figure 3.1 The study site, beach profile and model grid. (a) Geographical location of the beach, located on Virginia Key, in the north of Biscayne Bay, and to the southeast of Miami, FL. (b) Google Earth aerial photo of the beach (imagery date of March 31, 2010), which is 1600 m long and northwest-southeast oriented. The positions of tide and wave recorder (TWR), meteorological station (Weatherpak), and NOAA Virginia Key station (VK) are indicated by the triangle, square, and diamond, respectively. The approximate location of water sampling transect is illustrated by a red pushpin. (c) Cross-shore beach profile (heavy solid line) and model coordinate. The coordinate origin is always set at the waterline, moving with the tides. The mean sea level (MSL), reference supratidal (η_H) and subtidal (η_L) lines are illustrated by light solid and dashed lines. The actual tidal elevation (η) is indicated by the black dots with the dots showing the grid points. The first ten grid points (red dots) are microbial source points in the model. (d) Illustration of the 1-D staggered grid used by the numerical computation. The grid is equally spaced (Δx = 1 m). The microbial level (C_j) and source term (S_j) are positioned at the cell centers (j = 1, 2… N-1, N) whereas diffusive flux terms (Q_j) are at the cell edges (j = 1, 2… N, N+1) and N is the total number of cells.

In view of this, a model capable of simulating time-varying microbial levels at a nonpoint source beach is an imperative, especially given the significance of intertidal sediments and stormwater observed in various studies. Only recently, mass balance models have been applied to estimate bacterial levels at nonpoint source beaches. Models developed for two California beaches identified that sand and groundwater are major contributors of FIB (Boehm et al., 2009; Russell et al., 2013).

The first and main objective of this study is to develop a new physically-based yet simple microbial balance model for nonpoint source beaches, taking into account loading, transport, and decay mechanisms. This mass balance model is a simplification of a prior process-based water quality model developed by Feng et al. (2013). The new mass balance model is not only computationally efficient, but also retains dominant physical and microbiological processes that govern the microbial balance in the nearshore water, where water quality monitoring and most recreational activities occur. As a case study, this model is optimized and validated with a 10-day hourly monitoring dataset at a well-studied subtropical municipal beach near Miami, Florida, USA (Figure 3.1). Multivariable linear regression equations that predict beach enterococci levels are also developed for comparative purposes. The second objective is to compare the balance model and regression equation in their ability to accurately predict beach advisories.

3.2 Materials and Methods

3.2.1 Simplified Microbial Balance Model

3.2.1.1 Simplification of Model Equations

The ultimate goal of this model is to predict time-varying microbial levels in order to guide water quality monitoring and beach advisories. We start from a two-

dimensional (2D) depth-averaged microbial balance equation between microbial advection, diffusion, source loading, and a first-order biological decay (e.g., Sanders, et al., 2005; Liu et al., 2006; Feng et al., 2013):

$$\frac{\partial hC}{\partial t}+\frac{\partial uhC}{\partial x}+\frac{\partial vhC}{\partial y} = \sum_{i=1}^{N_s} s_i \delta\left(x-x_s^i\right)\delta\left(y-y_s^i\right)+\frac{\partial}{\partial x}\left[\varepsilon_x h\frac{\partial C}{\partial x}\right]+\frac{\partial}{\partial y}\left[\varepsilon_y h\frac{\partial C}{\partial y}\right]-k_d hC \quad (11)$$

where C is the depth-averaged microbial concentration (in Colony Forming Unit, CFU or Most Probable Number, MPN per m^3), h is water depth (in m), and u and v are depth-averaged cross-shore and alongshore velocities (in m/s) respectively. The first term on the right hand side (RHS) represents influx of microbes from point sources of multiple types, where N_s is the number of source types, s_i is influx rate (in CFU s^{-1}) of the ith type, δ is the Kronecker delta function (in m^{-1}), and x_s^i and y_s^i are coordinates of the source points. ε_x and ε_y are diffusivities (in m^2 s^{-1}) in cross-shore and alongshore directions, and k_d is a first-order decay rate (in s^{-1}). Note that Equation (11) may be applicable to all sorts of microorganisms (e.g. fecal bacteria, pathogen, and protozoan); in this study, we only focus on culturable enterococci, which are recommended by the EPA for water quality indication and has been monitored for decades (US EPA, 1986).

It is not possible to directly solve Equation (11) for microbial concentrations without resolving detailed hydrodynamics (i.e., u, v, h, ε_x, and ε_y) from momentum and continuity equations, so we simplified this equation based on the characteristics of the beach setting and hydrodynamic conditions outlined below.

Three transport-related assumptions can be made for many low-energy long beaches: (1) the beach is quasi-uniform alongshore ($\frac{\partial}{\partial y} \approx 0$); (2) cross-shore velocity is negligible ($u \approx 0$); and (3) the diffusion is assumed isotropic and homogenous. The first assumption applies only to the central part of the beach away from the lateral boundaries. Assuming a straight long beach with neither significant alongshore bathymetric variation nor flow convergence/divergence, the central portion of the beach can be considered alongshore uniform if the microbial sources along the shoreline are more or less uniform. A uniform shoreline is the characteristic of many beaches and would allow for applying this simplification to areas where flow patterns are approximately the same along the shoreline. The second assumption is also a reasonable assumption for these beaches where currents nearshore are very low. This is supported by both theoretical analysis of an ideal enclosed beach (Grant and Sanders, 2010), and the observations and other modeling efforts at the beach of this study (Zhu et al., 2011; Fiorentino et al., 2012; Feng et al., 2013). Finally, since the majority of the fecal bacteria originate from the beach shoreline and intertidal zone, there must be cross-shore gradients of bacteria levels. In this study, the diffusion process consists of both turbulent diffusion and tidal dispersion and a constant diffusivity, 0.03 m^2 s^{-1}, is used based on previous modeling efforts (Feng et al., 2013).

On the basis of the above assumptions, Equation (11) can be simplified as:

$$\frac{\partial hC}{\partial t} = \sum_{i=1}^{N_S} S_i \delta\left(x - x_s^i\right) + \frac{\partial}{\partial x}\left[\varepsilon_x h \frac{\partial C}{\partial x}\right] - k_d hC \tag{12}$$

where S_i represents source influx per meter shoreline (in CFU $m^{-1}s^{-1}$).

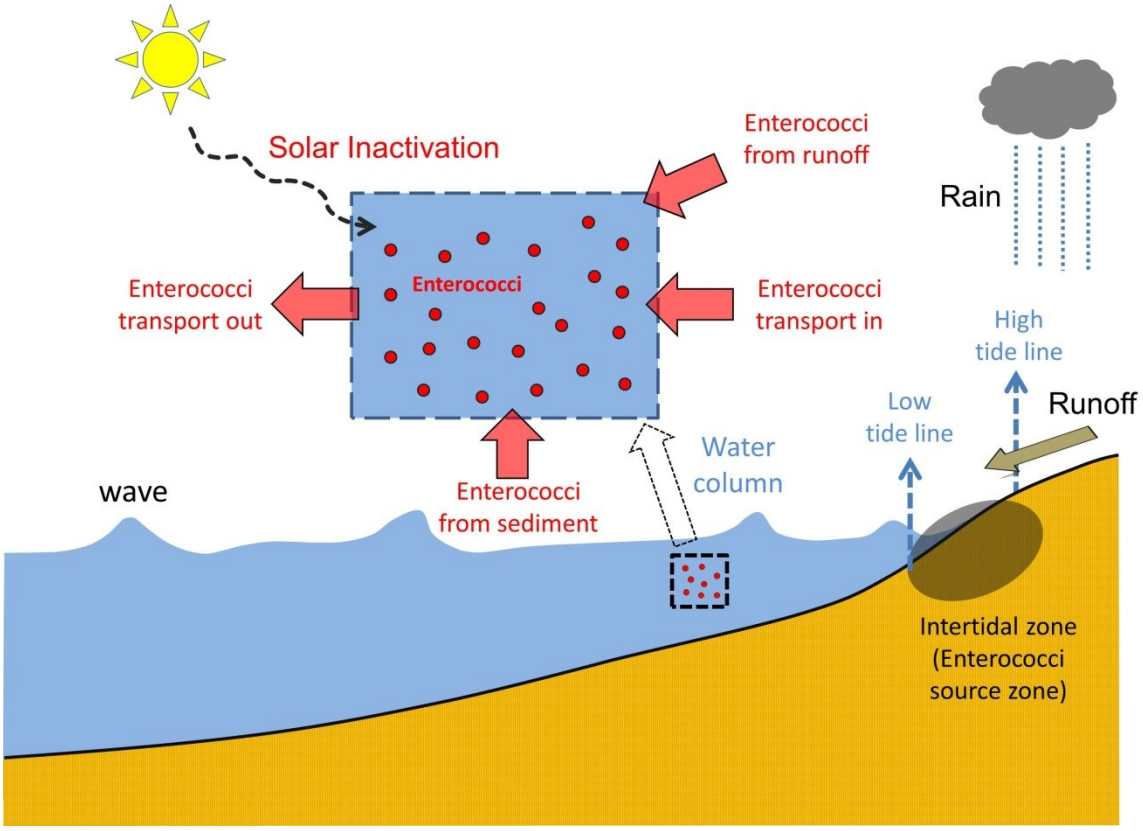

Figure 3.2 Graphic representations of the beach cross-shore section and processes in the balance model. The blue box illustrates the water column containing enterococci. The red arrows represent enterococci loading and transport processes and black dash arrow represents solar inactivation. The intertidal zone is the enterococci source. Enterococci enter the water column through rainfall runoff washing the beach face, and/or wave-induced sediment suspension and concomitant enterococci release.

3.2.1.2 Quantification of Source Loads and Decay

Our model takes into account contributions of two types of nonpoint sources: beach sediment and stormwater runoff (Figure 3.2). The influx terms of two sources are empirically provided by:

$$\sum_{i=1}^{N_S} S_i \delta\left(x - x_s^i\right) = \alpha\beta H_1^2 \delta(x - x_s^1) + \gamma I_r \delta(x - x_s^2) \tag{13}$$

where α is a wave pick-up coefficient (in CFU $m^{-3}s^{-1}$), β is a dimensionless tidal modulation factor, and γ is runoff loading coefficient (in CFU m^{-2}). H_1 represents significant wave height (in m) at a reference depth and I_r is the rainfall rate (in m s^{-1}). In addition, the source zones (x_s^1 and x_s^2) for both sediment and runoff loading are considered to be a 10 m wide cross-shore transect from the waterline to offshore (see Figure 3.1c red dots), equivalent to a typical width of intertidal zone at the study beach. Note that the source points in this model are not fixed because the waterline changes with rising and falling tides.

The first term on the RHS of Equation (13) quantifies microbial influx from the sand due to the wave effect under the influence of tides. Waves have been found to be an important agent to transport microbes shoreward or directly release them from the sand (Ge et al., 2012a; Ge et al., 2012b; Feng et al., 2013). Since wave-related bed shear stress suspends beach sands and releases attached microbes, we assume that the influx of microbes from the sands is linearly proportional to wave energy, or squared significant wave height. The above assumption also implies that bed sediments are infinite sources so that losses of enterococci are continuously compensated by settlement and/or regrowth

of enterococci in the sediment. The coefficient α is a fitting parameter, determined by minimizing least square errors between predictions and observations. The reference depth was set at 1 m, consistent with typical waist depth where water samples are routinely collected. Measured wave heights (H_0) are converted to the reference depth using a shoaling factor (K_s). The wave height at reference depth (H_1) is:

$$H_1 = H_0 K_s = H_0 \sqrt{\frac{C_{g0}}{C_{g1}}} \tag{14}$$

where C_{g0} and C_{g1} are wave group velocities at instrument and reference depths, derived from linear wave theory assuming that the incident wave direction is normal to the shoreline (Dean and Dalrymple, 1991). In addition, a minimal wave height of $H_{1,min}$ = 0.05 m is imposed to represent a background enterococci loading due to processes not present in the model, such as tidal washing and groundwater discharge (Boehm and Weisberg, 2005; Phillips et al., 2011b; Russell et al., 2012 & 2013; Feng et al., 2013).

The tidal modulation factor β is introduced to account for the fact that microbial levels in the sand decrease from supratidal to subtidal zones, as observed in many beaches (e.g., Whitman and Nevers, 2003; Yamahara et al., 2007; Wright et al., 2011; Piggot et al., 2012). We assume this factor has a maximum value of 1 at a reference supratidal point in the permanently dry upper beach, a minimum value of 0 at a reference subtidal point (i.e., permanently wet), and is linearly interpolated in between.

$$\beta = \begin{cases} 1, & if\ \eta \geq \eta_H \\ (\eta - \eta_L)/(\eta_H - \eta_L), & if \eta_L < \eta < \eta_H \\ 0, & if\ \eta \leq \eta_L \end{cases}$$

(15)

where η_H (= 0.5 m) and η_L (= -0.5 m) denote elevations of the supratidal and subtidal reference lines (see Figure 3.1c).

The second term on the RHS of Equation (13) represents loading flux of the stormwater runoff as a prior study has observed high levels of fecal indicator bacteria in runoff water at this beach (Wright et al., 2011). The coefficient γ (= 2.6×10^8 CFU m^{-2}) was determined based on the rational formula (Lindeburg, 1986) for estimating the volume of runoff coupled with a typical level of bacteria in the runoff (Wright et al. 2011). The derivation procedures of the coefficient value can be found in Feng et al. (2013).

The solar inactivation effect, represented by the last term on RHS of Equation (12), is formulated according to a first-order exponential decay, in which the decay coefficient is linearly proportional to solar insolation (Sinton et al., 2002):

$$k_d = \kappa I_s$$

(16)

where the κ is the solar inactivation coefficient (in $m^2\ J^{-1}$) and I_s is the solar insolation (in W m^{-2}). In this model, a constant $\kappa = 3.68\times10^{-7}\ m^2\ J^{-1}$ is adopted based upon the work of Zhu et al. (2011).

The final balance model equation is:

$$\frac{\partial hC}{\partial t} = \alpha\beta H_1^2 \delta(x - x_s^1) + \gamma I_r \delta(x - x_s^2) + \frac{\partial}{\partial x}\left[\varepsilon_x h \frac{\partial C}{\partial x}\right] - \kappa I_s hC$$

(17)

3.2.1.3 Numerical Computation

Equation (17) was discretized in a 1-D staggered grid (Figure 3.1d). During the computation, the whole grid moved simultaneously with the tides so that model origin can always be placed at the waterline. This was done to circumvent the wetting and drying of grid points in the intertidal zone. The transformation from traditional fixed grid to the moving grid has negligible effects on the computations due to the slowly varying nature of local tide and its small tidal range (See Appendix-C).

To update microbial levels in time, i.e. solving the first term of Equation (17), we used a fourth-order Runge-Kutta method (RK-4), chosen for its high accuracy and large stability region (Hundsdorfer and Verwer, 2003). The updated microbial level was imposed with a minimum value of 1 CFU/100 mL, assumed to be the background enterococci level of the beach water. This was set due to the detection limit of traditional membrane filtration methods using a typical dilution of 100 mL water. The time step was 15 seconds to meet the stability criterion (See Appendix-D). The model was initialized from the minimum level of 1 CFU/100 mL in the entire model domain. We applied Dirichlet boundary condition at the closed waterline boundary assuming zero flux value (i.e., $Q_1 = 0$; see Figure 3.1d). A Neumann-type offshore boundary was used by imposing zero flux gradients (i.e., $Q_{N+1} = Q_N$). In this case, offshore boundary allows microbes to leave the computational domain because the sources are in the beach side, but not the ocean side. Additional details about the numerical methods can be found in Appendix-D. The total computational time for a 10-day period trial was less than 2 minutes on a laptop computer using computational codes written in Matlab (MathWorks, Natick, MA).

3.2.2 Multivariable Linear Regression Equation

In this study, we utilized EPA's Virtual Beach (VB) version 2.3 (Frick et al., 2008; Cyterski et al., 2012) to construct the regression equations from a number of independent explanatory variables:

$$log_{10}ENT = B_0 + \sum_{i=1}^{n} B_i V_i + e \tag{18}$$

where $log_{10}ENT$ is $\log_{10}$-transformed enterococci level (in $\log_{10}${CFU/100 mL}), n is the number of explanatory variables, V_i and B_i are ith explanatory variable and corresponding regression coefficient, and e is the residual error.

The candidate explanatory variables include: tidal elevation (η in m), squared wave height (H^2 in m^2), solar insolation (I_s in W/m^2), and 4-hour antecedent cumulative rainfall (I_{4h} in mm).These variables were also compatible with the input variables in the microbial balance model in previous subsection and were uncorrelated, satisfying an important assumption when conducting multi-regression analysis (Ge and Frick, 2007). An exhaustive search on all variable combinations was performed, and the best-fit equation was chosen with the smallest Akaike information criterion or *AIC* value (Akaike, 1974; Cyterski et al., 2012), defined as:

$$AIC = 2p + N * ln \sum_{i=1}^{N} (log_{10}P_i - log_{10}O_i)^2 \tag{19}$$

where p is the number of variables, N is the number of observations, and P and O represent model-predicted and field-observed enterococci levels. AIC includes a penalty associated with increasing number of variables, and hence discourages over-fitting.

3.2.3 Field Dataset

The data utilized for model training and evaluation purposes were collected in June 1 to 11, 2010. Water was sampled hourly at the knee depth (~0.3 m) and every six hours at the waist depth (~1.0 m). Enterococci levels of the water samples were measured by membrane filtration method. Tide and wave conditions were measured by a bottom-mounted tide and wave recorder (RBR TWR-2050, Ottawa, ON, Canada). Solar insolation and rainfall rate were recorded by a research weather station (Weatherpak, Seattle, WA) every 2 minutes at the University of Miami Rosenstiel School (Figure 1b). The model inputs of solar insolation and rainfall rate were hourly moving averages of the raw measurements. The details of this experiment were described in Enns et al. (2012) and Feng et al. (2013).

The whole dataset was split into two subsets, one from 1300 (Eastern Daylight Time or EDT hereafter) June 1st to 2300 June 7th and the other after 0000 June 8th. The first subset was used to identify the optimized coefficient α (= 1.645×10^{4} CFU $m^{-3}s^{-1}$) for the balance model (see Appendix-E) and also to build regression equations. The second subset was then used to validate both the balance model and regression equations. Because enterococci levels have high spatial variability, we did not attempt to aggregate the observations at different locations to construct a unified regression equation. Instead, we built the regression relationships for enterococci levels of the knee and waist depths separately.

3.2.4 Statistical Analyses

All enterococci levels were $\log_{10}$-transformed ($\log_{10}ENT$) to achieve normality. One-way analysis of variance (ANOVA) was conducted using Matlab statistical toolbox to compare significant differences of the model and observational results.

Model performances were assessed by two typical statistical measures, mean absolute error (*MAE*) and root mean square error **(***RMSE*), which are traditional dimensioned measures of average model-performance errors (Willmott and Matsuura, 2005).

$$MAE = \sum_{i=1}^{N} |log_{10}P_i - log_{10}O_i|/N \tag{20}$$

$$RMSE = \left[\sum_{i=1}^{N} (log_{10}P_i - log_{10}O_i)^2/N\right]^{1/2} \tag{21}$$

3.2.5 Beach Advisory Assessment

Based on EPA's single sample threshold, an exceedance (or a positive outcome) occurs when sampled or predicted enterococci level exceeds 104 CFU/100 mL. Type-I error (or a false positive outcome) occurs when enterococci level above threshold value is predicted by the method but actual water sample is below the threshold. On the contrary, Type-II error (or a false negative outcome) means that predicted enterococci level is below 104 CFU/100 mL but actual water sample exceeds, which may result in public exposure to microbial contaminations when beaches are still open. Three other metrics that evaluate model's performance in predicting advisories are:

$$Accuracy = (N_{TP} + N_{TN})/N$$

(22)

$$Specificity = N_{TN}/(N_{TN} + N_{FP})$$

(23)

$$Sensitivity = N_{TP}/(N_{TP} + N_{FN})$$

(24)

where N, N_{TP},N_{TN},N_{FP}, and N_{FN} are numbers of observations, true positives, true negatives, false positives, and false negatives. Accuracy is the percentage of correct advisory predictions. Specificity and sensitivity are rates of correctly predicted non-exceedance and exceedance, respectively. All three metrics range from 0 to 1, with 1 being perfect.

3.3 Results

3.3.1 Microbial Balance Model

Model hindcast of enterococci levels using input variables of wave, tide, rainfall, and solar radiation demonstrated substantial spatiotemporal variation from the shoreline to 200-m offshore (Figure 3.3e). The spatiotemporal patterns of enterococci levels agreed well with those shown by a much more sophisticated process model in Feng et al (2013). The most important spatial pattern is the substantial decrease of enterococci levels from the waterline to offshore boundary. For both model and observation, mean $\log_{10}ENT$ of the knee depth are more than one order of magnitude higher than the waist depth ($p <$ 0.001; Table 3.1). Such a spatial pattern is due to enterococci release at the shoreline source zone with subsequent offshore transport and dilution.

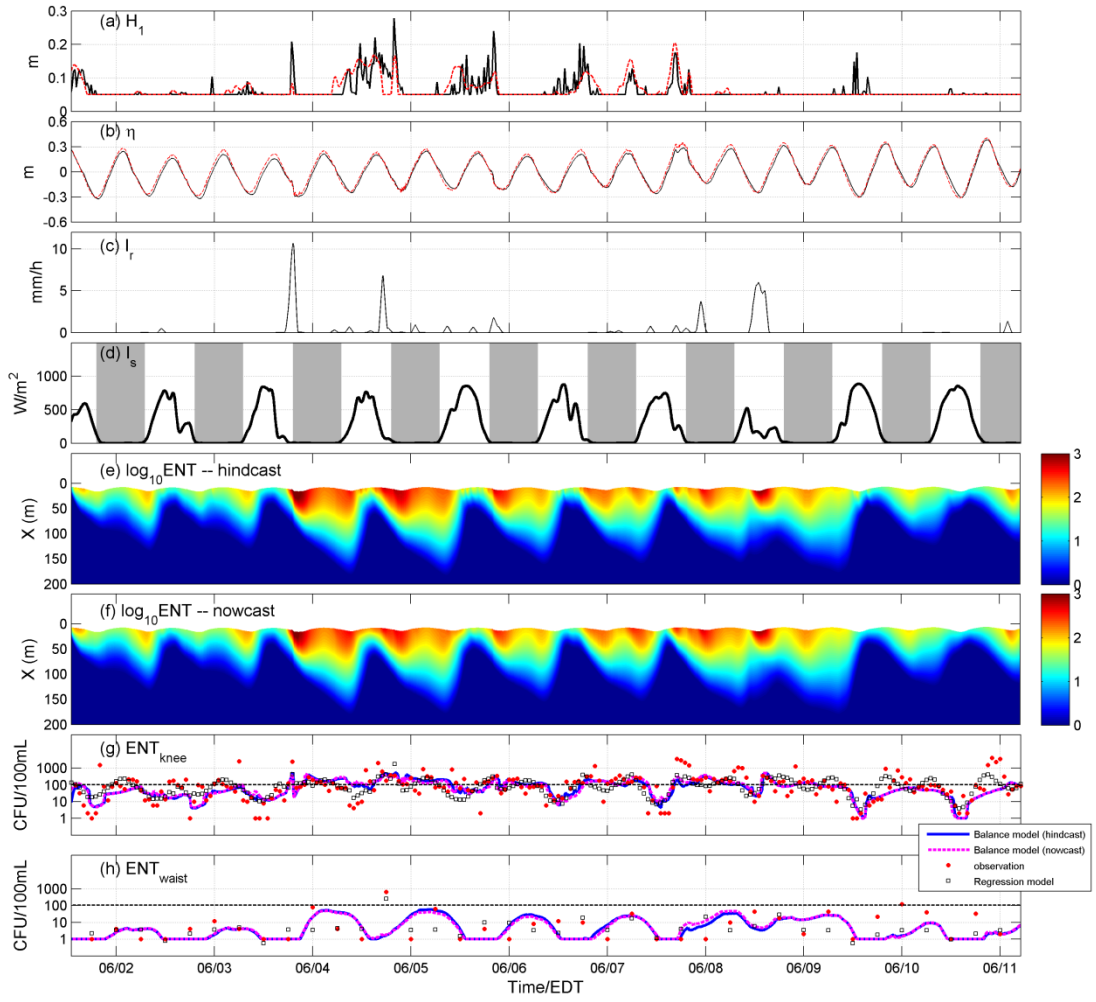

Figure 3.3 Microbial balance model input variables and outputs of enterococci levels from June 1st to 11th, 2010. (a) Measured (black line) and wind-retrieved (red line) wave heights. (b) Tides in situ (black line) and at a nearby NOAA station (red line). (c) Hourly moving-averaged rainfall rates. (d) Hourly moving-averaged solar insolation. The grey stripes indicate nighttime conditions. (e) Contour of $\log_{10}ENT$ in hindcast mode using in situ wave and tide measurements. It illustrates the cross-shore transect from waterline to about 200 m offshore. Color bar is in the unit of $\log_{10}$(CFU/100 mL). (f) Contour of $\log_{10}ENT$ in nowcast mode using wind-retrieved wave heights and NOAA tides as surrogates. (g) Comparisons of balance model, regression equation and observation at knee-depth locations. Blue solid and magenta dashed lines are balance model outcomes based on measured and wind-retrieved wave heights, respectively. Red dots and black squares show observations and regression equation results. Black dashed line is the EPA single sample threshold, 104 CFU/100 mL. (h) Comparisons at waist-depth locations.

Table 3.1 Comparisons of mean (and standard deviation) $\log_{10}$-transformed enterococci levels of knee- versus waist depth, day versus night, high versus low tide, ebb versus flood tide, and large versus small wave.

	Sample	Model
Knee-depth (N = 233)	1.85 (± 0.76)	1.76 (± 0.52)
Waist-depth (N =38)	0.73 (± 0.77)	0.62 (± 0.57)
One-way ANOVA	$p < 0.001$	$p < 0.001$
Day (N = 114)	1.54 (± 0.82)	1.64 (± 0.55)
Night (N = 119)	2.14 (± 0.56)	2.00 (± 0.41)
One-way ANOVA	$p < 0.001$	$p < 0.001$
High-tide (N = 32)	2.24 (± 0.67)	1.79 (± 0.31)
Low-tide (N = 36)	1.22 (± 0.73)	1.17 (± 0.67)
One-way ANOVA	$p < 0.001$	$p < 0.001$
Ebb-tide (N = 120)	1.93 (± 0.81)	1.94 (± 0.49)
Flood-tide (N = 113)	1.77 (± 0.70)	1.68 (± 0.54)
One-way ANOVA	$p = 0.11$	$p = 0.019$
Large-wave (N = 25)	2.07 (± 0.87)	2.07 (± 0.45)
Small-wave (N = 208)	1.82 (± 0.74)	1.72 (± 0.52)
One-way ANOVA	$p = 0.12$	$p = 0.001$

Notes: The unit is $\log_{10}$(CFU/100 mL). The day sample is defined as a sample collected from 7:00 am and 6:59 pm (EDT), when the beach is open to the public. The sample taken after 7:00 pm and before 6:59 am next morning is defined as a night sample. High- (or low-) tide sample is collected when tidal elevation is above 0.2 m (or below -0.2 m) with respect to MSL. Ebb- (or flood-) tide sample is a sample collected at a time when tide is falling (or rising). The cutoff wave height to distinguish large/small wave is 0.1 m. For inter-comparison purposes, model outputs were subsampled to the time when water samples were collected. For day/night, ebb/flood, high/low tide, and large/small wave comparisons, only knee depth was utilized.

The most apparent temporal pattern is the diurnal variation, with lower enterococci levels in the daytime and higher in the nighttime, mainly resulting from sunlight inactivation during the day (Figure 3.3d). Mean daytime $\log_{10}ENT$ is significantly lower than the nighttime ($p < 0.001$; Table 3.1). Another temporal pattern is associated with the semidiurnal tidal fluctuations (Figure 3.3b). Enterococci levels during the high tides are significantly higher than those during the low tides ($p < 0.001$; Table 3.1). In addition, enterococci levels in the ebb phase are slightly higher than those in the flood phase, although not very significant ($p = 0.11$ for observation and $p = 0.019$ for model).

Elevated enterococci levels occur with the presence of local wind waves, shown as red patches in the contours (Figure 3.3e & f). Mean enterococci levels during large waves are higher than small or no wave conditions (Table 3.1). The significance level calculated from the observation is not as high as the model, mainly due to the larger standard deviation associated with the observations. Meanwhile, rainfall only functions as an intermittent source. For instance, the maximum enterococci loading rate during a summer afternoon thunderstorm with the peak rainfall rate of 10 mm/h could reach 722 CFU $m^{-2}s^{-1}$. This rate is more than half of the loading rate (1332 CFU $m^{-2}s^{-1}$) from the sand in a condition of largest observed wave height (of 0.3 m) during spring high tide (of 0.4 m). However, because precipitation in this 10-day period was sporadic and short-lived, rainfall was of secondary importance compared to the release of bacteria from sand through wave and tidal actions.

Model and observations agreed particularly well in the middle part of the 10-day period (Figure 3.3g & h). However, the balance model generally underpredicted

enterococci levels in the first and last two days when wave and rainfall were predominantly small to minimal. Also, observed enterococci levels were highly variable with extreme values of the knee-depth samples up to thousands of CFU/100 mL, whereas the modeled maximum enterococci levels of knee-depth water never exceeded 600 CFU/100 mL. Such difference was also shown in the box-whisker diagram that observed enterococci levels had a nearly one order of magnitude higher upper whisker than modeled ones (Figure 3.4e).

The model performance was further evaluated with statistical measures. The subsets for model training and validation have very similar error values (Table 3.2). The *MAE* and *RMSE* of the knee depth are around 0.5 and 0.65, respectively. In addition, slightly larger errors were found in waist-depth predictions. All these results indicate approximately half an order of magnitude average error existing in enterococci predictions by the balance model.

3.3.2 Regression Model

The multivariable linear regression equations to predict the knee- and waist-depth enterococci levels based on Subset-1 can be written as:

$$log_{10}ENT_{knee} = 1.9632 + 1.6976\eta + 20.5628H_1^2 - 0.001058I_s + 0.03931I_{4h} \quad (25)$$

$$log_{10}ENT_{waist} = 0.5298 + 45.1858H_1^2 - 0.0009412I_s + 0.1486I_{4h} \quad (26)$$

Table 3.2 Assessment of balance model and regression equation performance using the mean absolute error (*MAE*) and root mean square error (*RMSE*). See Equations (20) and (21) for definitions.

Subset	Location	Model vs. Sample	*MAE* (log_{10}CFU/100 mL)	*RMSE* (log_{10}CFU/100 mL)
Subset-1 (training)	Knee (*N* = 155)	Balance	0.508	0.663
		Regression	0.474	0.604
	Waist (*N* = 25)	Balance	0.569	0.800
		Regression	0.452	0.565
Subset-2 (validation)	Knee (*N* = 78)	Balance	0.474	0.665
		Regression	0.490	0.605
	Waist (*N* = 13)	Balance	0.721	0.920
		Regression	0.739	0.892

Model fit and variable statistics for two equations above were shown in Table 3.3. The regression equation could predict 35% and 34% of the variance of the knee and waist depths, respectively. For the knee-depth relationship, all four explanatory variables are statistically significant. Surprisingly, tide is not significant in waist-depth relationship. Due to the limited number of samples for regression fitting to the waist depth (*N* = 25), the best-fit relationship is rather crude and may not capture all significant variables.

3.3.3 Application in Beach Advisories

Predicted enterococci levels were visualized against measured values in scatterplots to analyze beach advisory decisions according to EPA's single-sample enterococci criteria of 104 CFU/100 mL (Figure 3.4 and Table 3.4). 43.8% of the total

knee-depth samples exceeded the threshold, whereas only 5.3% of the waist-depth samples were above the threshold. Note that the study beach is only open to the public during the daytime from sunrise to sunset according to the regulation of Miami-Dade County, which implies that only advisories using day samples/predictions may be directly relevant to human health protection. In a scenario only accounting for day samples/predictions, lower rates of advisories would be issued no matter whether observations or models are utilized.

Table 3.3 Regression equation parameters and fit statistics based on the Subset-1

Model statistics	Explanatory Variable	Coefficient	Standard error	P-value
Knee (N = 155)	Constant	1.9632	0.0702	< 0.001
AIC = 10.85	Tidal elevation (η)	1.6976	0.3196	< 0.001
Adjusted R^2 = 0.35	Squared wave height (H_1^2)	20.5628	6.5487	0.002
	Solar radiation (I_s)	-0.001058	0.0002	< 0.001
	4-h Rainfall (I_{4h})	0.03931	0.0203	0.0545
Waist (N = 25)	Constant	0.5298	0.1769	0.0069
AIC = 5.06	Squared wave height (H_1^2)	45.1858	24.2050	0.0760
Adjusted R^2 = 0.329	Solar radiation (I_s)	-0.0009412	0.0004	0.0340
	4-h Rainfall (I_{4h})	0.1486	0.0895	0.1118

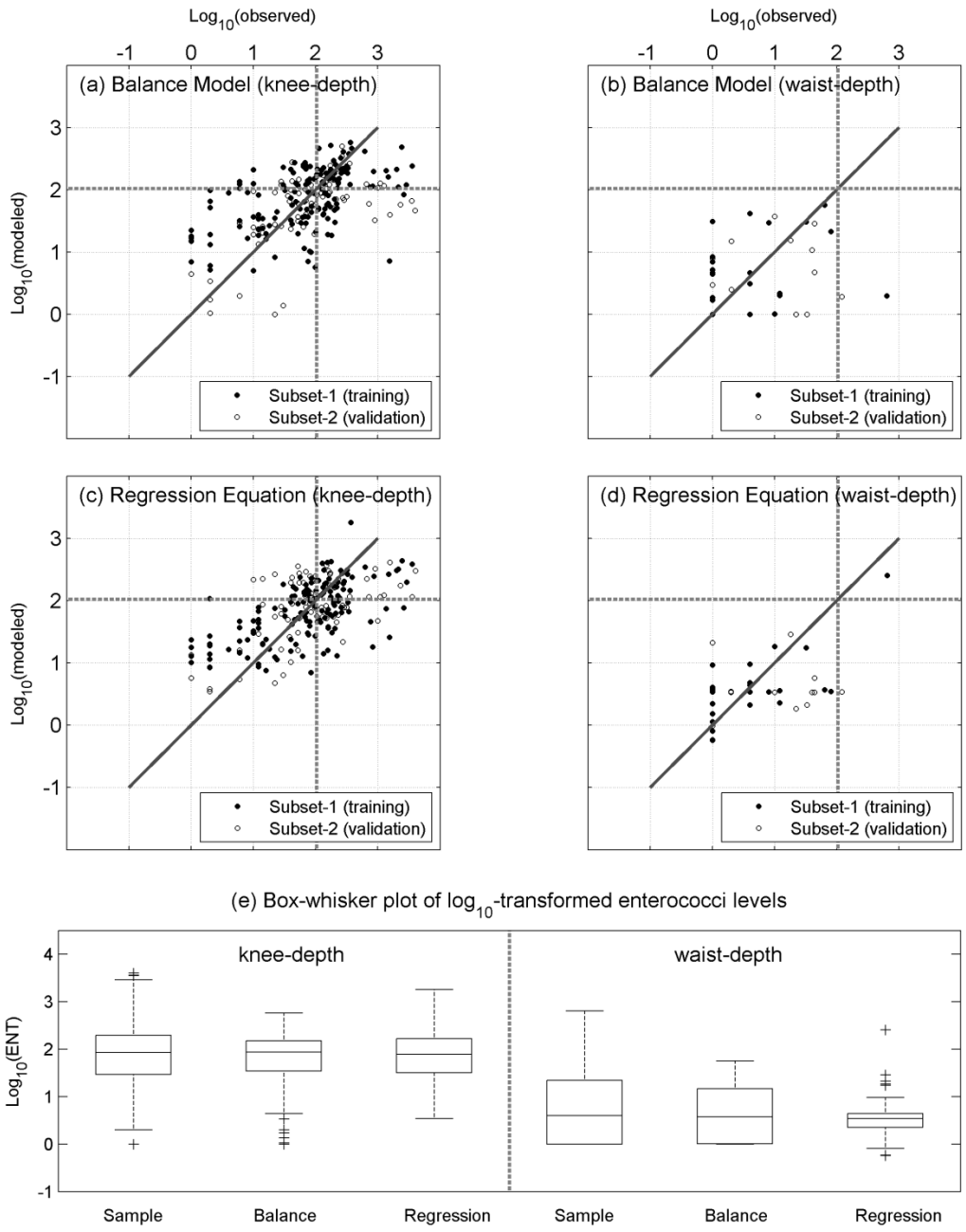

Figure 3.4 Scatter and box-whisker plots showing observed versus modeled enterococci levels at the knee and waist locations. (a) Balance model results at the knee depth. Dash lines are EPA-recommended single sample threshold of 104 CFU/100 mL and solid lines are where model and observation have perfect agreement. (b) Balance model results at the waist depth. (c) Regression equation results at the knee depth. (d) Regression equation results at the waist depth. (e) Box-whisker plot of measured and modeled enterococci levels. On each box, the central line is the median, the edges of the box are the 25th and 75th percentiles, the whiskers extend to the most extreme data points not considered outliers, and outliers are plotted with crosses.

Table 3.4 Summary of beach advisory evaluation based on water sample, balance model in hindcast (H) and nowcast (N) modes, and regression equation at the knee- and waist-depth locations.

Location	Method	Positive	Exceedance Rate (%)	True Positive	True Negative	Type-I error	Type-II error	Accuracy	Specificity	Sensitivity
						False Positive	False Negative			
Knee (N = 233)	Sample	102	43.8	-	-	-	-	-	-	-
	Balance (H)	86	36.9	58	103	28	44	0.691	0.786	0.569
	Balance (N)	87	37.3	61	105	26	41	0.712	0.801	0.598
	Regression	96	41.2	58	93	38	44	0.648	0.71	0.569
Knee (day sample only, N = 114)	Sample	31	27.2	-	-	-	-	-	-	-
	Balance (H)	25	21.9	12	70	13	19	0.719	0.843	0.387
	Balance (N)	31	27.2	15	67	16	16	0.719	0.807	0.484
	Regression	26	22.8	15	72	11	16	0.763	0.867	0.484
Waist (N = 38)	Sample	2	5.3	-	-	-	-	-	-	-
	Balance (H)	0	0	0	36	0	2	0.947	1	0
	Balance (N)	0	0	0	36	0	2	0.947	1	0
	Regression	1	2.6	1	36	0	1	0.974	1	0.5
Waist (day sample only, N = 19)	Sample	1	5.3	-	-	-	-	-	-	-
	Balance (H)	0	0	0	18	0	1	0.947	1	0
	Balance (N)	0	0	0	18	0	1	0.947	1	0
	Regression	1	5.3	1	18	0	0	1	1	1

The balance model and regression equation yielded accuracy values of 0.691 and 0.648 using knee-depth samples (Table 3.4). If only daytimes or beach open hours are evaluated, both methods performed better, with accuracy values of 0.719 (balance model) and 0.763 (regression equation), respectively. Waist-depth enterococci levels rarely exceeded the EPA threshold. Notice that neither the balance model nor regression equation can circumvent false positive/negative predictions at the knee depth due to the fact that enterococci levels have much larger variability than environmental variables in time and space (see Figure 3.3). Both methods were better in predicting non-exceedances (specificity > 0.6) than exceedances (sensitivity < 0.6).

3.4 Discussion

3.4.1 Model Nowcast

In previous section, the hindcast ability of the balance model has been explored; however, in order to apply it practically, the nowcast capability is a necessity. Typically, in situ tide and wave measurements are unavailable and therefore surrogates are required. Tides can be acquired from nearby National Oceanic and Atmospheric Administration (NOAA) tidal gauges as water level observations or harmonic tidal predictions (http://tidesandcurrents.noaa.gov/). Here, we obtained tidal records at the Virginia Key station which is very close to the beach (see Figure 3.1b). In lieu of direct wave measurements, nearshore wave models (e.g., Ge et al., 2010) or, in some particular cases, wind observations can be used. For the study site, a good correlation between onshore wind speed and observed wave height was found ($r = 0.718$, $p < 0.001$). This correlation can be explained by the fact that the beach is mainly impacted by locally generated wind waves, and the onshore wind direction is approximately aligned with the longest wind

fetch within the Biscayne Bay. Using the wind and wave measurements, we fitted a linear curve between onshore wind speed and significant wave height (see Appendix-F):

$$H_1 = \begin{cases} 0.02, & if\ u_c < 0\ m \cdot s^{-1} \\ 0.02u_c + 0.02, & if\ u_c \geq 0\ m \cdot s^{-1} \end{cases} \quad (27)$$

where u_c is the cross-shore wind speed (in m s^{-1}, positive onshore and negative offshore). Hence, in the absence of wave observations or modeling, Equation (27) was applied to retrieve wave height from the wind at this beach.

The contours of cross-shore distributions of $Log_{10}ENT$ obtained from model hindcast and nowcast seem almost identical to each other (Figure 3.3e & f) and the values are highly correlated (r = 0.995). With respect to triggering beach advisories, the results based on hindcast and nowcast are comparable to each other, in terms of accuracy, specificity, and sensitivity (Table 3.4). This suggests that at this site, retrieved waves from the cross-shore winds and tidal levels observed at nearby NOAA station are feasible and satisfactory surrogates when there are no in situ measurements.

3.4.2 Model Implications for Beach Management

One major advantage of the balance model compared to the regression equation is that it provides a synoptic view of spatiotemporal distributions of microbial levels in the nearshore water, rather than only predicting microbial levels at relatively fixed locations (for instance, knee or waist depth). Our results confirm a prior study suggesting that spatial and temporal variations in indicator microbes substantially impact management decisions in recreational beaches (Enns et al., 2012). The high spatiotemporal variability of FIB is not unique at the study beach, but can also be found at other beaches (e.g., Boehm et al., 2002; Boehm, 2007; Ge et al., 2012a).

A prior study at this beach not only identified a variety of pathogens (e.g., yeasts, pathogenic bacteria, protozoa, viruses, and helminthes) in the sand, but also found significant correlations between some indicator microbes and pathogens (Shah et al., 2011). Moreover, epidemiologic studies demonstrated positive dose-response relationships of reported skin illness to both enterococci levels (Fleisher et al., 2010; Sinigalliano et al., 2010) and 24-hour antecedent rainfall (Sinigalliano et al., 2010). Another study at 7 U.S. beaches suggested sand contact activities were positively associated with gastrointestinal illness and diarrhea (Heaney et al., 2009). Our model results showed a substantial increase of enterococci loading to the beach water occurs when local wind waves coincide with high tide. Therefore, it is possible that wave-induced sediment resuspension may release pathogens from the sand reservoir. If that is the case, these environmental phenomena should be taken into account in regular beach monitoring practices.

Abdelzaher et al. (2013) proposed a framework of Comprehensive Toolbox within an Approval Process (CTBAP), with the objective of designing site-specific beach regulation for better public health protection, and ensuring protection consistency nationwide. The model approach developed in this study can be readily incorporated as a component in this suggested framework. The model can serve as a nowcast tool to provide an independent estimate of cross-shore microbial distributions. This model can also be used as a tool to examine beach responses to various “worst-case” scenarios. For example, an overnight heavy rainfall event, although it did not occur within evaluated data sets, will likely flush large amounts of enterococci onto the beach water. Our model can provide a quick estimation of enterococci condition in the early morning, which may

help the local beach managers in the decision process. These scenario tests will facilitate decision making in the case of extreme events such as thunderstorms. Last but not least, the model outcome may also be useful in guiding sampling strategy.

In addition, the balance model may have potential use in estimating counts of indicator organisms by culture-independent methods, notably quantitative polymerase chain reaction (qPCR). Some studies have found associations between gastrointestinal illness among swimmers and qPCR-measured enterococci at both freshwater and marine beaches (Wade et al. 2006 and 2010). Recently, the rapid qPCR method has been recommended in the new recreational water quality criteria (US EPA, 2012). However, the response of qPCR counts to environmental conditions may be different from culture-based counts (Boehm et al., 2009; Byappanahalli et al., 2010; Sassoubre et al., 2012). Therefore, the skill of the balance model in predicting culture-independent counts of fecal bacteria requires further model refinement and validation using new qPCR monitoring datasets in the future.

3.4.2 Model Application and Limitation

The main difference between the balance model of this study and the prior process-based water quality model (Feng et al., 2013) is in the resolution of the detailed hydrodynamic and sediment transport processes. The balance model here takes an empirical approach to directly parameterize bacterial loading with wave and tidal conditions, which essentially saves considerable time and computational resources. Due to the simplicity, however, the application of the balance model is restricted to certain types of beaches situated in coastal embayment or lakes without significant longshore current gradient and topographic variations. Moreover, sand and stormwater have to be a

prevailing source of bacteria, which also implies that the beach is not directly affected by point sources of microbial pollution (such as rivers and sewage outfalls).

The under-prediction of enterococci levels by the balance model in last two days (see Figure 3.3) may suggest that additional sources, possibly a thick wrack line observed at site, could contribute to the enterococci loading. Prior studies suggested that beach wrack is an FIB reservoir and may also provide favorable conditions for FIB survival and regrowth (Whitman et al., 2003; Shibata et al., 2004; Imamura et al., 2011). However, due to a lack of wrack quantification in the field study, the present model does not include the wrack source term. The incorporation of other potential sources into the model could improve model performance in the future.

Model adaption (i.e., parameter tuning) is a prerequisite when applying this model to other similar beaches or if the beach conditions are dramatically changed as a result of episodic events, such as beach renovations (Hernandez et al., 2014; Rippy et al., 2013) and tropical storms (Gast et al., 2011). For example, the release of microbes from the sand, tied to the wave pick-up coefficient α in Equation (17), is controlled by both sediment and microbial characteristics of the sand (Feng et al., 2013). The sediment characteristics, such as grain size and distribution, affect sediment suspension and deposition (Soulsby, 1997). The microbial characteristics, such as biofilm, mineral composition, abundance of microbes in the sand, and attachment of microbes to the sand grains, affect the amount of microbial release under external forcing (Yamahara et al., 2009; Piggot et al., 2012; Russell et al., 2012; Phillips et al., 2014). One particular example in the study site was a recent beach renovation activity in 2010 that significantly reduced enterococci levels within the sand after the renovation (Hernandez et al., 2014).

Such reduction would very likely result in less enterococci influx from the shoreline sand and thereby smaller wave pick-up coefficient, as indicated by the significant decrease of enterococci levels and exceedances in post- versus pre-renovation periods (Hernandez et al., 2014).

3.5 Concluding Remarks

In this chapter, a simplified microbial balance model is developed, specifically for low-energy beaches where sand and stormwater are major nonpoint sources. This model has been applied to a typical beach to solve the time-varying cross-shore distribution of enterococci levels. The inputs to the model are readily-available environmental factors (i.e., wind, tide, wave, solar radiation, and precipitation), which are used in the mass balance considerations of source loading, transport, and biological decay. The significant advantage of this model is its easy implementation and a detailed description of the cross-shore distribution of enterococci levels which should be useful for beach management purposes. The performance of the balance model is evaluated by comparing predicted exceedances of a beach advisory threshold value to field data, and to a traditional regression equation model. Model results represented the temporal patterns of enterococci levels associated with the diurnal cycles of solar radiation and the semidiurnal tidal oscillations. The predominant spatial pattern was as an average 1 log reduction of enterococci levels from the knee to waist depths. Both the balance model and regression equation predicted approximately 70% the advisories correctly at the knee depth and over 90% at the waist depth. The balance model has the advantage over the regression equation in its ability to simulate spatiotemporal variations of microbial levels and is recommended for making more informed beach management decisions

Chapter 4 FLORIDA BEACH WATER QUALITY: HYDROLOGIC, HYDROMETEOROLOGIC, AND GEOMORPHIC IMPACTS

4.1 Introductory Remarks

Recreational beaches are monitored for their bacterial safety through measures of fecal indicator bacteria (FIB), as some studies have shown relationships between FIB levels and gastrointestinal illness (Wade et al. 2003 & 2006). The sources of bacteria that cause illness at beaches include point sources such as sewage outfalls (Cabelli et al. 1982), and/or non-point sources such as beach sand (Heaney et al. 2009; Fleisher et al. 2010; Sinigalliano et al. 2010) and stormwater runoff (Haile et al. 1999; Colford et al. 2007; Colford et al. 2012).

Many studies have been conducted to evaluate environmental factors that influence microbial water quality at recreational beaches since the causes of microbial pollution may be site-specific, including proximity to point sources (e.g., sewage outfalls and river outflows), high background levels of bacteria and other pathogens in beach sand and wrack, dog feces, bather shedding, rainfall runoff, and/or low mixing and exchange. Beach sand has been identified as an important and pervasive source of FIB (Whitman and Nevers, 2003; Shibata et al., 2004; Yamahara et al., 2007; Halliday and Gast, 2011; Byappanahalli et al., 2012). Stormwater runoff, usually containing large amounts of FIB, is another important nonpoint source (Ahn et al, 2005; Parker et al., 2010; Wright et al. 2011).

The loading, transport, distribution, and persistence of microbial pollutants in the water column are largely determined by hydrologic, hydrometeorologic, and geomorphologic factors and processes. Wave- and/or current-induced resuspension may release sediment-bound bacteria (Feng et al., 2013; Thupaki et al. 2013). Once bacteria

enter the water column, their concentrations depend furthermore on the dilution associated with fluid mixing and circulation (Liu et al., 2006; Fiorentino et al., 2012; Ge et al., 2012). Moreover, bacterial survival in the water is highly susceptible to environmental stresses, particularly sunlight and increased temperature (Davies-Colley et al., 1999; Sinton et al., 1999; Enns et al. 2012). Shortwave ultraviolet sunlight can cause direct damage to DNA of microorganisms, while indirect inactivation is related to photo-oxidative reactions (Boehm et al., 2009; Sassoubre et al., 2012). Studies have found that natural mortality rates of FIB decrease with decreasing water temperature primarily due to lowered metabolic activities (e.g., Burkhardt et al., 2000; Hipsey et al., 2008).

Beaches along the Atlantic and Gulf of Mexico (GoM) coasts are invaluable tourism and recreational resources, which contribute significantly to the economy of the State of Florida. For health protection purposes, State beaches are regularly monitored through the Florida Healthy Beach Program, administrated by the Florida Department of Health (http://www.floridahealth.gov/). All 34 coastal counties joined this statewide program in 2000, and began to collect water samples every-other week, transitioning in 2002 to sampling on a weekly basis. As a result, a dataset of decade-long near-continuous observations of FIB has been generated across the entire state. In the past, historical water quality records in California have revealed decadal to shorter period FIB variability. The 43-year-long total coliform measurements at Huntington Beach, CA demonstrated the responses of surfzone water quality to wastewater infrastructure changes, El Nino events, and seasonal variations of rainfall (Boehm et al., 2002). A later study suggested that elevated coliform levels in the summer can be attributed to weakened stratification and persistence of FIB in cooler than average waters, while

elevated coliform levels in the winter are mainly caused by increased rainfall and stormwater runoff (Boehm et al., 2004b). The 32-year-long coliform measurements at 25 sampling sites of Newport Bay, CA showed that seasonal and inter-annual variability in rainfall runoff explains about 70% of the coliform variability; and bacterial level variations within the bay are strongly influenced by tidal mixing (Pednekar et al., 2005).

The unique FHBP historical water quality dataset allows us to examine not only the temporal, but also spatial patterns of microbial variations and their responses to the environmental forcing. To our best knowledge, no prior study has assessed water quality of so many beaches, consisting of a variety of hydrologic and geomorphic features and spanning such a long coastline (approximately 2,000 km). The specific objectives of this chapter are (1) to provide a synoptic picture of beach water quality exceedances in Florida; and (2) to determine which hydrometeorological, hydrological, and geomorphologic factors may affect microbial patterns in the intra- to inter-annual time scales.

4.2 Materials and Methods

The methods focused on collecting available long-term FIB (enterococci and fecal coliform) data and compiling environmental measures from diverse sources, including hydrometeorological factors (i.e. solar radiation and precipitation), hydrologic variables (i.e. water temperature and wave height), and beach morphologic characteristics that influence fluid mixing (i.e. beach slope and degree of exposure to waves) for the individual beaches monitored in the Florida Healthy Beaches Program.

4.2.1 Fecal Indicator Bacteria Monitoring Data

FIB data were obtained from the archives of the Florida Department of Health. Beaches considered were those included as part of the Florida Healthy Beaches Program. This Program began in 1998, with 11 Florida coastal counties participating through the monitoring and reporting of fecal coliform levels every two weeks. In August 2000, the Program was expanded to include all 34 coastal counties. In August 2002, the counties began collecting weekly samples for both enterococci and fecal coliform analyses.

The datasets used in this study were nearly decade long, from August 2000 to December 2009, when both enterococci and fecal coliform were monitored. This time frame was thus chosen to compile environmental variables from diverse sources. The original database included over 300 beaches; however, only 262 beaches with a minimum of 409 sampling events (i.e., less than 10% missing samples) were selected for further analyses. For plotting purposes, beaches were numbered from 1 to 262 starting at the northeast corner of the State in Nassau County, and proceeding clockwise along the coastline to the northwestern corner in Escambia County (see Appendix-G).

According to the Florida Healthy Beaches Program sampling protocol, beach water was sampled at waist depth in the morning by trained personals from county health departments, and samples were analyzed by standard membrane filtration culture method. Samples below the detection limit were assigned a value of 0.5 CFU/100 mL, half the detection limit of 1 CFU/100 mL.

To achieve normality, logarithmic transforms were performed on the levels of enterococci ($\log_{10}ENT$) and fecal coliform ($\log_{10}FC$) before averaging. Log-means, other than arithmetic means, were calculated because FIB data can vary substantially, by at

least 3 orders of magnitude. The data were evaluated on both long-term (i.e. 10 year) and seasonal basis. The four seasons were defined as January-February-March (JFM), April-May-June (AMJ), July-August-September (JAS), and October-November-December (OND).

The Florida county health departments issue health warnings or advisories when bacterial levels exceed a set threshold level based upon either geometric mean or single sample analyses (Table 4.1). Warnings are issued based upon fecal coliform measures whereas advisories are issued based upon enterococci measures. Given the high variability of the bacterial levels observed at Florida beaches, health advisories and warnings are issued only when two consecutive single-sample exceedances are observed. However, these resamples after exceedances were excluded for our analyses to eliminate bias towards exceedance events.

Table 4.1 Thresholds for Beach Warnings and Advisories Based Upon Fecal Coliform and Enterococci Concentrations, Respectively. The single-sample thresholds are utilized in this study.

	Fecal Coliform [a] (CFU/100 ml)	Enterococci [b] (CFU/100 ml)
Monthly Geometric Mean	≥ 200	≥ 35
Single Sample Threshold	**≥ 400**	**≥ 104**

a. Source: the Florida Department of Environmental Protection surface water quality criteria;
b. Source: the US EPA Ambient Water Quality Criteria for Bacteria (1986).

In order to put the monitoring results in terms of beach warnings or advisories, the CFU/100 mL concentration measures included in the database were converted to either an "exceedance" or a "non-exceedance" values based upon the single sample threshold levels listed in Table 4.1. The results for the whole 10-year period were then reported as percent exceedance, which represents the percentage of the sampling points within that period exceeding either 400 or 104 CFU/100 mL for fecal coliform or enterococci, respectively. Percent exceedance based on long-term monitoring records can provide a relative measure of overall health and quality of beach recreational waters. We further defined that a beach exceeding less than 2.5% of the time was rated as a rare-exceedance beach, while a beach exceeding more than 10% was a high-exceedance beach.

4.2.2 Beach Classifications

The first beach classification is purely based upon geographic location. The Atlantic beaches are those along the Florida Atlantic coast, from northernmost Nassau County at the Florida-Georgia border through Miami-Dade County. The GoM beaches start from southernmost Monroe County (i.e. Florida Keys), along the concave GoM coastline, and end at Escambia County at the Florida-Alabama border (See Appendix-G).

The second beach classification is based upon the wave energy level, depending on beach exposure to or sheltering from wave action. On one hand, high-energy (or exposed) beaches are directly open to the sea and frequently exposed to offshore waves; therefore, they are more energetic with relatively high fluid mixing rates. These beaches are located in the barrier islands along the Florida Atlantic coast and some parts of the GoM coast. On the other hand, low-energy (or sheltered) beaches are sheltered from offshore wave action and therefore have low fluid mixing rates. These beaches can be

typically found within the coastal bays, surrounded by marshes, protected by manmade structures, behind broad coral reefs, or inside the Intracoastal Waterway. Google Earth images of typical high- and low-energy beaches are provided in Appendix-H.

4.2.3 Environmental Measures

Environmental measures compiled for study beaches included wave, sea surface temperature (SST), solar radiation, and precipitation. The beach sampling locations, provided through the FHBP archives, were used as reference locations for data compilation.

4.2.3.1 Wave

Wave information was obtained through National Oceanic and Atmospheric Administration (NOAA) National Center for Environmental Prediction (NCEP) WAVEWATCH III Global wave model hindcast using the Climate Forecast System Reanalysis Winds (Chawla et al., 2013). Along the U.S. east coast and GoM, this database provided 1/15° grid resolution wave hindcast every 3 hours. The hindcasts of significant wave height (h_s) agree well with observations at four National Data Buoy Center (NDBC) stations, with the correlation coefficients all above 0.9 (see Appendix-I). Significant wave heights were obtained at an offshore location 3 model grid points (~20 km) away from the beach in the normal direction, which represented deep-water wave climate outside the nearshore zone. This offshore location, other than beach location, was chosen due to model limitations in spatial resolution and underrepresentation of processes in the nearshore (Chawla et al., 2013). Beach offshore wave heights were calculated through a two-dimensional (2-D) linear interpolation. As for low-energy beaches, wave heights were assumed zero all the time. In relatively large bays or long

waterways, local wind may sometimes generate waves; however, the wave heights are mostly small, and would be minimal if averaged on seasonal or longer time scales. The overall wave energy level of each beach is quantified by averaging wave heights in the 10-year time period.

4.2.3.2 Solar Radiation

Solar radiation was calculated using the Simple Model for the Atmospheric Radiative Transfer of Sunshine (SMARTS), given typical cloudless atmospheric conditions (i.e., U.S. Standard Atmosphere) on the surface of the water at the beach locations (Gueymard, 2003a & 2003b). Model-predicted direct beam broadband irradiances (W m^{-2}) were verified with radiometer irradiance measurements for a whole year (see Appendix-J). Agreement between model and observation was high ($r = 0.88$, $p < 0.01$), although overestimation sometimes occurred in the daytime because of the cloudless-sky model assumption. Monthly mean daily-total direct beam irradiations (MJ m^{-2}) at all beaches were calculated with a model-provided input option. First, we obtained yearly-total irradiances by integrating daily-total irradiances. Then, the daily-total values were integrated within each of the four seasons and averaged to seasonal mean daily-total irradiation.

4.2.3.3 Sea Surface Temperature

Sea surface Temperature (SST) was obtained from NOAA National Climatic Data Center high-resolution SST analysis products. The analyses of Advanced Very High Resolution Radiometer (AVHRR) infrared satellite data yielded a spatial resolution of 1/4° daily global SST (Reynolds et al., 2007). Correlations of satellite-retrieved daily SST and daily-averaged water temperature observations at four aforementioned NDBC

stations were all above 0.96 (see Appendix-K). Since the water areas very close to the land were masked, SSTs of each beach were extracted from the nearest position with SST output.

4.2.3.4 Precipitation

The precipitation data were obtained from National Aeronautics and Space Administration (NASA) Tropical Rainfall Measuring Mission (TRMM) products, which have been extensively validated in Florida (Wolff et al., 2005; Amitai et al., 2006; Wang and Wolff, 2012). We extracted a series of maps of daily cumulative rainfall covering the whole Florida (spatial resolution of 1/4°), and daily precipitations were then interpolated at corresponding beach locations for the study period.

4.2.3.5 Beach Slope

Beach slope was retrieved based on 3 arc-second (~90 m) bathymetric dataset of NOAA's U.S. Coastal Relief Model (http://www.ngdc.noaa.gov/mgg/coastal/coastal.html). The slope was calculated from the elevation difference between two points. The starting point is located at the mean sea level waterline, and then extended normally offshore by a distance of 3 grid points (9 arc-second) to reach the end point. The elevations of these two points were linearly interpolated from the bathymetry. An index of mean beach slope was obtained by dividing elevation difference by the distance. In this study, the beach slope was assumed to be fairly stable throughout the time.

4.2.4 Statistical Analyses

One-way analysis of variance (ANOVA) was conducted in Matlab Statistical Toolbox (Mathworks, Natick, MA). The correlation coefficient was also calculated in Matlab with a *p*-value less than 0.05 regarded as significant.

4.3 Results

4.3.1 Exceedance Percentage

Overall, the majority of the studied Florida beaches have good water quality (Fig 4.1a and 4.1b). Based upon enterococci, about 61% of the total beaches were characterized by rare occurrences of beach advisories as the criteria are exceeded less than 2.5% of the time (Table 4.2). If fecal coliform is utilized as the indicator microbe, 76% were considered to have rare occurrences. With respect to high exceedance (exceedances occurring more than 10% of the time), 9.2% (n = 24) of the beaches fell within this category based upon enterococci and 3% (n = 8) based upon fecal coliform. Hot spots of the most severe water quality were identified in the swampy Big Bend area and west Florida Panhandle along the northern GoM coast as a series of beaches in these areas exceeding enterococci threshold more than 20% of the time (Figure 4.1a). Interestingly, the beaches of the Big Bend do not emerge as hot spots based on fecal coliform (Figure 4.1b), mainly because of higher threshold level for fecal coliform than for enterococci (400 versus 104 CFU/100 mL; Table 4.1). Other possibilities are that fecal coliform and enterococci may originate from different sources and behave differently in the environment. Fecal coliform and enterococci observations are generally comparable, with moderate correlations of 0.2 to 0.7 between $\log_{10}ENT$ and $\log_{10}FC$ (Figure 4.1c).

4.3.2 Comparison of Exceedance: High- versus Low-energy Beaches

Wave energy level strongly influences beach water quality. High- and low-energy beaches have very different water quality characteristics. Over 80% of the high-energy beaches were in the rare exceedance category and only one high-energy beach was in the high exceedance category based on enterococci and none were in this category based on fecal coliform (Table 4.2). On the contrary, for low-energy beaches, only 15.0% are in the rare exceedance category, whereas 26.4% are in the high exceedance category for enterococci. The differences between high- and low-energy beaches were statistically significant ($p < 0.01$).

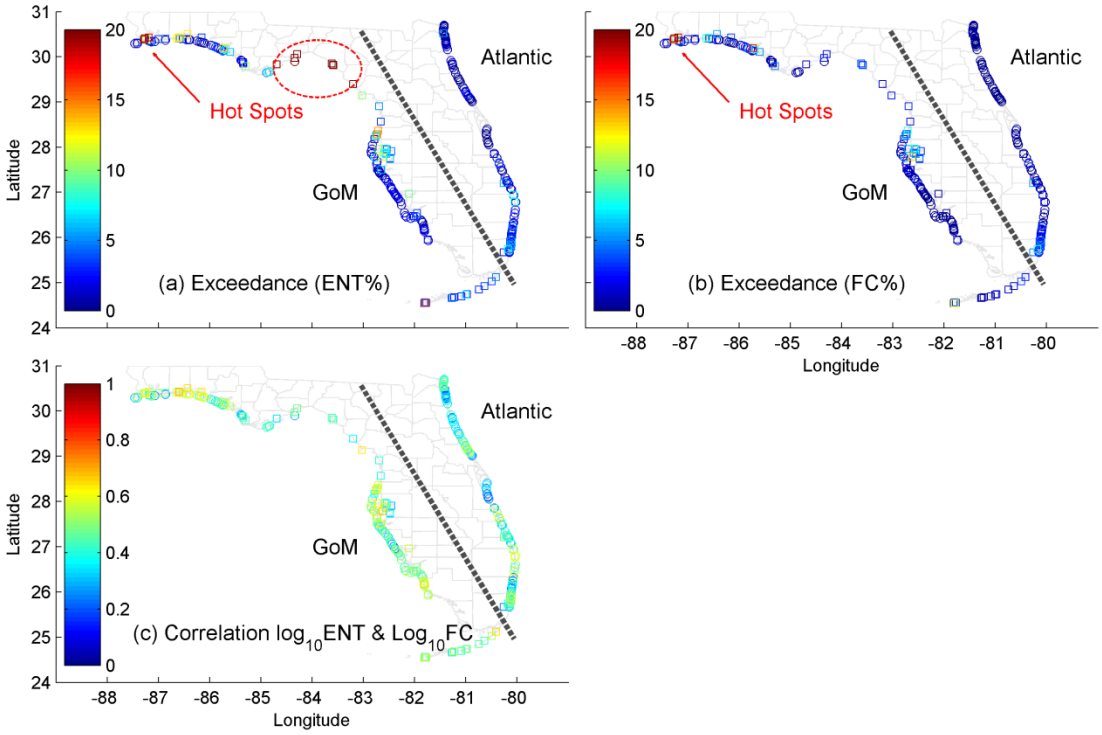

Figure 4.1 Percentage of water samples exceeding regulatory thresholds at 262 Florida beaches based on (a) enterococci levels and (b) fecal coliform levels. (c) Correlations between $\log_{10}ENT$ and $\log_{10}FC$. Correlation coefficients are shown only when p-values are less than 0.05. Circles and squares indicate high- and low-energy beaches. The color bars indicate exceedance percentage in 4.1a and 4.1b, and correlation coefficient in 4.1c. The dashed line separates Atlantic and GoM beaches.

4.3.3 Comparison of Exceedance: Atlantic versus GoM Beaches

The occurrence of FIB exceedances shows spatial heterogeneities. Taken as a whole, Atlantic beaches have better water quality than GoM ones (Figure 4.1 and Table 4.2). All high exceedance beaches are located along the GoM side, whereas the majority of the Atlantic beaches (~80%) rarely exceed fecal indicator thresholds. The average enterococci exceedance percentage of 106 Atlantic beaches is 1.52%, significantly lower than 5.07%, average of 156 GoM beaches ($p < 0.01$). Mean fecal coliform exceedance percentages of Atlantic and GoM beaches are 0.94% and 2.38%, and their differences are also significant ($p < 0.01$).

4.3.4 Relationships between Exceedances and Environmental Factors

Beach slope (Figure 4.2a) negatively correlated with enterococci percent exceedance ($r = -0.31$, $p < 0.01$). Long-term mean wave height (Figure 4.2b) also negatively correlated with enterococci percent exceedance ($r = -0.51$, $p < 0.01$). Similarly, negative correlations were found between fecal coliform percent exceedance and beach slope ($r = -0.21$, $p < 0.01$) as well as long-term mean wave height ($r = -0.46$, $p < 0.01$). In other words, the mild sloping beach and lower wave energy level correspond to higher exceedance percentages. In contrast, lower exceedance percentage coincides with intermediate to steep sloping beach and higher wave energy level. More significantly, hot spots of persistent exceedance occurrences in the Big Bend area correspond to zero wave energy at flat beaches.

No significant correlations were found between exceedance percentages and long-term mean SST, yearly total irradiance or yearly total rainfall. The mean water temperature and irradiance were mostly latitude dependent (higher values in lower

latitude and vice versa), except for the coastal waters in southeast Florida that are warmed up by the Gulf Stream (Figure 4.2c and 4.2d). Mean yearly rainfall is highest in southeast Florida and western Florida Panhandle while lowest in the Florida Keys (Figure 4.2e). The spatial patterns of temperature, solar radiation, and rainfall distributions do not coincide with the patterns of FIB exceedance, beach slope or wave height.

Table 4.2 Comparison of exceedance percentages of high- versus low-energy and Atlantic versus GoM beaches

Beach Classification		Total Number	Rare Exceedance (≤ 2.5%)		Medium Exceedance (2.5-10%)		High Exceedance (≥ 10%)	
			ENT	FC	ENT	FC	ENT	FC
All		262	159 (60.7%)	198 (75.6%)	79 (30.1%)	56 (21.4%)	24 (9.2%)	8 (3.0%)
Wave Energy Level	High-energy	175	**146 (83.4%)**	**157 (89.7%)**	28 (16.0%)	18 (10.3%)	1 (0.6%)	0 (0%)
	Low-energy	87	13 (15.0%)	41 (47.1%)	51 (58.6%)	38 (43.7%)	**23 (26.4%)**	**8 (9.2%)**
Geographic Location	Atlantic	106	**83 (78.3%)**	**89 (84.0%)**	23 (21.7%)	17 (16.0%)	0 (0%)	0 (0%)
	GoM	156	76 (48.7%)	109 (69.9%)	56 (35.9%)	39 (25.0%)	**24 (15.4%)**	**8 (5.1%)**

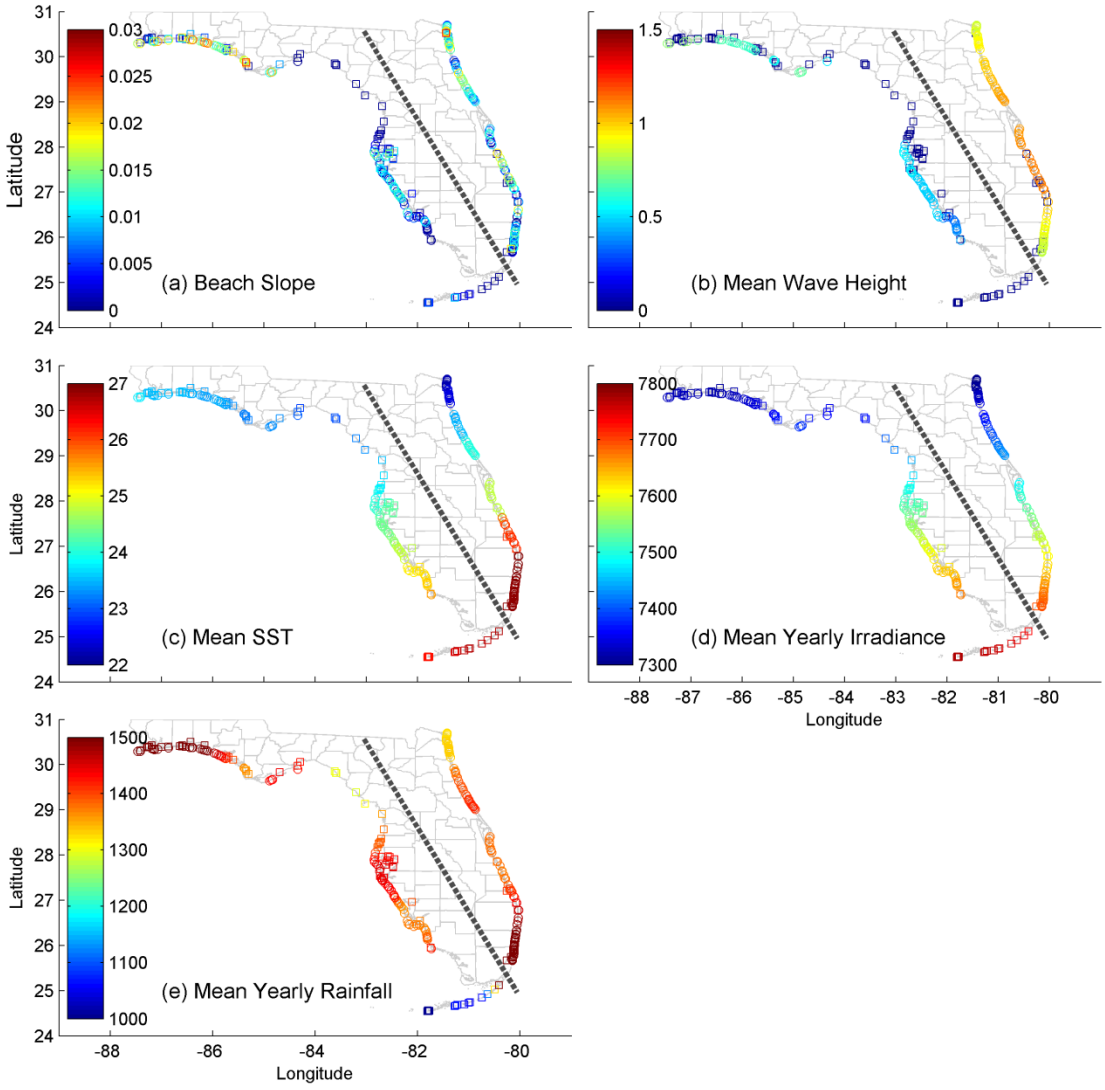

Figure 4.2 Long-term mean environmental variables: (a) beach slope; (b) wave heights (m); (c) mean SST (°C); (d) yearly total irradiation (MJ m^{-2}); and (e) yearly total rainfall (mm).

4.3.5 Seasonal Variations

FIB levels demonstrated seasonal variability, covarying with water temperature, solar radiation, wave height, and precipitation in the intra- to inter-annual time scales (Figure 4.3). In general, seasonal FIB variations in Atlantic and GoM beaches are out of phase. Along the Atlantic coast, FIB levels tend to be higher in the winter months (i.e., dry season with bigger waves, lower temperature and radiation) and lower in the summer (i.e., wet season with smaller waves, higher temperature and radiation). Seasonal mean $\log_{10}ENT$ and $\log_{10}FC$ have positive correlations with wave heights but negative correlations with both water temperature and solar radiation (Figure 4.4). This may be explained by the facts that waves resuspend sediment and concurrently release bacteria from the sand (Feng et al., 2013; Thupaki et al., 2013), which can then survive longer in the relatively cooler temperature and less solar radiation (Sinton et al., 1999; Boehm et al. 2004). The negative correlations between seasonal mean FIB levels and cumulative rainfall at some Atlantic beaches seem to be counterintuitive because it is unlikely that more rainwater runoff leads to less bacterial presence in beach water. Since there are limited rivers and insignificant river outflows onto the Florida Atlantic coast, rainfall is less likely to be a dominant factor at Atlantic beaches. Seasonal variations of FIB are likely governed by combined effects of wave, water temperature, and solar radiation.

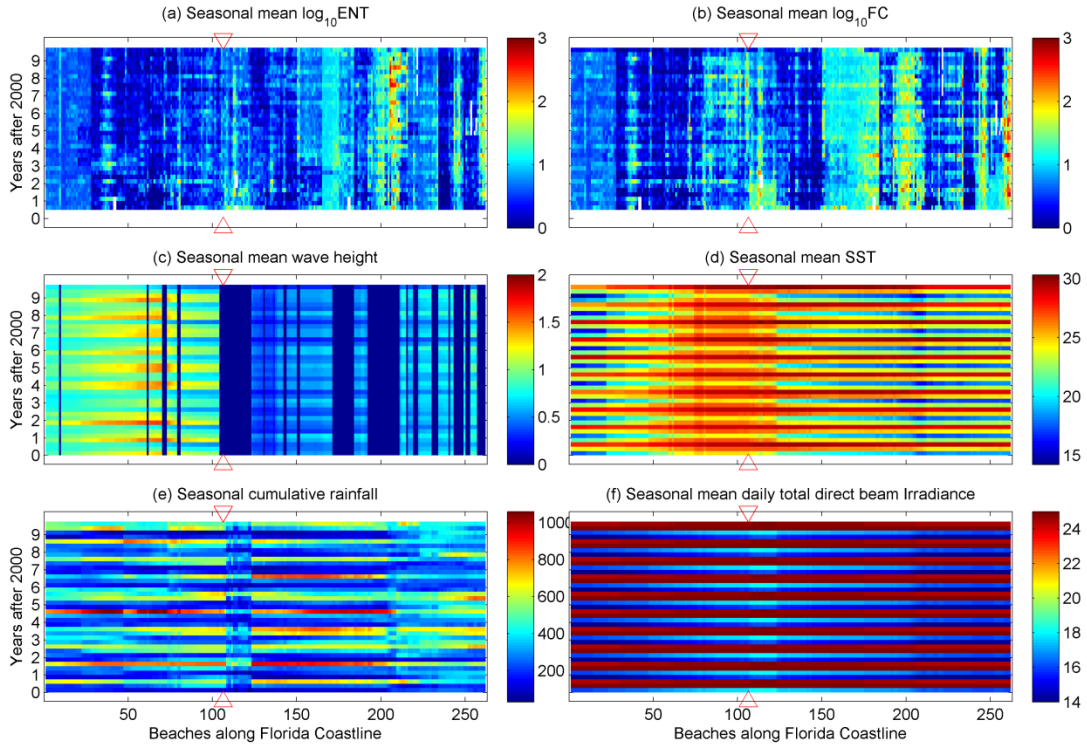

Figure 4.3 Seasonal means. (a) $\log_{10}ENT$ (in $\log_{10}${CFU/100 mL}); (b) $\log_{10}FC$ (in $\log_{10}${CFU/100 mL}); (c) wave height (in m); (d) SST (in °C); (e) cumulative rainfall (in mm); and (c) daily total direct-beam irradiation (in MJ m^{-2}). The red triangles divide Atlantic beaches to the left and GoM beaches to the right.

GoM beaches display the opposite seasonal patterns to Atlantic ones. FIB levels are relatively higher in the summer seasons and lower in the winter. It was found that mean log-transformed FIB levels positively correlate with cumulative rainfall at a majority of GoM beaches (Figure 4.4). Therefore, elevated FIB levels at GoM beaches in the wet seasons are likely dominated by bacterial and nutrient loading from the river effluent and runoff associated with rainfall. This is further supported by the fact that major rivers in Florida discharge into the GoM (see Appendix-K), although seasonal rainfall on both sides of the coast is in phase with each other.

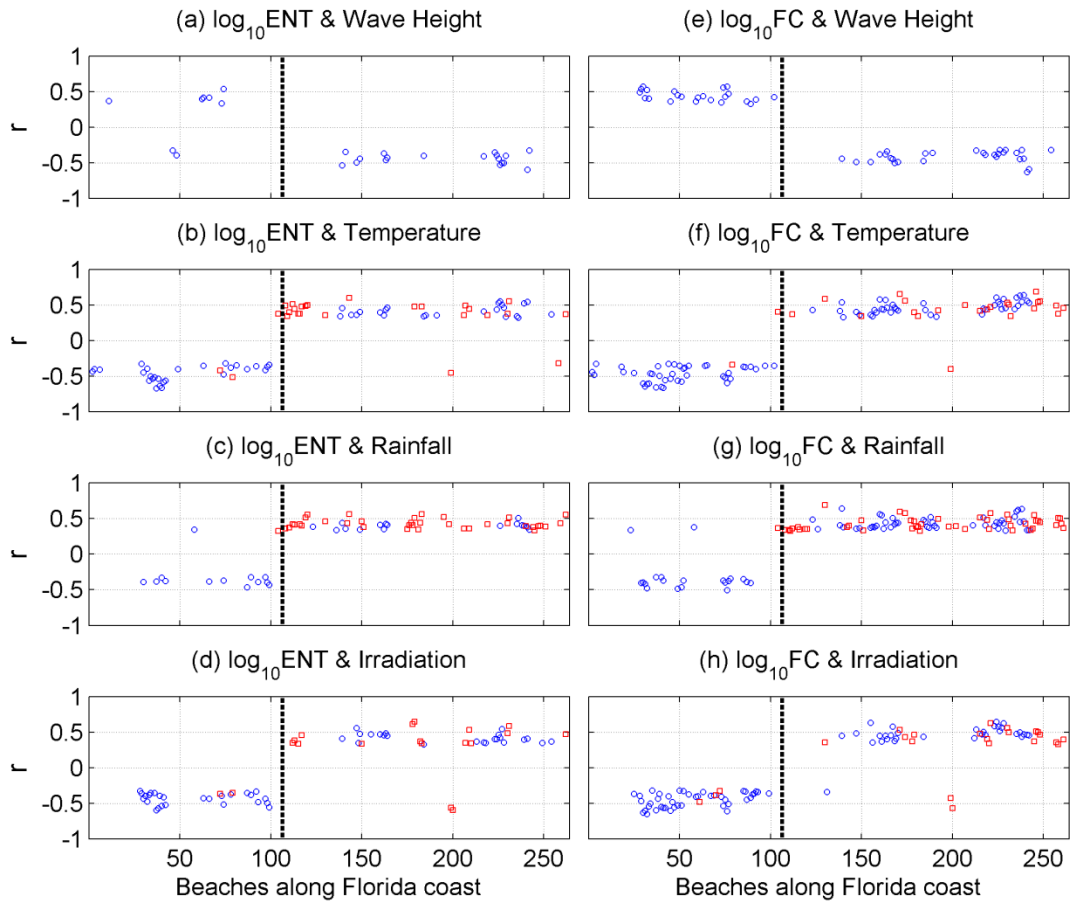

Figure 4.4 Correlations between seasonal mean $\log_{10}ENT$ (left panels) or $\log_{10}FC$ (right panels) and seasonal mean significant wave heights, water temperature, cumulative rainfall, and irradiation. Correlation coefficients are shown only when *p*-values are less than 0.05. The blue circles and red squares represent high- and low-energy beaches, respectively. The vertical dash line divides Atlantic and GoM beaches.

4.4 Discussion

4.4.1 Beach Wave Energy Level

Beach wave energy level may control the abundance of bacteria in the sand, as well as fluid mixing, which further determine water quality characteristics. The settlement and regrowth capability of bacteria in the sand reservoir is restricted when sediment is consistently reworked by waves breaking and dissipating in the nearshore zone (Yamahara et al., 2007). The wave energy patterns observed in this study are supported by a prior shoreline change study showing that the more energetic Florida Atlantic coast has much larger longshore sediment transport rate than the less energetic GoM coast (Absalonsen and Dean, 2011). At high wave energy beaches, even if microbial pollution may occur within the nearshore zone, the pollutants would unlikely accumulate or deposit due to vigorous turbulent mixing and strong surfzone currents (Grant et al., 2005; Rippy et al., 2013).

In contrast, at the GoM Big Bend coast, low energy level, mild beach slope, and calm water environment may facilitate bacterial settlement, aggregation, and even replication in the sand under certain environmentally favorable conditions, such as tide-induced intermittent wetting/drying (Yamahara et al., 2009). The surrounding muddy shoreline and river inflow to this region may function as putative FIB sources and also provide necessary nutrients for FIB regrowth (Litton et al., 2010).

The above hypothesis linking beach energy level to bacterial abundance of the sand and beach water quality is supported by prior multi-beach studies in California and Florida (Yamahara et al. 2007; Phillips et al., 2011a). The California coast sand survey of 55 beaches found that enterococci levels of the sand are highest at sheltered beaches

associated with nearby potential FIB sources (Yamahara et al., 2007). Sand sampling campaigns at eight South Florida beaches suggested that beaches with higher sand enterococci levels generally have more enterococci exceedances (Phillips et al., 2011a).

4.4.2 Implications for Water Quality Management

The opposite patterns in FIB exceedances and seasonal variations among the Atlantic versus GoM beaches have important implications for beach management practices in the State of Florida, particularly the GoM beaches where FIB exceedances are much more likely to occur. We recommend that FIB inputs to rivers and stormwater should be minimized in the Gulf coast counties. The State currently has on-going programs (http://www.dep.state.fl.us/water/tmdl/) to minimize the Total Daily Maximum Loads within the State's interior waters and these programs should continue, especially for rivers that discharge towards the Gulf of Mexico, in light of the patterns observed in coastal FIB levels.

4.5 Concluding Remarks

This chapter evaluated the relationships between beach water quality and hydrologic, hydrometeorologic, and geomorphic factors using historical records of FIB data for 262 beaches within the State of Florida. Results showed that low-wave-energy beaches exceeded the EPA thresholds significantly more than high-wave-energy beaches ($p < 0.01$), and that GoM beaches have significantly worse microbial water quality than Atlantic ones ($p < 0.01$). Percent exceedances negatively correlated with both long-term mean wave energy and beach slope, suggesting that beach wave energy level is an important factor in determining overall microbial water quality. In addition, we found that seasonal FIB variations in Atlantic and Gulf of Mexico (GoM) beaches are generally

out of phase. There are opposite correlations in seasonal mean log-transformed FIB levels and environmental variables (i.e., wave height, water temperature, solar radiation, and precipitation) between Atlantic versus GoM beaches. Microbial variations on each of Florida coasts are likely controlled by different mechanisms, which would require different beach management strategies to minimize FIB exceedances.

Chapter 5 CONCLUSIONS AND RECOMMENDATIONS

5.1 Conclusions

The overall goal of this dissertation is to elucidate the loading, transport, and fate of fecal indicator bacteria (FIB) at nonpoint source beaches in subtropical marine environments. The goal has been achieved through three studies in Chapter 2 to 4.

The first major contribution of this dissertation is the development of an innovative coupled microbe-hydrodynamic-morphological model, which accounts for nonpoint source loads of enterococci from sediment, bed pore water, and runoff (Chapter 2). This modeling work highlights the mechanisms of waves and tides in moving enterococci out from the sediment reservoir to the beach water.

The second major contribution is a new mass balance model, which provides quick estimations of transient cross-shore distribution of enterococci at nonpoint source beaches where sand and runoff are primary source (Chapter 3). Compared to traditional multivariable linear regression model, the balance model has similar accuracy in predicting beach advisory but provides synoptic information instead of single point predictions. The time-varying distribution of enterococci levels could be useful to beach managers for making more informed management decisions.

The scope of this dissertation is greatly broadened by assessing overall water quality patterns of 262 beaches across the State of Florida over 10 years (Chapter 4). The synthesis of decade-long weekly measurements of enterococci and fecal coliform levels reveal the dramatic differences in water quality exceedances among Atlantic versus Gulf of Mexico beaches, as well as high- versus low-wave-energy beaches. The other striking finding is that the seasonal FIB variations along the Atlantic and Gulf of Mexico coasts

are generally out of phase. Further analyses with environmental variables suggest that different mechanisms possibly dominate two sides of the Florida coast, which would require different management strategies to minimize the FIB exceedances.

5.2 Recommendations

More work is needed to study the intrinsic characteristics of the sand (e.g., sand mineralogy, grain size distribution, porosity, hydraulic conductivity, and biofilm) and the environment (e.g., salinity, temperature, nutrient, and moisture content) in controlling the abundance, regrowth, and redistribution of bacteria in the sand and attachment/detachment mechanisms. The advancement in studying sand-bacteria relationships would contribute to further model development from at least two points.

First, through-beach transport, a pathway by which bacteria may be transported downward from the sand to the groundwater, is a missing link in present coupled model (Chapter 2) and in the vast majority of existing water quality models. Field studies at multiple beach sites have revealed that bacteria are the most abundant in the dry sand above the high tide line (e.g., Whitman and Nevers, 2003; Yamahara et al., 2007; Piggot et al., 2012). However, this part of the beach can only be inundated during spring high tide or swash uprush. Few studies have investigated the role of swash infiltration/exfiltration in mobilizing bacteria within the sand and porewater. Improved understanding of coupling between swash, infiltration/exfiltration, and groundwater flow would be vital in successfully quantifying microbial mass balance budget and exchange within the beach-aquifer-ocean system.

Second, the regrowth and redistribution processes of bacteria have not been incorporated in present model or, to the best of my knowledge, any other water quality

model. Although the constant sand reservoir assumption in this modeling effort works quite well at the case study beach (see subsection 2.4.2), this assumption may not hold at some other sites or under abnormal circumstances. For instance, a prior sand core study has demonstrated the redistribution of enterococci in the sand under beach erosion and accretion during storm conditions. One unique feature of the coupled model is that it allows tracking, varying, and redistributing contaminated sand fractions over the entire model domain, as well as in the layered bed (subsection 2.2.4.3.1). With more laboratory and field experiments, the regrowth and redistribution of FIB can be implemented as time-varying fractions of contaminated sand in future model versions.

Newly emerging molecular and culture-independent methods for FIB, such as quantitative polymerase chain reaction (qPCR), may provide additional data sources for model development and validation, in conjunction with traditional culture-based measurements. The cultivation and molecular methods were combined to examine the photoinactivation mechanisms of enterococci (Boehm et al., 2009; Sassoubre et al., 2012). The qPCR datasets were also utilized to construct multivariable regression models (e.g. Byappanahalli et al.; 2010; Gonzalez and Noble, 2014). However, few studies have incorporate both culture-based and qPCR measurements into the process-based models. This is a future direction of the water quality modeling.

Appendix-A Sediment Transport in XBeach

Suspended sediment transport is calculated from a depth-averaged advection-diffusion equation (Galappatti and Vreugdenhil, 1985):

$$\frac{\partial hC_{s,i}}{\partial t} + \frac{\partial hC_{s,i}u^E}{\partial x} + \frac{\partial hC_{s,i}v^E}{\partial y} - \frac{\partial}{\partial x}\left[D_h h \frac{\partial C_{s,i}}{\partial x}\right] - \frac{\partial}{\partial y}\left[D_h h \frac{\partial C_{s,i}}{\partial y}\right] = \frac{hC_{eq,s,i} - hC_{s,i}}{T_{s,i}} \quad \text{(A1)}$$

where $C_{s,i}$ represents the depth-averaged suspended sediment concentration of sediment class i, with class 1 and 2 representing contaminated and clean sand, respectively; D_h is the sediment diffusion coefficient, h the local water depth, and u^E and v^E are short-wave-averaged Eulerian velocities (see Roelvink et al., 2009 for details).

The uptake of sediment is represented by an adaptation time $T_{s,i}$, given by a simple approximation based on the local water depth h and sediment fall velocity w_s:

$$T_{s,i} = \max\left(0.05\frac{h}{w_s}, 0.2\ s\right) \quad \text{(A2)}$$

where a small value of $T_{s,i}$ corresponds to nearly instantaneous sediment response (Reniers et al., 2004). Uptake of sediment, U, occurs if there is a positive difference between the equilibrium concentration, $C_{eq,s,i}$, and the actual sediment concentration, $C_{s,i}$, thus representing the source term in the sediment transport equation (see Figure 2.2). Deposition, D, occurs when there is a negative difference and thus represents a sink term for the suspended sediment.

The equilibrium suspended sediment concentration is calculated with the sediment transport formulation of Soulsby-van Rijn (Soulsby, 1997), considering the stirring due to both Eulerian mean velocity u^E and near-bed short wave orbital velocity u_{rms}:

$$C_{eq,s,i} = p_i \frac{A_{ss,i}}{h}\left[\left(|u^E|^2 + 0.018\frac{u_{rms}^2}{C_{d,i}}\right)^{0.5} - u_{cr}\right]^{2.4}(1 - \alpha_b m) \quad \text{(A3)}$$

where p_i represents the fraction of sediment class i within the active layer at the bed (top sediment layer in Figure 2.2). Suspended load coefficient $A_{ss,i}$ is a function of sediment grain size, relative density of the sediment and the local water depth (see Soulsby, 1997 for details). $C_{d,i}$ is the drag coefficient due to flow velocity only. A threshold velocity u_{cr} must be exceeded before sediment is set to motion. Bed slope (m) and a calibration factor (α_b) are introduced to account for bed-slope effects.

The near-bed short wave orbital velocity, u_{rms}, is obtained using linear wave theory:

$$u_{rms} = \frac{\pi H_{rms}}{T_{rep}\sqrt{2}\sinh(kh)} \tag{A4}$$

where H_{rms} is the root-mean-squared wave height calculated from a wave action balance equation (see Roelvink et al., 2009 for details), and T_{rep} is the representative intrinsic wave period.

The critical velocity is given by (Soulsby, 1997):

$$u_{cr} = \begin{cases} 0.19(d_{50})^{0.1}\log_{10}\left(\frac{4h}{d_{90}}\right) & \text{for } 0.1 \le d_{50} \le 0.5 \text{ mm} \\ 8.5(d_{50})^{0.6}\log_{10}\left(\frac{4h}{d_{90}}\right) & \text{for } 0.5 \le d_{50} \le 2.0 \text{ mm} \end{cases} \tag{A5}$$

where d_{50} is medium grain diameter and d_{90} is the grain diameter where 90% of the sediment is finer.

Cross-shore suspended sediment transport due to advection and diffusion is given by:

$$S_{s,i,x}(x,y,t) = hC_{s,i}u^E - D_h h\frac{\partial C_{s,i}}{\partial x} \tag{A6}$$

And similarly for the alongshore transport:

$$S_{s,i,y}(x,y,t) = hC_{s,i}v^E - D_h h\frac{\partial C_{s,i}}{\partial y} \tag{A7}$$

The bed-load sediment transport is assumed to react instantaneously to the near-bed velocity and is given by:

$$S_{b,i,x}(x,y,t) = C_{eq,b,i}u^E \tag{A8}$$

$$S_{b,i,y}(x,y,t) = C_{eq,b,i}v^E \tag{A9}$$

where the equilibrium bed-load concentration ($C_{eq,b,i}$) is also given by the Soulsby-van Rijn formulation (Soulsby, 1997):

$$C_{eq,b,i} = p_i \frac{A_{sb,i}}{h}\left[\left(|u^E|^2 + 0.018\frac{u_{rms}^2}{C_{d,i}}\right)^{0.5} - u_{cr}\right]^{2.4}(1-\alpha_b m) \tag{A10}$$

where $A_{sb,i}$ is bed load coefficient.

By summing the calculated sediment transport rates for all sediment classes, the change in bed elevation is computed from the sediment balance:

$$\frac{\partial z_b}{\partial t} + \frac{f_{mor}}{(1-n_p)}\left[\frac{\partial \sum_i (S_{s,i,x}+S_{b,i,x})}{\partial x} + \frac{\partial \sum_i (S_{s,i,y}+S_{b,i,y})}{\partial y}\right] = 0 \tag{A11}$$

where z_b is bed level, n_p is porosity, and f_{mor} represents a morphological factor to speed up the bed evolution (e.g., Reniers et al., 2004; f_{mor} = 0 means constant bed level).

Appendix-B Groundwater Flow in XBeach

Groundwater system is an ongoing developing module in XBeach (R. McCall personal communication). Darcy's law is utilized to calculate horizontal flow velocities from the groundwater head (p_{gw}) gradient, assuming laminar flow conditions for sandy beaches:

$$u_{gw} = -\kappa_x \frac{\partial p_{gw}}{\partial x} \tag{B1}$$

$$v_{gw} = -\kappa_y \frac{\partial p_{gw}}{\partial y} \tag{B2}$$

where u_{gw} and v_{gw} are groundwater flow velocities (in m/s), and k_x and k_y are hydraulic conductivities (also in m/s).

The groundwater head is determined as follows:

If there is no surface water (i.e., a dry grid), the groundwater head is equal to the groundwater surface level (η_{gw}) of the same grid at previous time step:

$$\left[p_{gw}\right]_{i,j}^{n} = \left[\eta_{gw}\right]_{i,j}^{n-1} \qquad \text{where } wetz_{i,j}^{n-1} = 0 \tag{B3}$$

where wetz is a wet-dry grid identifier, which is equal to 1 when a grid is wet and 0 when it is dry.

For a wet cell with surface water, if groundwater surface level is higher or equal to the bed level z_b, the groundwater head is equal to the surface water head z_s. When groundwater level is more than a depth value ($d_{wetlayer}$) below the bed, the groundwater head is no longer affected by the surface water head but equal to groundwater level. Within the intermediate depth or the interaction layer, linear interpolation is conducted using a relative groundwater level (fac), defined as:

$$\mathrm{fac}_{i,j}^{n}=\begin{cases}0\,, & \text{if } [z_b]_{i,j}^{n-1}-\left[\eta_{gw}\right]_{i,j}^{n-1}<0\\ \left([z_b]_{i,j}^{n-1}-\left[\eta_{gw}\right]_{i,j}^{n-1}\right)/d_{wetlayer}\,, & \text{if } 0\le [z_b]_{i,j}^{n-1}-\left[\eta_{gw}\right]_{i,j}^{n-1}\le d_{wetlyaer}\\ 1\,, & \text{if } [z_b]_{i,j}^{n-1}-\left[\eta_{gw}\right]_{i,j}^{n-1}>d_{wetlyaer}\end{cases} \tag{B4}$$

where $d_{wetlayer}$ is the thickness of surface-subsurface water interaction layer.

The groundwater head is thereby determined as:

$$\left[p_{gw}\right]_{i,j}^{n}=\left[\eta_{gw}\right]_{i,j}^{n-1}+\left(1-\mathrm{fac}_{i,j}^{n}\right)\left([z_s]_{i,j}^{n-1}-\left[\eta_{gw}\right]_{i,j}^{n-1}\right)\quad \text{if } \mathrm{wetz}_{i,j}^{n-1}=1 \tag{B5}$$

The vertical flow across the sediment-water interface, referred to as exfiltration or infiltration, is also simulated in XBeach. This flow is defined positive downward from surface to groundwater and is given in terms of surface water for the continuity equation (i.e., 100% porosity). Such flow may have important implications to the microbial balance that involves the convective microbial exchange between surface water and groundwater.

Exfiltration takes place when groundwater level exceeds the bed level. That exceeding amount of groundwater determines the flow rate and also joins in the surface water in the same numerical time step:

$$w_{i,j}^{n}=\left(\frac{[z_b]_{i,j}^{n-1}-[\eta_{gw}]_{i,j}^{n-1}}{\Delta t}\right)n_p \qquad if\ \left[\eta_{gw}\right]_{i,j}^{n-1}\ge [z_b]_{i,j}^{n-1} \tag{B6}$$

where n_p is the porosity.

Infiltration can occur where surface water is on top of bed and groundwater level is below bed. XBeach models infiltration uses a quasi-3D model and Darcy flow:

$$w=-k_z\left(\frac{\partial p_{gw}}{\partial z}+1\right)n_p \tag{B7}$$

$$w_{i,j}^{n} = \begin{cases} 0\,, & if\ \ wetz_{i,j}^{n-1} = 0\ and\ \left[\eta_{gw}\right]_{i,j}^{n-1} < \left[z_b\right]_{i,j}^{n-1} \\ \left[\left(1 - fac_{i,j}^{n}\right)\frac{\left[z_b\right]_{i,j}^{n-1} - \left[\eta_{gw}\right]_{i,j}^{n-1}}{\Delta t} + fac_{i,j}^{n} k_z \left(\frac{\left[z_s\right]_{i,j}^{n-1} - \left[z_b\right]_{i,j}^{n-1}}{\left[d_{infiltration}\right]_{i,j}^{n}} + 1\right)\right] n_p & \\ & if\ \ wetz_{i,j}^{n-1} = 1\ and\ \left[\eta_{gw}\right]_{i,j}^{n-1} < \left[z_b\right]_{i,j}^{n-1} \end{cases} \tag{B8}$$

where $d_{infiltration}$ is the thickness of infiltration layer, which increases at the end of each time step by the infiltration water.

$$\left[d_{infiltration}\right]_{i,j}^{n} = \left[d_{infiltration}\right]_{i,j}^{n-1} + \frac{w_{i,j}^{n}\Delta t}{n_p} \tag{B9}$$

The infiltration velocity is limited by the amount of water available or surface water depth in the cell:

$$w_{i,j}^{n} \le \frac{h_{i,j}^{n-1}}{\Delta t} \tag{B10}$$

For numerical stability, $d_{infiltration}$ is restricted to a minimum of one third of $d_{wetlayer}$, (i.e., corresponding to the centroid of the instantaneous infiltration part) and the maximum is equal to the depth of groundwater level below the bed level. Once a cell is dry, the corresponding $d_{infiltration}$ is reset to the minimum value.

$$\left[d_{infiltration}\right]_{i,j}^{n-1} = \frac{1}{3} d_{wetlayer},\quad if\ wetz_{i,j}^{n-1} = 0 \tag{B11}$$

$$\frac{1}{3} d_{wetlayer} \le \left[d_{infiltration}\right]_{i,j}^{n-1} \le \left[z_b\right]_{i,j}^{n-1} - \left[\eta_{gw}\right]_{i,j}^{n-1},\quad if\ wetz_{i,j}^{n-1} = 1 \tag{B12}$$

The continuity equation for groundwater system can be written as:

$$\frac{\partial \eta_{gw}}{\partial t} + \frac{\partial u_{gw} h_{ugw}}{\partial x} + \frac{\partial v_{gw} h_{vgw}}{\partial y} = \frac{w}{n_p} \tag{B13}$$

where the effective depths (h_{ugw} and h_{vgw}) are calculated by taking the mean differences between the groundwater level and bed of the aquifer ($z_{b,aquifer}$) in the surrounding η-points:

$$\left[h_{ugw}\right]_{i,j}^{n} = \frac{\left[\eta_{gw} - z_{b,aquifer}\right]_{i,j}^{n} + \left[\eta_{gw} - z_{b,aquifer}\right]_{i+1,j}^{n}}{2} \tag{B14}$$

$$\left[h_{vgw}\right]_{i,j}^{n} = \frac{\left[\eta_{gw} - z_{b,aquifer}\right]_{i,j}^{n} + \left[\eta_{gw} - z_{b,aquifer}\right]_{i,j+1}^{n}}{2} \tag{B15}$$

The new groundwater level can then be solved from continuity equation:

$$\left[\eta_{gw}\right]_{i,j}^{n+1} = \left[\eta_{gw}\right]_{i,j}^{n} + \Delta t\left(-\frac{\left[u_{gw}h_{ugw}\right]_{i,j}^{n} - \left[u_{gw}h_{ugw}\right]_{i-1,j}^{n}}{x_{u,i,j} - x_{u,i-1,j}} - \frac{\left[v_{gw}h_{vgw}\right]_{i,j}^{n} - \left[v_{gw}h_{vgw}\right]_{i,j-1}^{n}}{y_{v,i,j} - y_{v,i,j-1}} + \frac{w_{i,j}^{n}}{n_p}\right) \tag{B16}$$

Appendix-C Grid Transformation and Coordinate Mapping

The wetting and drying of grid points in the intertidal zone due to tidal variations are sometimes complicated to deal with in numerical computations. In Chapter 3, I utilize a moving mesh where instantaneous waterline is always treated as the model origin (x = 0 m). Consequently, the reference (fixed) physical space (x, t) has to be mapped to a new set of independent variables in transformed space (ξ, τ), where

$$\xi = \xi(x, t) \tag{C-1}$$

$$\tau = \tau(t) \tag{C-2}$$

In this application, the new ξ-variable can be related to the location of waterline (x_w) and reference space; in the meantime, new time variable is equivalent to the reference time. Therefore,

$$\xi = x + x_w \tag{C-3}$$

$$\tau = t \tag{C-4}$$

The position of waterline can be calculated from the tidal elevation (η) and slope of the cross-shore profile (Figure C-1).

$$x_w = -\frac{\eta}{\tan\theta} \tag{C-5}$$

where η is assumed positive upward and $tan\theta$ is the constant beach slope.

Note that the study beach is dominated by principal lunar semi-diurnal tide (M_2 constituent). As a result, we can express tidal elevation as a simple trigonometry function,

$$\eta = A \sin\left(\frac{2\pi t}{T} - \varphi_0\right) \tag{C-6}$$

where A is local M_2 tidal amplitude (~ 0.3 m), T is the M_2 tidal period (= 12.42 hour), and φ_0 is the tidal phase.

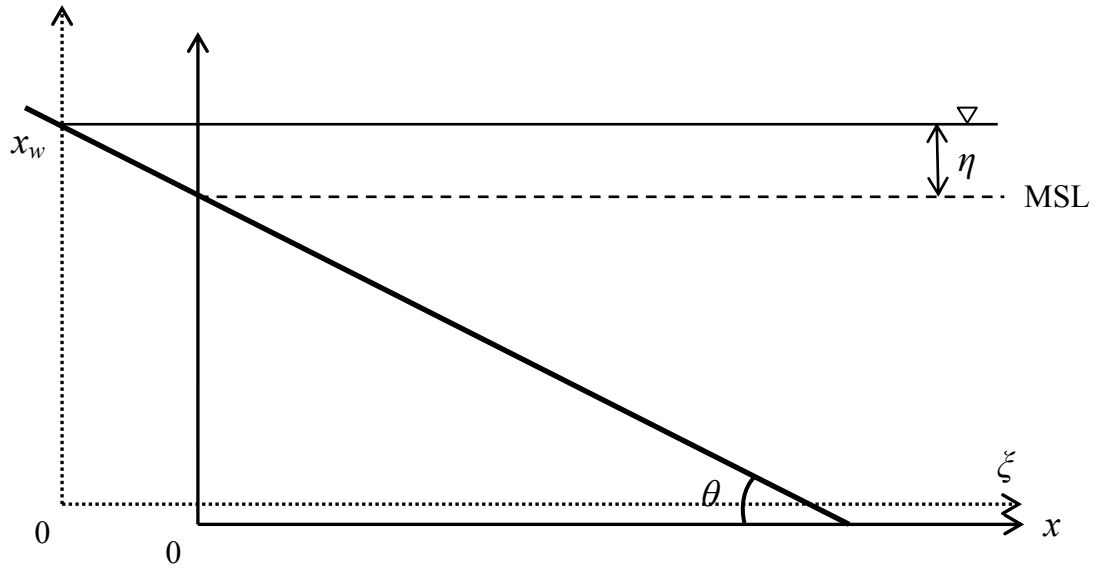

Figure C-1 Cross-shore transection of the beach. The solid line and dashed line arrows indicate the reference (fixed) and transformed (moving) axes. θ, η, and x_w are beach slope, tidal elevation, and waterline.

Combining equations (C-3) to (C-6), we have the expression of ξ with respect to x and t and vice versa.

$$\xi = x - \frac{A}{\tan\theta}\sin\left(\frac{2\pi t}{T} - \varphi_0\right) \tag{C-7}$$

By applying the chain rule of differential calculus to equations, we obtained the following relationships,

$$\frac{\partial}{\partial x} = \frac{\partial \xi}{\partial x}\frac{\partial}{\partial \xi} + \frac{\partial \tau}{\partial x}\frac{\partial}{\partial \tau} = \frac{\partial}{\partial \xi} \tag{C-8}$$

$$\frac{\partial}{\partial t} = \frac{\partial \xi}{\partial t}\frac{\partial}{\partial \xi} + \frac{\partial \tau}{\partial t}\frac{\partial}{\partial \tau} = \frac{2\pi A}{\mathrm{T}\tan\theta}\cos\left(\frac{2\pi t}{T} - \varphi_0\right)\frac{\partial}{\partial \xi} + \frac{\partial}{\partial \tau} \tag{C-9}$$

At first glance, the spatial partial derivatives are the same for two spaces (C-8) whereas the temporal partial derivative (C-9) introduces an additional term due to the transformation. However, when the terms are discretized in time, we can show that this term is much smaller and negligible compared to the other term due to the fact that tide is so slowly varying and tidal range is small.

$$\frac{\Delta}{\Delta t} = \frac{2\pi A}{\mathrm{T}\tan\theta}\cos\left(\frac{2\pi t}{T} - \varphi_0\right)\frac{\Delta}{\Delta \xi} + \frac{\Delta}{\Delta \tau} \tag{C-10}$$

Normalize (C-10) by Δt, then consider a uniform grid spacing of 1.0 m for both reference and moving grid systems, a constant time step of 15 s, tidal amplitude and period of 0.3 m and 12.42 hours, and a mean slope 1/25 of intertidal zone in this study, we obtain

$$\frac{2\pi A}{\mathrm{T}\tan\theta}\cos\left(\frac{2\pi t}{T} - \varphi_0\right)\frac{\Delta \mathrm{t}}{\Delta \xi} \leq \frac{2\pi A}{\mathrm{T}\tan\theta}\frac{\Delta t}{\Delta x} = 0.016 \ll 1 \tag{C-11}$$

Therefore, we can readily neglect this additional term introduced by the grid transformation and keep the calculations as neat as possible.

Appendix-D Numerical Computations for Microbial Balance Model

The partial differential equation to be numerically solved is (see Equation 17 in Chapter 3):

$$\frac{\partial hC}{\partial t} = S + \frac{\partial}{\partial x}\left[\varepsilon_x h \frac{\partial C}{\partial x}\right] - \kappa I_s hC \tag{D-1}$$

where $S = \alpha\beta H_1^2 \delta(x - x_S^1) + \gamma I_r \delta(x - x_S^2)$ is the source loading rate.

The above equation is solved with a second-order finite difference scheme in a 1-D staggered grid (Figure 3.1 d). All terms on the right hand side (RHS) of Equation (D-1) is evaluated at present time step (i.e., an explicit scheme). The discretization can be expressed as:

$$S + \frac{\partial}{\partial x}\left[\varepsilon_x h \frac{\partial c}{\partial x}\right] - \kappa I_s hc = S_i + \frac{1}{\Delta x}\left[Q_{j+1} - Q_j\right] - \kappa I_s h_i c_i \tag{D-2}$$

$$Q_j = \varepsilon_x h_{e\,j}\left(c_j - c_{j-1}\right)/\Delta x \tag{D-3}$$

where $h_{e\,j}$ is the water depth at the cell edge, given by the average depth of two neighboring cells.

$$h_{e\,j} = \left(h_{j-1} + h_j\right)/2 \tag{D-4}$$

Once the RHS is computed, a fourth order Runge-Kutta method (RK-4) is applied for time evolution. The time step is chose to satisfy stability criterion for a 1-D pure diffusion equation using 2nd-order central discretization (Hundsdorfer and Vermer, 2003).

$$\frac{\varepsilon_x \Delta t}{\Delta x^2} < \frac{1}{2}$$

(D-5)

Hence, based on grid spacing of 1 m and diffusivity of 0.03 $m^2 s^{-1}$, the time step must satisfy:

$$\Delta t < \frac{\Delta x^2}{2\varepsilon_x} = 16.67\ s$$

(D-6)

Therefore, the time step of 15 s guarantees stability.

Appendix-E Parameter Optimization for Wave Pick-up Coefficient

The wave pick-up coefficient α was determined by an optimization procedure that minimized an objective function that quantifies the goodness of fit between model results and observations. We applied a common least square objective function (Little and Williams, 1992), which is given by the sum of normalized weighted squared errors (residuals):

$$WLSE = \min \frac{1}{N} \sum_{i=1}^{N} W_i (log_{10} O_i - log_{10} P_i)^2 \quad \text{(E-1)}$$

where O_i and P_i are ith set of observed and predicted enterococci levels (in CFU/100 mL) with corresponding weight W_i, and N is the total number of prediction-observation pairs. In the study, we assigned equal weights to all observations (i.e., $W_i = 1$).

Table E-1 Optimization experiments for wave pick-up coefficient α

Trial #	Starting Point ($\times 10^4$)	Bounds ($\times 10^4$)	Iterations	Objective Function	Final Point ($\times 10^4$)
1	0.2	0.1~10	5	0.491	1.644
2	0.5	0.1~10	7	0.491	1.645
3	1.0	0.1~10	6	0.491	1.645
4	5.0	0.1~10	7	0.491	1.645
5	8.0	0.1~10	8	0.491	1.644

To find optimal α value, a series of numerical experiments were conducted in Matlab Optimization Toolbox (MathWorks, Natick, MA) using constrained nonlinear minimization function (fmincon). Regardless of the starting points, the final points converge toward the same value, 1.645×10^4 (Table E-1). Therefore, in Chapter 3, we set a constant α (= 1.645×10^4 CFU $m^{-3}s^{-1}$) to run balance model simulations.

Appendix-F Linear Fit of Significant Wave Height and Onshore Wind Component

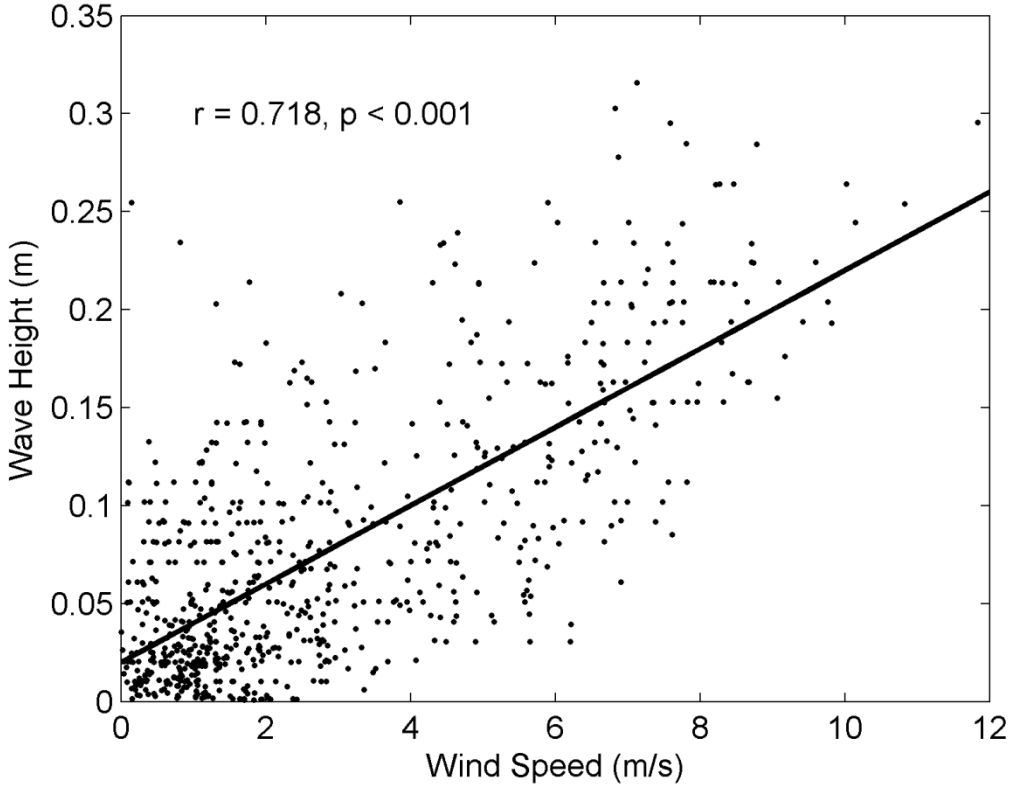

Figure F-1 Linear fit of significant wave height and onshore wind component. Wind speeds are 1-hour moving averaged. All offshore winds are assigned with zero speed assuming waves generated by offshore wind have minimal effect on this beach. The solid line shows linearly fitted wind-wave curve of Equation (27).

Appendix-G Florida Beaches and Observational Stations

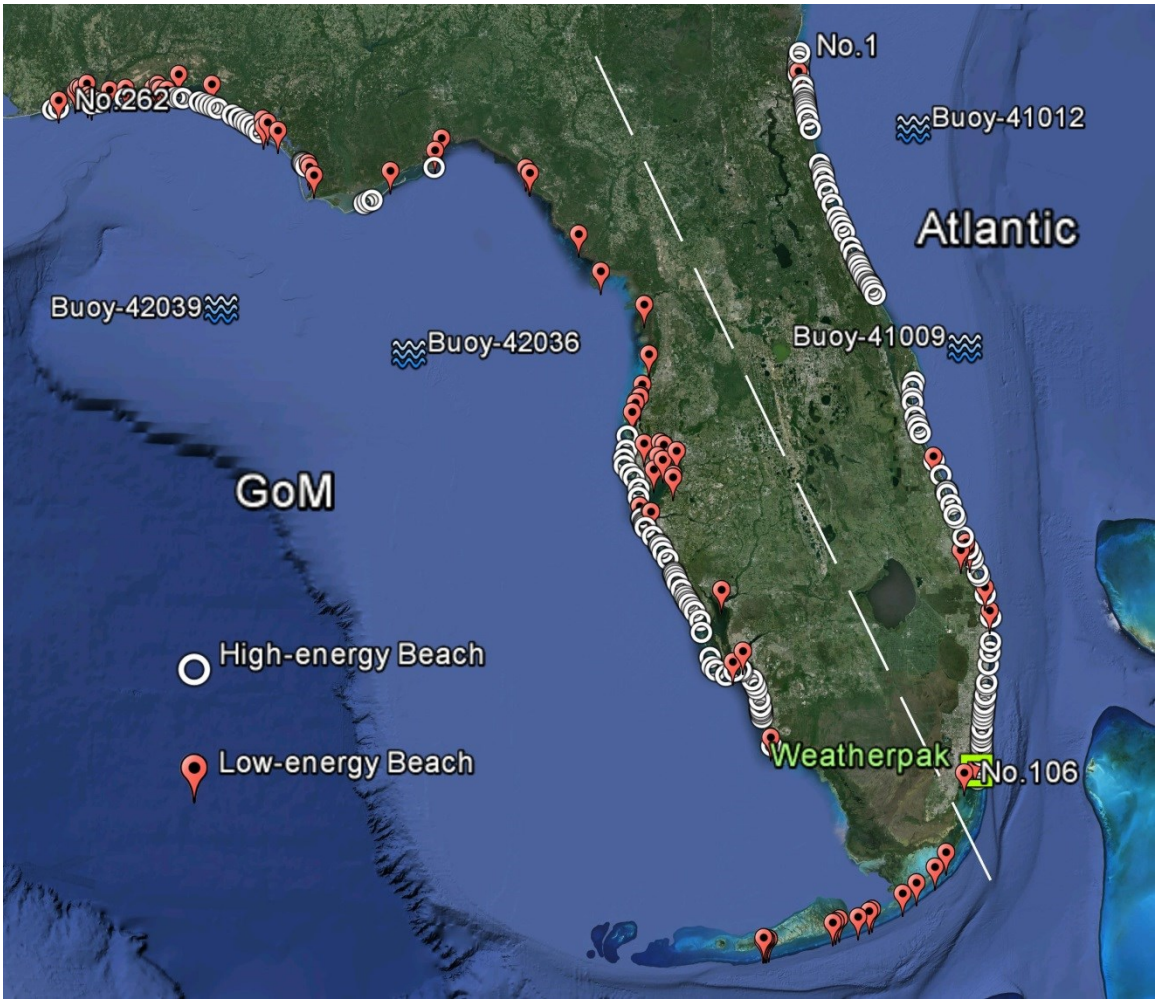

Figure G-1 Florida beaches and observational stations used in this study. Four NDBC buoys are illustrated by wave symbols and the weatherpak station is illustrated by a green square. High- and low-energy beaches are shown with white circles and red balloons, respectively. The white dashed line separates Atlantic and GoM beaches. In this study, beaches are numbered from 1 to 262 starting at the northeast corner of the State, in Nassau County, and proceeding clockwise along the coastline to the northwestern corner, in Escambia County. Three representative beaches are illustrated in this figure. No. 1 is the first or northernmost Atlantic beach in Nassau County; No. 106 is the last or southernmost Atlantic beach in Miami-Dade County; No. 262 is the last GoM beaches in Escambia County.

Appendix-H Google Earth Images of Typical High- and Low-energy Beaches

High-energy Beaches:

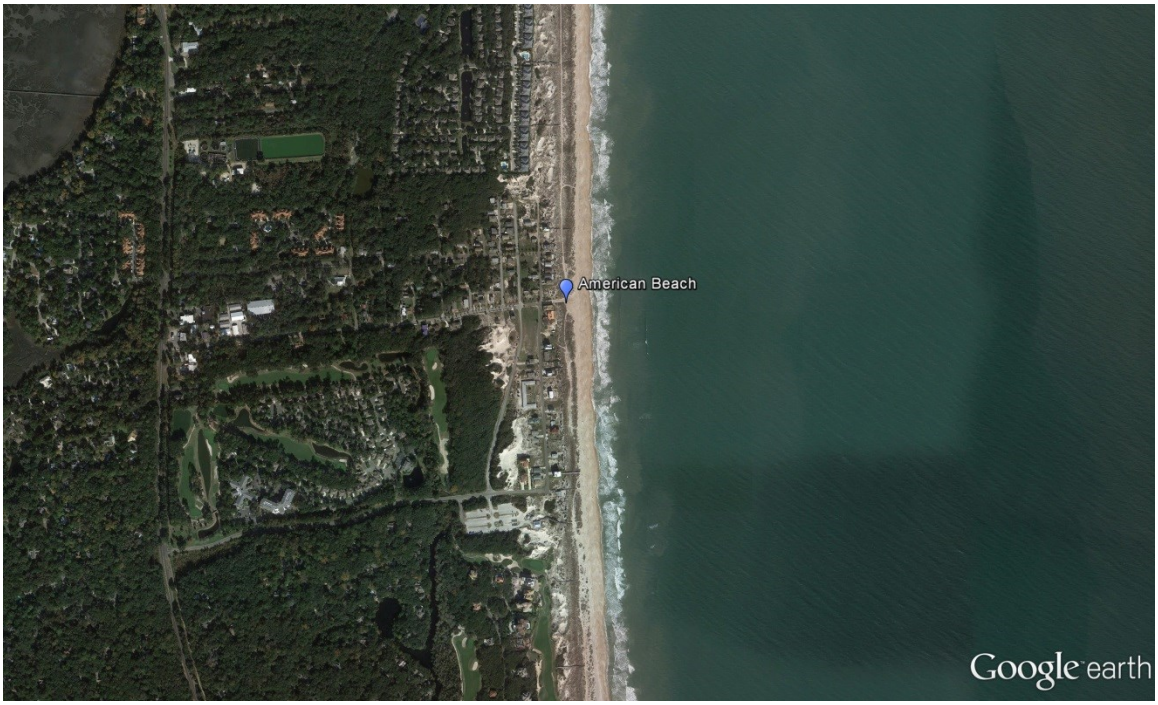

Figure H-1 American beach in Nassau County (a high-energy beach).

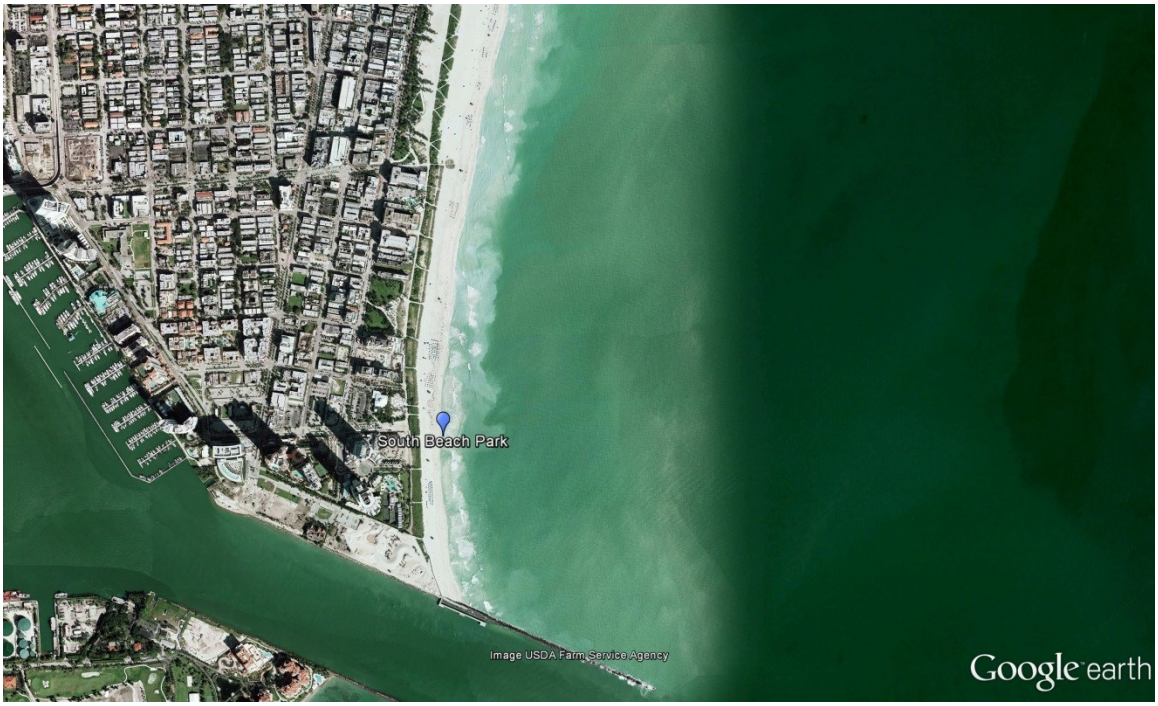

Figure H-2 South Beach in Miami-Dade County (a high-energy beach)

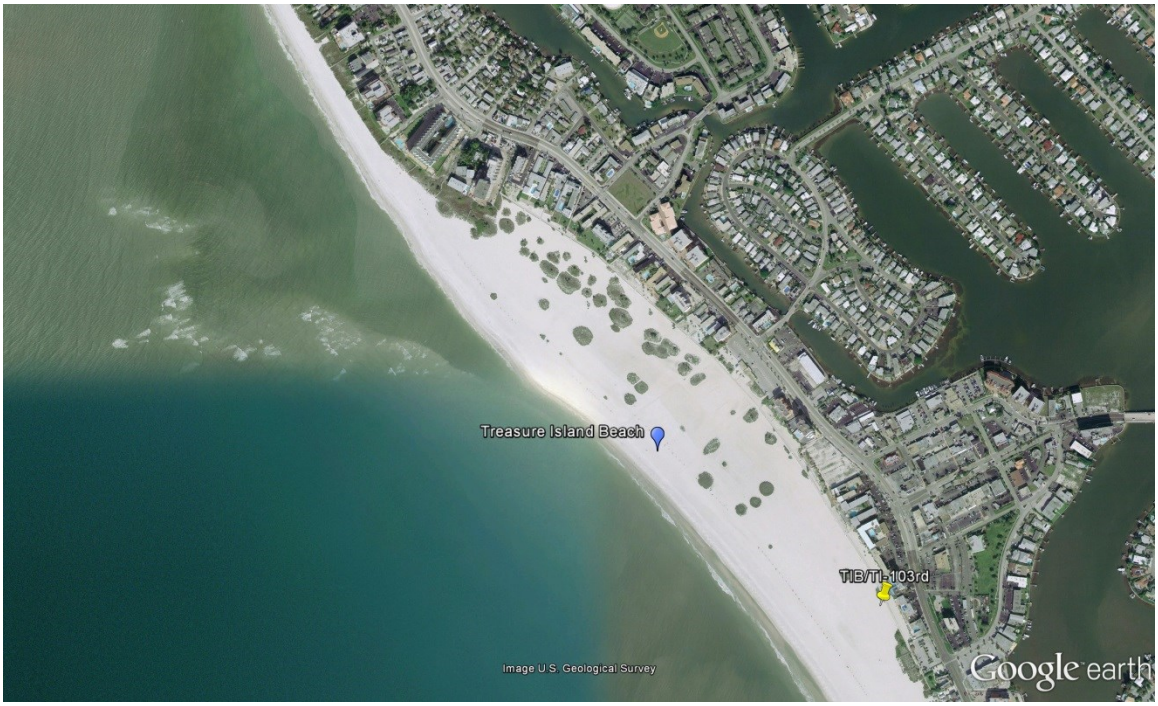

Figure H-3 Treasure Island Beach in Pinellas County (a high-energy beach)

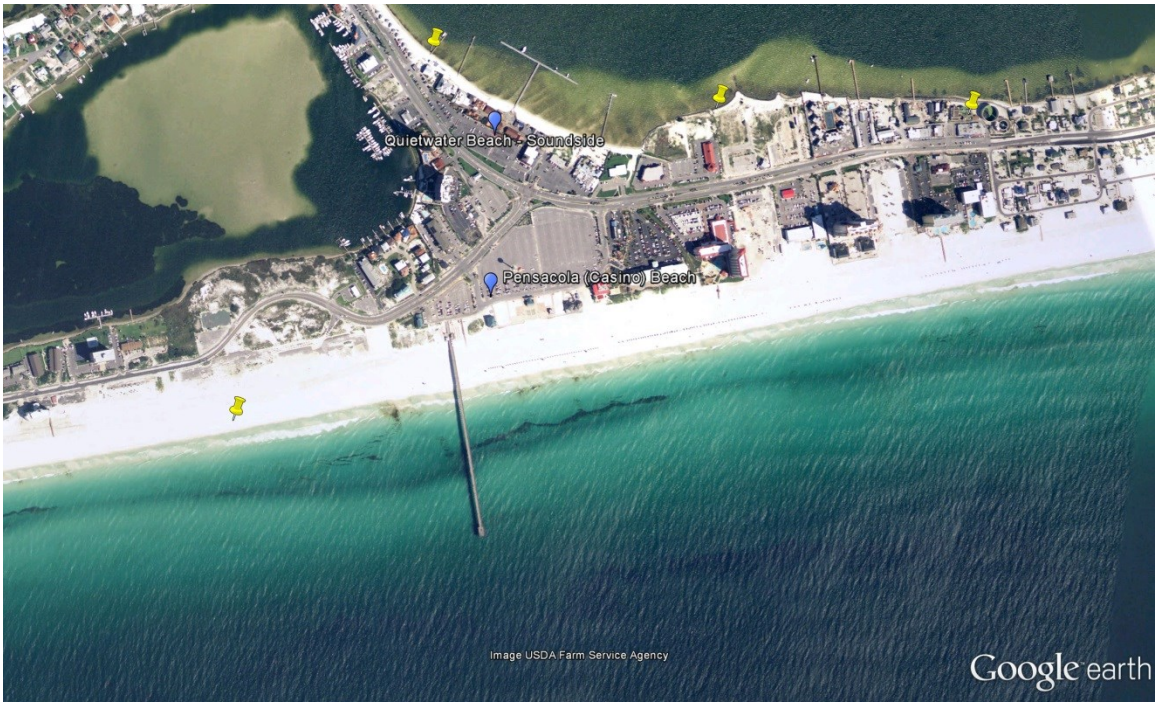

Figure H-4 Pensacola Beach in Escambia County (a high-energy beach)

Low-energy Beaches:

Figure H-5 Hobie Beach in Miami-Dade County (a low-energy beach). This beach is located inside Biscayne Bay.

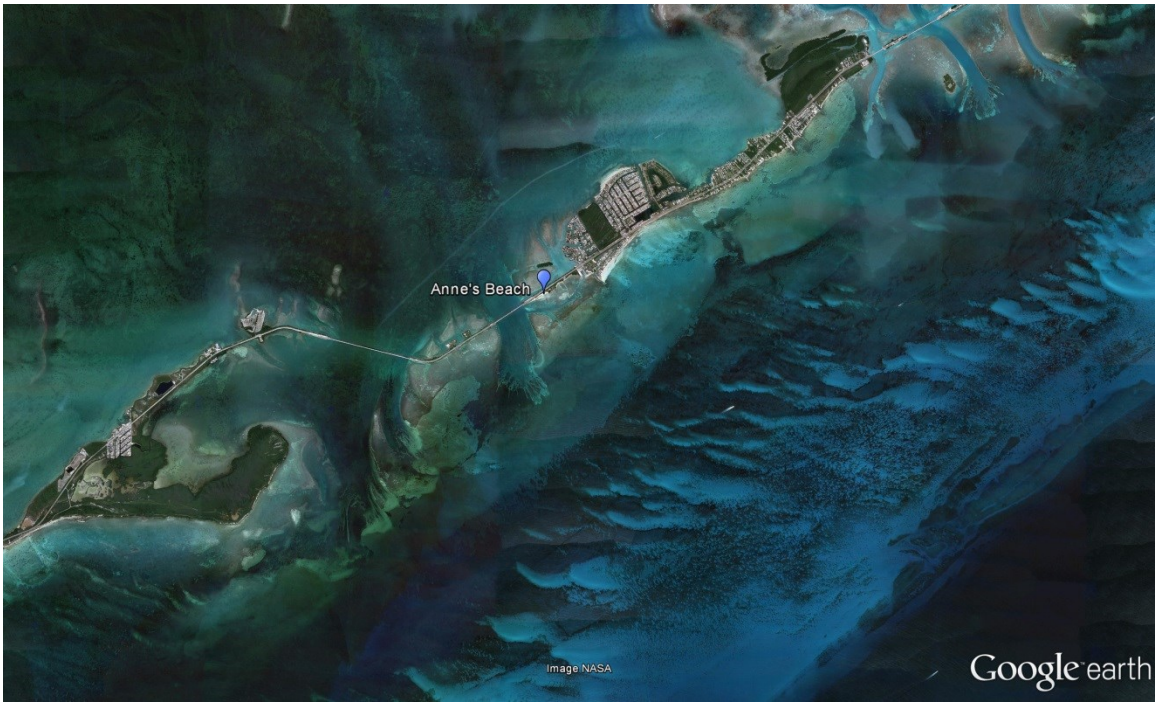

Figure H-6 Anne's Beach in Monroe County (a low-energy beach). This beach is behind coral reefs.

Figure H-7 Hagen's Cove Beach in Taylor County (a low-energy beach). This beach is located in the Big Bend area, surrounded by marshes.

Figure H-8 Harry Harris County Park in Monroe County (a low-energy beach). This beach is fully protected by a coral rock barrier.

Appendix-I Validation of Wave Model Hindcasts with Observations

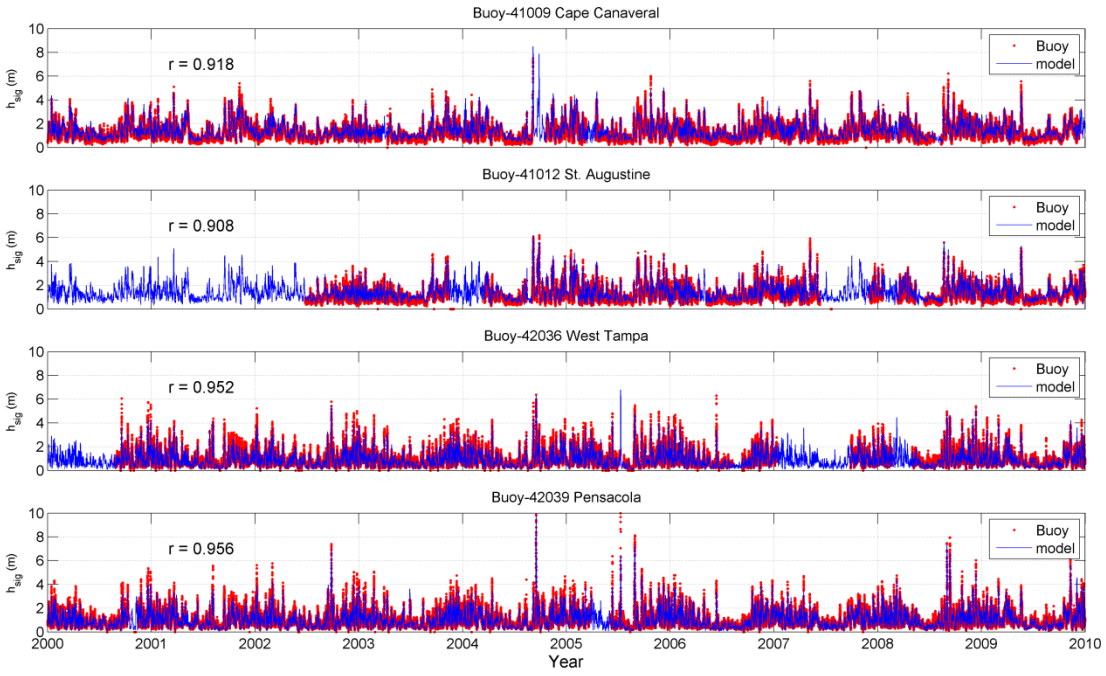

Figure I-1 Comparisons of significant wave height between WAVEWATCH-III hindcasts and NDBC buoy observations at four stations from 2000 to 2009. (a) Buoy-41009 Cape Canaveral; (b) Buoy-41012 St. Augustine; (c) Bouy-42036 West Tampa; and (d) Buoy-42039 Pensacola. Data gaps exist in the observations (red dots). Model outcomes and observations agree well with correlation coefficient all above 0.9.

Appendix-J Validation of Ideal Direct-beam Irradiance with Observations

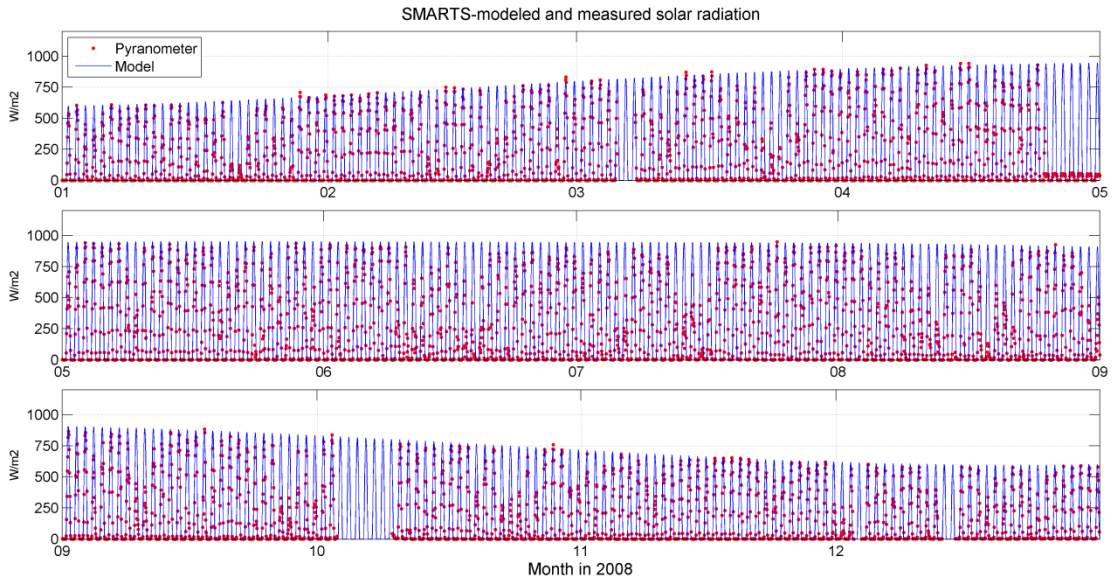

Figure J-1 Comparisons of direct-beam irradiance calculated from SMART model under ideal conditions and hourly-averaged spectral pyranometer observations at RSMAS Weatherpak Station in 2008. For better visualization, the whole year is divided into three subplots each containing time series of four months. The model outcomes agree well with the observations (r = 0.88). Model sometimes overestimates daytime irradiance because of the idealized clear sky assumption.

Appendix-K Validation of Satellite-retrieve SST with Observations

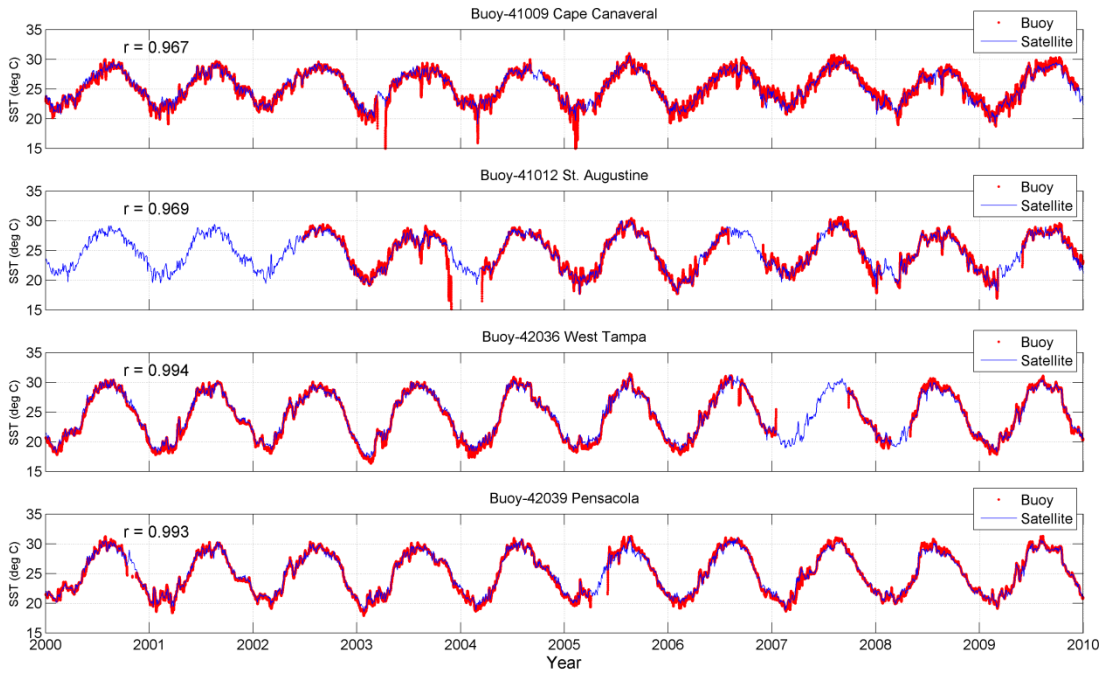

Figure K-1 Comparisons between satellite-retrieved daily SST and daily-averaged observations at NDBC four stations from 2000 to 2009. (a) Buoy-41009 Cape Canaveral; (b) Buoy-41012 St. Augustine; (c) Bouy-42036 West Tampa; and (d) Buoy-42039 Pensacola. Sattelite-retrieved SSTs agree well with buoy observations and their correlations are all above 0.96. Notice that sudden and drastic decreases or increases in temperature observations may not be captured by the satellite.

Appendix-L Florida Hydrologic Map

Figure L-1 Rivers and lakes in the State of Florida (obtained from www.geology.com)

REFERENCES

Abdelzaher, A.M., M.E. Wright, C. Ortega, H.M. Solo-Gabriele, G. Miller, S. Elmir, X. Newman, P. Shih, J.A. Bonilla, T.D. Bonilla, C.J. Palmer, T. Scott, J. Lukasik, V.J. Harwood, S. McQuaig, C. D. Sinigalliano, M.L. Gidley, L.R.W. Plano, X. Zhu, J.D. Wang, L.E. Fleming, 2010. Presence of pathogens and indicator microbes at a non-point source subtropical recreational marine beach, Appl. Environ. Microbiol. 76(3), 724-732.

Abdelzaher, A.M., Wright, M.E., Ortega, C., Hasan, a R., Shibata, T., Solo-Gabriele, H.M., Kish, J., Withum, K., He, G., Elmir, S.M., Bonilla, J.A., Bonilla, T.D., Palmer, C.J., Scott, T.M., Lukasik, J., Harwood, V.J., McQuaig, S., Sinigalliano, C.D., Gidley, M.L., Wanless, D., Plano, L.R.W., Garza, A.C., Zhu, X., Stewart, J.R., Dickerson, J.W., Yampara-Iquise, H., Carson, C., Fleisher, J.M., Fleming, L.E., 2011. Daily measures of microbes and human health at a non-point source marine beach. J. Water Health 9, 443–457.

Abdelzaher, A.M., Solo-Gabriele, H.M., Phillips, M.C., Elmir, S.M., Fleming, L.E., 2013. An alternative approach to water regulations for public health protection at bathing beaches. J. Environ. Public Health 2013, 1-9.

Absalonsen, L., Dean, R., 2011. Characteristics of the shoreline change along Florida sandy beaches with an example for Palm Beach County. J. Coast. Res. 27, 16–26.

Ahn, J. H., Grant, S. B., Surbeck, C. Q., DiGiacomo, P. M., Nezlin, N. P., & Jiang, S., 2005. Coastal water quality impact of stormwater runoff from an urban watershed in southern California. *Environmental science & technology*, *39*(16), 5940–5953.

Akaike, H. 1974. A new look at the statistical model identification. *IEEE Transactions on Automatic Control*, 19(6), 716-723.

Amitai, E., Marks, D.A., Wolff, D.B., Silberstein, D.S., Fisher, B.L., Pippitt, J.L., 2006. Evaluation of radar rainfall products: lessons learned from the NASA TRMM validation program in Florida. J. Atmos. Ocean. Technol. 23, 1492–1505.

Badgley, B.D., Thomas, F.I.M., Harwood, V.J., 2011. Quantifying environmental reservoirs of fecal indicator bacteria associated with sediment and submerged aquatic vegetation. Environ. Microbiol. 13, 932–942.

Boehm, A., 2007. Enterococci concentrations in diverse coastal environments exhibit extreme variability. Environ. Sci. Technol. 41, 8227–8232.

Boehm, A.B., Weisberg, S.B., 2005. Tidal forcing of enterococci at marine recreational beaches at fortnightly and semidiurnal frequencies. Environ. Sci. Technol. 39, 5575–5583.

Boehm, A.B., Grant, S.B., Kim, J.H., Mowbray, S.L., McGee, C.D., Clark, C.D., Foley, D.M., Wellman, D.E., 2002. Decadal and shorter period variability of surf zone water quality at Huntington Beach, California. Environ. Sci. Technol. 36, 3885–3892.

Boehm, A.B., Shellenbarger, G.G., Paytan, A., 2004a. Groundwater discharge: potential association with fecal indicator bacteria in the surf zone. Environ. Sci. Technol. 38, 3558–3566.

Boehm, A.B., Lluch-Cota, D.B., Davies, K.A., Winant, C.D., Monismith, S.G., 2004b. Covariation of coastal water temperature and microbial pollution at interannual to tidal periods. Geophys. Res. Lett. 31, 1–5.

Boehm, A.B., Keymer, D.P., Shellenbarger, G.G., 2005. An analytical model of enterococci inactivation, grazing, and transport in the surf zone of a marine beach. Water Res. 39, 3565–3578.

Boehm, A.B., Yamahara, K.M., Love, D.C., Peterson, B.M., McNeill, K., Nelson, K.L., 2009. Covariation and photoinactivation of traditional and novel indicator organisms and human viruses at a sewage-impacted marine beach. Environ. Sci. Technol. 43, 8046–8052.

Brodtkorb, P.A., P. Johannesson, G. Lindgren, I. Rychlik, J. Ryden, and E. Sjo, 2000. WAFO - a Matlab toolbox for analysis of random waves and loads, Proc. 10th Int. Offshore and Polar Eng. Conf., Seattle, USA, Vol III, pp. 343-350.

Burkhardt, W., Calci, K.R., Watkins, W.D., Rippey, S.R., Chirtel, S.J., 2000. Inactivation of indicator microorganisms in estuarine waters. Water Res. 34, 2207–2214.

Byappanahalli, M.N., Whitman, R.L., Shively, D. A, Nevers, M.B., 2010. Linking non-culturable (qPCR) and culturable enterococci densities with hydrometeorological conditions. Sci. Total Environ. 408, 3096–3101.

Byappanahalli, M.N., Nevers, M.B., Korajkic, A., Staley, Z.R., Harwood, V.J., 2012. Enterococci in the environment. Microbiol. Mol. Biol. Rev. 76, 685–706.

Cabelli, V.J., Dufour, A.P., McCabe, L.J., Levin, M.A., 1982. Swimming-associated gastroenteritis and water quality. Am. J. Epidemiol. 115, 606–616.

Chawla, A., Spindler, D.M., Tolman, H.L., 2013. Validation of a thirty year wave hindcast using the Climate Forecast System Reanalysis winds. Ocean Model. 70, 189–206.

Colford, J.M., Wade, T.J., Schiff, K.C., Wright, C.C., Griffith, J.F., Sandhu, S.K., Burns, S., Sobsey, M., Lovelace, G., Weisberg, S.B., 2007. Water quality indicators and the risk of illness at beaches with nonpoint sources of fecal contamination. Epidemiology 18, 27–35.

Colford, J.M., Schiff, K.C., Griffith, J.F., Yau, V., Arnold, B.F., Wright, C.C., Gruber, J.S., Wade, T.J., Burns, S., Hayes, J., McGee, C., Gold, M., Cao, Y., Noble, R.T., Haugland, R., Weisberg, S.B., 2012. Using rapid indicators for enterococcus to assess the risk of illness after exposure to urban runoff contaminated marine water. Water Res. 46, 2176–2186.

Cyterski, M., Galvin, M., Wolfe, K., and Parmar, R., 2012. Virtual Beach v. 2.3 User Guide. Center for Exposure Assessment Modeling (CEAM), U.S. Environmental Protection Agency, Athens, GA.

Davies-Colley, R.J., Donnison, A.M., Speed, D.J., Ross, C.M., Nagels, J.W., 1999. Inactivation of faecal indicator micro-organisms in waste stabilisation ponds: interactions of environmental factors with sunlight. Water Res. 33, 1220–1230.

Dean, R. G., and Dalrymple, R.A., 1991. Water wave mechanisms for engineers and scientists. World Scientific.

Desmarais, T.R., Solo-Gabriele, H.M., Palmer, C.J., 2002. Influence of soil on fecal indicator organisms in a tidally influenced subtropical environment. Appl. Environ. Microbiol. 68, 1165-1172.

Elmir, S.M., 2006. Development of a water quality model which incorporates non-point microbial sources, Ph.D. thesis, Univ. of Miami, Coral Gables, Florida, USA.

Elmir, S.M., Wright, M.E., Abdelzaher, A., Solo-Gabriele, H.M., Fleming, L.E., Miller, G., Rybolowik, M., Peter Shih, M.-T., Pillai, S.P., Cooper, J. A, Quaye, E. A, 2007. Quantitative evaluation of bacteria released by bathers in a marine water. Water Res. 41, 3–10.

Elmir, S.M., Shibata, T., Solo-Gabriele, H.M., Sinigalliano, C.D., Gidley, M.L., Miller, G., Plano, L.R.W., Kish J., Withum, K., Fleming, L.E., 2009. Quantitative evaluation of enterococci and Bacteroidales released by adults and toddlers in marine water. Water Res. 43, 4610-4616.

Enns, A.A., Vogel, L.J., Abdelzaher, A.M., Solo-Gabriele, H.M., Plano, L.R.W., Gidley, M.L., Phillips, M.C., Klaus, J.S., Piggot, A.M., Feng, Z., Reniers, A.J.H.M., Haus, B.K., Elmir, S.M., Zhang, Y., Jimenez, N.H., Abdel-Mottaleb, N., Schoor, M.E., Brown, A., Khan, S.Q., Dameron, A.S., Salazar, N.C., Fleming, L.E., 2012. Spatial and temporal variation in indicator microbe sampling is influential in beach management decisions. Water Res. 46, 2237–2246.

Feng, Z., Reniers, A., Haus, B., Solo-Gabriele, H., Fiorentino, L., Olascoaga, M., MacMahan, J., 2012. Modeling microbial water quality at a beach impacted by multiple non-point sources. Coast. Eng. Proc., 1(33), management.74. doi:10.9753/icce.v33.management.74

Feng, Z., Reniers, A., Haus, B.K., Solo-Gabriele, H.M., 2013. Modeling sediment-related enterococci loading, transport, and inactivation at an embayed nonpoint source beach. Water Resour. Res. 49, 693–712.

Fiechter, J., Steffen, K.L., Mooers, C.N.K., Haus, B.K., 2006., Hydrodynamics and sediment transport in a southeast Florida tidal inlet, Estuar. Coast. Shelf Sci., 70, 297-306.

Fiorentino, L.A., Olascoaga, M.J., Reniers, A., Feng, Z., Beron-Vera, F.J., MacMahan, J.H., 2012. Using Lagrangian coherent structures to understand coastal water quality. Cont. Shelf Res. 47, 145–149.

Fleisher, J.M., Fleming, L.E., Solo-Gabriele, H.M., Kish, J.K., Sinigalliano, C.D., Plano, L., Elmir, S.M., Wang, J.D., Withum, K., Shibata, T., Gidley, M.L., Abdelzaher, A., He, G., Ortega, C., Zhu, X., Wright, M., Hollenbeck, J., Backer, L.C., 2010. The BEACHES Study: health effects and exposures from non-point source microbial contaminants in subtropical recreational marine waters. Int. J. Epidemiol. 39, 1291–1298.

Fleming, L.E., Solo-Gabriele, H., Elmir, S., Shibata, T., Squicciarini Jr., D., Quirino, W., Arguello, M., Van de Bogart, G., 2004. A pilot study of microbial contamination of subtropical recreational waters. Florida J. Environ. Health, 29-33.

Fleming, L.E., Broad, K., Clement, A., Dewailly, E., Elmir, S., Knap, A., Pomponi, S.A., Smith, S., Solo-Gabriele, H., Walsh, P., 2006. Oceans and human health: emerging public health risks in the marine environment. Mar. Pollut. Bull. 53, 545-560.

Frick, W.E., Ge, Z., Zepp, R.G., 2008. Nowcasting and forecasting concentrations of biological contaminants at beaches: a feasibility and case study. Environ. Sci. Technol. 42, 4818–4824.

Galappatti, R., Vreugdenhil C.B. 1985. A depth integrated model for suspended transport, J. Hydraul. Res., 23, 359-377.

Gast, R. J., Gorrell, L., Raubenheimer, B., Elgar, S., 2011. Impact of erosion and accretion on the distribution of enterococci in beach sands. Continental shelf research, 31(14), 1457–1461. doi:10.1016/j.csr.2011.06.011

Gonzalez, R. A, Noble, R.T., 2014. Comparisons of statistical models to predict fecal indicator bacteria concentrations enumerated by qPCR- and culture-based methods. Water Res. 48, 296–305.

Ge, Z., Frick, W.E., 2007. Some statistical issues related to multiple linear regression modeling of beach bacteria concentrations. Environ. Res. 103, 358–364.

Ge, Z., Nevers, M.B., Schwab, D.J., Whitman, R.L., 2010. Coastal loading and transport of *Escherichia coli* at an embayed beach in Lake Michigan. Environ. Sci. Technol. 44, 6731–6737.

Ge, Z., Whitman, R., Nevers, M., Phanikumar, M.S., Byappanahalli, M.N., 2012a. Nearshore hydrodynamics as loading and forcing factors for *Escherichia coli* contamination at an embayed beach. Limnol. Oceanogr. 57, 362–381.

Ge, Z., Whitman, R.L., Nevers, M.B., Phanikumar, M.S., 2012b. Wave-induced mass transport affects daily Escherichia coli fluctuations in nearshore water. Environ. Sci. Technol. 46, 2204–2211.

Goodwin, K., Matragrano, L., Wanless, D., Sinigalliano C.D., LaGier M.J., 2009. A preliminary investigation of fecal indicator bacteria, human pathogens, and source tracking markers in beach water and sand. Environ. Res, 2(4). 395-417.

Grant, S. B., Sanders, B. F., 2010. Beach boundary layer: a framework for addressing recreational water quality impairment at enclosed beaches. Environ. Sci. Technol., 44(23), 8804–8813. doi:10.1021/es101732m

Grant, S.B., Sanders, B.F., Boehm, A B., Redman, J. A, Kim, J.H., Mrse, R.D., Chu, A K., Gouldin, M., McGee, C.D., Gardiner, N. A, Jones, B.H., Svejkovsky, J., Leipzig, G. V, Brown, a, 2001. Generation of enterococci bacteria in a coastal saltwater marsh and its impact on surf zone water quality. Environ. Sci. Technol. 35, 2407–2416.

Grant, S. B., Kim, J.H., Jones, B.H., Jenkins, S.A., Wasyl, J., and Cudaback, C., 2005. Surf zone entrainment, along-shore transport, and human health implications of pollution from tidal outlets. J. Geophys. Res. 110, C10025.

Grant, S.B., Litton-Mueller, R.M., Ahn, J.H., 2011. Measuring and modeling the flux of fecal bacteria across the sediment-water interface in a turbulent stream, Water Resour. Res., 47, W05517, doi:10.1029/2010WR009460.

Gueymard, C., 2003a. Direct solar transmittance and irradiance predictions with broadband models. Part I: detailed theoretical performance assessment. Sol. Energy 74, 355–379.

Gueymard, C., 2003b. Direct solar transmittance and irradiance predictions with broadband models. Part II: validation with high-quality measurements. Sol. Energy 74, 381–395.

Haile, R.W., Witte, J.S., Gold, M., Cressey, R., McGee, C., Millikan, R.C., Glasser, A., Harawa, N., Ervin, C., Harmon, P., Harper, J., Dermand, J., Alamillo, J., Barrett, K., Nides, M., Wang, G., 1999. The health effects of swimming in ocean water contaminated by storm drain runoff. Epidemiology 10, 355–363.

Halliday, E., Gast, R.J., 2011. Bacteria in beach sands: an emerging challenge in protecting coastal water quality and bather health. Environ. Sci. Technol. 45, 370–379.

Hannouche, A., Chebbo, G., Ruban, G., Tassin, B., Lemaire, B.J., Joannis, C., 2011. Relationship between turbidity and suspended solids concentration within a combined sewer system, Water Sci. Technol., 64(12), 2445-2452.

Heaney, C.D., Sams, E., Wing, S., Marshall, S., Brenner, K., Dufour, A.P., Wade, T.J., 2009. Contact with beach sand among beachgoers and risk of illness. Am. J. Epidemiol. 170, 164–172.

Hernandez, R.J., Hernandez, Y., Jimenez, N.H., Piggot, A.M., Klaus, J.S., Feng, Z., Reniers, A., Solo-Gabriele, H.M., 2014. Effects of full-scale beach renovation on fecal indicator levels in shoreline sand and water. Water Res. 48, 579–591.

Hipsey, M.R., Antenucci, J.P., Brookes, J.D., 2008. A generic, process-based model of microbial pollution in aquatic systems. Water Resour. Res. 44, 1–26.

Hundsdorfer, W., Verwer J.G., 2003. Numerical solution of time-dependent advection-diffusion-reaction equations. Springer, Berlin, Germany, 471p.

Imamura, G.J., Thompson, R.S., Boehm, A.B., Jay, J.A., 2011. Wrack promotes the persistence of fecal indicator bacteria in marine sands and seawater. FEMS microbial. ecology. 77(1), 40–49.

Kim, J. H., Grant, S. B., McGee, C. D., Sanders, B. F., Largier, J. L., 2004. Locating sources of surf zone pollution: a mass budget analysis of fecal indicator bacteria at Huntington Beach, California. Environ. Sci. Technol., 38(9), 2626–2636.

Lindeburg, M.R., 1986. Civil engineering reference manual, 4th ed., Prof. Pub., San Carlos, California.

Little, K.W., and Williams, R.E., 1992. Least-squares calibration of QUALE2E. Water Environ. Res., 64(2), 179-185.

Litton, R.M., Ahn, J.H., Sercu, B., Holden, P.A., Sedlak, D.L., Grant, S.B., 2010. Evaluation of chemical, molecular, and traditional markers of fecal contamination in an effluent dominated urban stream. Environ. Sci. Technol. 44, 7369–7375.

Liu, L., Phanikumar, M.S., Molloy, S.L., Whitman, R.L., Shively, D.A., Nevers, M.B., Schwab, D.J., Rose, J.B., 2006. Modeling the transport and inactivation of E. coli and enterococci in the near-shore region of Lake Michigan. Environ. Sci. Technol. 40, 5022–5028.

McCall, R.T., Van Thiel de Vries, J.S.M., Plant, N.G., Van Dongeren, A. R., Roelvink, J. A., Thompson, D.M., Reniers, A. J.H.M., 2010. Two-dimensional time dependent hurricane overwash and erosion modeling at Santa Rosa Island. Coast. Eng. 57, 668–683.

National Resources Research Council, 2011. Testing the waters 2011: A Guide to Water Quality at Vacation Beaches, 21st annual report.

National Resources Research Council, 2012. Testing the waters 2012: A Guide to Water Quality at Vacation Beaches, 22nd annual report.

Nevers, M.B., Whitman, R.L., 2005. Nowcast modeling of *Escherichia coli* concentrations at multiple urban beaches of southern Lake Michigan. Water Res. 39, 5250-5260.

Nielsen, P., 1990. Tidal dynamics of the water table in beaches, Water Resour. Res., 26(9), 2127-2134.

Nielsen, P., 1999. Groundwater dynamics and salinity in coastal barriers, J. Coast. Res., 15(3), 732-740.

Olyphant, G.A., 2005. Statistical basis for predicting the need for bacterially induced beach closures: emergence of a paradigm? Water Res., 39, 4953-4960.

Orzech, M.D., Reniers, A.J.H.M., Thornton, E.B., MacMahan, J.H., 2011. Megacusps on rip channel bathymetry: Observations and modeling. Coast. Eng. 58, 890–907.

Palmer, C.J., Bonilla, J.A., Bonilla, T.D., Goodwin, K.D., Elmir, S.M., Abdezaher, A.M., Solo-Gabriele, H.M., 2008. Future of microbial ocean water quality monitoring. In: Walsh, P.J., Smith, S.L., Fleming, L.E., Solo-Gabriele H.M., and Gerwick, W.H. (eds). Oceans and human health: risks and remedies for the seas. Acedemic Press, Burlington, MA.

Parker, J.K., McIntyre, D., Noble, R.T., 2010. Characterizing fecal contamination in stormwater runoff in coastal North Carolina, USA. Water Res. 44, 4186–4194.

Pednekar, A.M., Grant, S.B., Jeong, Y., Poon, Y., Oancea, C., 2005. Influence of climate change, tidal mixing, and watershed urbanization on historical water quality in Newport Bay, a saltwater wetland and tidal embayment in southern California. Environ. Sci. Technol. 39, 9071–9082.

Piggot, A.M., Klaus, J.S., Johnson, S., Phillips, M.C., Solo-Gabriele, H.M., 2012. Relationship between enterococcal levels and sediment biofilms at recreational beaches in South Florida. Appl. Environ. Microbiol. 78, 5973–5982.

Phillips, M.C., Solo-Gabriele, H.M., Piggot, A.M., Klaus, J.S., Zhang, Y., 2011a. Relationships between sand and water quality at recreational beaches. Water Res. 45, 6763–6739.

Phillips, M.C., Solo-Gabriele, H.M., Reniers, a J.H.M., Wang, J.D., Kiger, R.T., Abdel-Mottaleb, N., 2011b. Pore water transport of enterococci out of beach sediments. Mar. Pollut. Bull. 62, 2293–2298.

Phillips, M.C., Feng, Z., Vogel, L.J., Reniers, A.J.H.M., Haus, B.K., Enns, A. A., Zhang, Y., Hernandez, D.B., Solo-Gabriele, H.M., 2014. Microbial release from seeded beach sediments during wave conditions. Mar. Pollut. Bull. 79, 114-122.

Pierce, R.H., Henry, M.S., Blum, P.C., Lyons, J., Cheng, Y.S., Yazzie, D., Zhou, Y., 2003. Brevetoxin concentrations in marine aerosol: human exposure levels during a Karenia brevis harmful algal bloom, Bull. Environ. Contam. Toxicol., 70, 161-165.

Plano, L.R., Garza, A.C., Shibata, T., Elmir, S.M., Kish, J., Sinigalliano, C.D., Gidley, M.L., Miller, G., Withum, K., Fleming, L.E., Solo-Gabriele, H.M., 2011. Shedding of *Staphylococcus aureus* and methicillin-resistant *Staphylococcus aureus* from adult and pediatric bathers in marine waters, BMC Microbiology, 11(5), 1-10.

Reeves, R. L., Grant, S. B., Mrse, R. D., Copil Oancea, C. M., Sanders, B. F., Boehm, A. B., 2004. Scaling and management of fecal indicator bacteria in runoff from a coastal urban watershed in southern California. Environ. Sci. Technol. 38(9), 2637–2648.

Reidenbach, M.A., Limm, M., Hondzo, M., Stacey, M.T., 2010. Effects of bed roughness on boundary layer mixing and mass flux across the sediment-water interface, Water Resour. Res., 46, W07530, doi: 10.1029/2009WR008248.

Reniers, A.J.H.M., Roelvink, J.A., Thornton, E.B., 2004. Morphodynamic modeling of an embayed beach under wave group forcing. J. Geophys. Res. 109, 1–22.

Reniers, A. J.H.M., MacMahan, J.H., Thornton, E.B., Stanton, T.P., Henriquez, M., Brown, J.W., Brown, J. A., Gallagher, E., 2009. Surf zone surface retention on a rip-channeled beach. J. Geophys. Res. 114, C10010.

Reniers, A., Gallagher, E.L.L., MacMahan, J.H., Brown, J., van Rooijen, A., van Thiel de Vries, J., van Prooijen, B.C., 2013. Observations and modeling of steep-beach grain-size variability. J. Geophys. Res. 118, 1–15.

Reynolds, R.W., Smith, T.M., Liu, C., Chelton, D.B., Casey, K.S., Schlax, M.G., 2007. Daily high-resolution-blended analyses for sea surface temperature. J. Clim. 20, 5473–5496.

Rippy, M. A, Franks, P.J.S., Feddersen, F., Guza, R.T., Moore, D.F., 2013. Physical dynamics controlling variability in nearshore fecal pollution: fecal indicator bacteria as passive particles. Mar. Pollut. Bull. 66, 151–157.

Rippy, M. A, Franks, P.J.S., Feddersen, F., Guza, R.T., Warrick, J. A, 2013. Beach nourishment impacts on bacteriological water quality and phytoplankton bloom dynamics. Environ. Sci. Technol. 47, 6146–54.

Roelvink, D., Reniers, A., van Dongeren, A., van Thiel de Vries, J., McCall, R., Lescinski, J., 2009. Modelling storm impacts on beaches, dunes and barrier islands. Coast. Eng. 56, 1133–1152.

Russell, T. L., Yamahara, K. M., Boehm, A. B., 2012. Mobilization and transport of naturally occurring enterococci in beach sands subject to transient infiltration of seawater. Environ. Sci. Technol. 46(11), 5988–5996.

Russell T. L., Sassoubre L. M., Wang D., Masuda S., Chen H., Soetjipto C., Hassaballah A., Boehm A. B., 2013. A coupled modeling and molecular biology approach to microbial source tracking at Cowell Beach, Santa Cruz, CA, United States. Environ. Sci. Technol. 47(18), 10231–10239.

Saltelli A., Chan, K., Scott, E.M., 2000. Sensitivity analysis, John Wiley & Sons, Chichester, England.

Sanders, B.F., Arega, F., Sutula, M., 2005. Modeling the dry-weather tidal cycle of fecal indicator bacteria in surface waters of an intertidal wetland. Water Res., 39, 3394-3408.

Sassoubre, L.M., Nelson, K.L., Boehm, A.B., 2012. Mechanisms for photoinactivation of Enterococcus faecalis in seawater. Appl. Environ. Microbiol. 78, 7776–7785.

Shah, A.H., Abdelzher, A.M., Phillips, M., Hernandez, R., Solo-Gabriele, H.M., Kish, J., Scorzetti, G., Fell, J.W., Diaz, M.R., Scott, T.M., Lukasik, J., Harwood, V.J., McQuaig, S., Sinigalliano, C.D., Gidley, M.L., Wanless, D., Ager, A., Lui, J., Stewart, J.R., Plano, L.R.W., Fleming, L.E., 2011. Indicator microbes correlate with pathogenic bacteria, yeasts and helminthes in sand at a subtropical recreational beach site. J. Appl. Microbiol. 110(6), 1571-1583.

Shibata, T., Solo-Gabriele, H.M., Fleming, L.E., Elmir, S., 2004. Monitoring marine recreational water quality using multiple microbial indicators in an urban tropical environment. Water Res. 38, 3119–3131.

Shibata, T., Solo-Gabriele, H.M., Sinigalliano, C.D., Gidley, M.L., Plano, L.R.W., Fleisher, J.M., Wang, J.D., Elmir, S. M., He, G., Wright, M.E., Abdelzher, A.M., Ortega, C., Wanless, D., Garza, A.C., Kish, J., Scott, T., Hollenbeck, J., Backer, L.C., Fleming, L.E., 2010. Evaluation of conventional and alternative monitoring methods for a recreational marine beach with nonpoint source of fecal contamination. Environ. Sci. Technol, 44, 8175-8181.

Shuval, H., 2003. Estimating the global burden of thalassogenic diseases: human infectious diseases caused by wastewater pollution of the marine environment. J. Water Health, 2, 53-64.

Sinigalliano, C.D., Fleisher, J.M., Gidley, M.L., Solo-Gabriele, H.M., Shibata, T., Plano, L.R.W., Elmir, S.M., Wanless, D., Bartkowiak, J., Boiteau, R., Withum, K., Abdelzaher, A.M., He, G., Ortega, C., Zhu, X., Wright, M.E., Kish, J., Hollenbeck, J., Scott, T., Backer, L.C., Fleming, L.E., 2010. Traditional and molecular analyses for fecal indicator bacteria in non-point source subtropical recreational marine waters. Water Res. 44, 3763–3772.

Sinton, L.W., Finlay, R.K., Lynch, P.A., 1999. Sunlight inactivation of fecal bacteriophages and bacteria in sewage-polluted seawater. Appl. Environ. Microbiol. 65, 3605–13.

Sinton, L.W., Hall, C.H., Lynch, P.A., Davies-Colley, R.J., 2002. Sunlight inactivation of fecal indicator bacteria and bacteriophages from waste stabilization pond effluent in fresh and saline waters. Appl. Environ. Microbiol. 68, 1122–1131.

Solo-Gabriele, H.M., Wolfert, M.A., Desmarais, T.R., and Palmer, C.J., 2000. Sources of *Escherichia coli* in a coastal subtropical environment. Appl. Environ. Microbiol., 66, 230-237.

Soulsby, R.L., 1997. Dynamics of marine sands, Thomas Telford, London, U.K.

Stewart, J.R., Fleming, L.E., Fleisher, J.M., Abdelzaher, A.M., and Lyons, M., 2011. Waterborn pathogens. In: Hester, R.E., and Harrison, R.M., (eds), Marine pollution and human health (Issues in Environmental Science and Technology), 25-67, DOI:10.1039/9781849732871-00025. Royal Society of Chemistry, Cambridge, UK.

Symonds, G., Zhong, L., Mortimer, N. A., 2011. Effects of wave exposure on circulation in a temperate reef environment. J. Geophys. Res. 116, C09010.

Thupaki, P., Phanikumar, M.S., Beletsky, D., Schwab, D.J., Nevers, M.B., Whitman, R.L., 2010. Budget analysis of *Escherichia coli* at a southern Lake Michigan beach. Environ. Sci. Technol. 44, 1010–1016.

Thupaki, P., Phanikumar, M., Schwab, D.J., Nevers, M.B., Whitman, R.L., 2013. Evaluating the role of sediment-bacteria interactions on Escherichia coli concentrations at beaches in Southern Lake Michigan. J. Geophys. Res. 118, 1–17.

US EPA, 1986. Ambient water quality criteria for bacteria. EPA 440/5-84-002. Washington D.C., U.S. Environmental Protection Agency.

US EPA, 2012. Recreational water quality criteria. Washington D.C., U.S. Environmental Protection Agency.

van de Mei, H.C., Meinders, J.M., Busscher, H.J., 1994. The influence of ionic strength and pH on diffusion of micro-organisms with different structural surface features, Microbiol., 140, 3413-3419.

van Rooijen, A.A., 2011. Modeling sediment transport in the swash zone, MSc thesis, Delft University of Technology, Delft, Netherlands.

Wade, T.J., Nitika, P., Eisenberg, J.N.S., Colford, J.M., 2003. Do US Environmental Protection Agency water quality guidelines for recreational waters prevent gastrointestinal illness? a systematic review and meta-analysis. Environ. Health Perspect. 1111, 1102–1109.

Wade, T.J., Calderon, R.L., Sams, E., Beach, M., Brenner, K.P., Williams, A.H., Dufour, A.P., 2006. Rapidly measured indicators of recreational water quality are predictive of swimming-associated gastrointestinal illness. Environ. Health Perspect. 114, 24–28.

Wang, J.D., Solo-Gabriele, H.M., Abdelzaher, A.M., Fleming, L.E., 2010. Estimation of enterococci input from bathers and animals on a recreational beach using camera images. Mar. Pollut. Bull. 60, 1270–1278.

Wang, J., Wolff, D.B., 2012. Evaluation of TRMM rain estimates using ground measurements over Central Florida. J. Appl. Meteorol. Climatol. 51, 926–940.

Whitman, R.L., and Nevers, M.B., 2003. Foreshore sand as a source of *Escherichia coli* in nearshore water of a Lake Michigan beach, Appl. Environ. Microbiol., 69(9), 5555-5562.

Whitman, R.L., Shively, D.A., Pawlik, H., Nevers, M.B., and Byappanahalli, M.N., 2003. Occurrence of *Escherichia coli* and enterococci in Cladophora (Chlorophyta) in nearshore water and beach sand of Lake Michigan. Appl. Environ. Microbiol., 69(8), 4714-4719.

Williams, J.J., de Alegría-Arzaburu, A.R., McCall, R.T., Van Dongeren, A., 2012. Modelling gravel barrier profile response to combined waves and tides using XBeach: Laboratory and field results. Coast. Eng. 63, 62–80.

Willmott C.J., and K. Matsuura, 2005. Advantage of the mean absolute error (MAE) over the root mean square error (RMSE) in assessing average model performance. Climate Research, 30, 79-82.

Willmott, C.J., Robeson, S.M., Matsuura, K., 2011. A refined index of model performance. Int. J. Climatol., DOI: 10.1002/joc.2419.

Wolff, D., Marks, D., Amitai, E., Silberstein, D.S., Fisher, B.L., Tokay, A., Wang, J., Pippitt, J.L., 2005. Ground validation for the Tropical Rainfall Measuring Mission (TRMM). J. Atmos. Ocean. Technol. 22, 365–380.

Wright, M.E., Solo-Gabriele, H.M., Elmir, S., Fleming, L.E., 2009. Microbial load from animal feces at a recreational beach. Mar. Pollut. Bull. 58, 1649–56.

Wright, M.E., Abdelzaher, A.M., Solo-Gabriele, H.M., Elmir, S., Fleming, L.E., 2011. The inter-tidal zone is the pathway of input of enterococci to a subtropical recreational marine beach. Water Sci. Technol. 63, 542–549.

Yamahara, K.M., Layton, B. A, Santoro, A.E., Boehm, A.B., 2007. Beach sands along the California coast are diffuse sources of fecal bacteria to coastal waters. Environ. Sci. Technol. 41, 4515–4521.

Yamahara, K.M., Walters, S.P., Boehm, A.B., 2009. Growth of enterococci in unaltered, unseeded beach sands subjected to tidal wetting. Appl. Environ. Microbiol. 75, 1517–1524.

Yamahara, KM, Sassoubre, L.M., Goodwin, K.D., Boehm, A.B., 2012. Occurrence and persistence of bacterial pathogens and indicator organisms in beach sand along the California coast. Appl. Environ. Microbiol. 78, 1733–1745.

Young, I.R., 1997. The growth rate of finite depth wind-generated waves, Coast. Eng., 32, 181-195.

Zhu, X., Wang, J.D., Solo-Gabriele, H.M., Fleming, L.E., 2011. A water quality modeling study of non-point sources at recreational marine beaches. Water Res. 45, 2985–2995.

VITA

Zhixuan Feng was born in Baoying, Yangzhou, Jiangsu Province, China on August, 1985. His parents are Zhaokui Feng and Xiyu Wang. He received his elementary education at Sheyanghu Elementary School and his secondary education at Sheyanghu Middle School and Baoying High School. In September 2003, he entered the Nanjing University, from which he graduated with Honors with a B.S. degree in Geography in June 2007. He studied at the Louisiana State University for two years, and earned a M.S. in Oceanography and Coastal Sciences. He was admitted to the Rosenstiel School of Marine and Atmospheric Science (RSMAS), University of Miami in 2009, and is completing his Ph.D. in Applied Marine Physics.